BAM
Bundesanstalt für Materialforschung und -prüfung

Freie Universität Berlin

Scandium in Bauxite Residues and other metallurgical by-products

Dissertation

Zur Erlangung des Grades eines Doktors der Naturwissenschaften

Doctor rerum naturalium

(Dr. rer. nat.)

Eingereicht im Fachbereich Geowissenschaften

der Freien Universität Berlin

Vorgelegt von:

Marie Christin Gentzmann

Berlin, Mai 2022

Erstgutachterin: Frau Dr. Christiane Stephan-Scherb
Zweitgutachterin: Frau Prof. Dr. Anna Gorbushina
Drittgutachter: Herr Prof. Dr. Lutz Hecht

Tag der Disputation: 12.12.2022

To search for the old
is to understand the new.
Gichin Funakoshi

Abstract

In the last two decades metallurgical industrial residues have become the focus of extensive research regarding circular economy concepts and sustainable sourcing of raw materials in the European Union. Those residues can be enriched in high-value technology metals, making them potential secondary resources. The technology metal Scandium (Sc) is one of those high-value elements and was found to be significantly enriched in a variety of different metallurgical residues worldwide. Even though several residues have been described to contain elevated Sc levels, a comprehensive overview and assessment of potential secondary Sc resources in Europe does not exist.

When it comes to Sc, one of the most widely considered secondary sources are bauxite residues (BR). These BRs accumulate when bauxites are treated in the Bayer process where alumina is extracted from the bauxite ore. Some of those BRs, also widely known as red muds, were found to be enriched in Sc. Even though these enrichments were already discovered in the early 90's, the Sc association and distribution as well as the link between the Sc occurrence in bauxite and BR remain unclear. This thesis therefore provides a first assessment of different metallurgical industrial residues in Europe and beyond and evaluates their potential as secondary Sc resources. It then strongly focuses on one selected residue of high potential, the BR, and delivers detailed insights into geochemical and mineralogical properties of the Sc occurrence in these materials.

Metallurgical residues originating from the production of alumina, titanium dioxide, nickel, tin, steel, fertilizer, and Al-Sc alloys were investigated in terms of their Sc mass fractions and their general mineralogy and chemistry. Data on annual accumulation and quantities in stockpiles was collected to calculate the theoretical amounts of Sc evident in those residues. The monetary value of the contained Sc was compared to the contained value of other rare earth elements.

The detailed investigation of the Sc association and distribution in different BRs was performed with wet chemical and mineralogical methods, including microtextural and structural analysis. The recoverability of the Sc was studied by leaching and subsequent mineralogical analyses whilst the major factors that influence the leaching process were studied by "Design of experiments", a methodology of applied statistics. Furthermore, the overall link between the Sc association in bauxite and its respective BR was studied by comparison of BRs of different geological backgrounds.

The liquid acid waste originating from Titanium dioxide production and BRs were identified to be the most promising secondary resources for Sc in Europe. The Sc recovery from BR will most likely be implemented alongside other recovery schemes that enable the reutilization of larger amounts of the BR. BRs derived from lateritic bauxites showed to be less

prone to Sc enrichment than those derived from karstic bauxites. Furthermore, the atmospheric conditions during bauxitization can influence the distribution of Sc between different minerals causing the Sc to be either incorporated into easily leachable or hardly leachable phases during Bayer processing and subsequent acid leaching. BR derived from karstic bauxites formed under partly reducing conditions were found to have a higher fraction of easily leachable Sc than karstic bauxites formed under predominantly oxidizing conditions. Lateritic bauxites in turn, tend to have even lower fractions of easily leachable Sc.

It can be summarized that the distribution and recoverability of Sc from BRs is linked to the original bauxite ore and plays an important role for the assessment of a BR as a secondary Sc resource. As BR represents one of the two most promising secondary resources for Sc in Europe these relationships are essential, when considering the establishment of a Sc supply chain in Europe.

Kurzfassung

In den vergangenen zwei Jahrzehnten sind metallurgische Industrierückstände in den Mittelpunkt umfangreicher Forschungsarbeiten gerückt. Dabei stehen Ansätze für die Integration der Kreislaufwirtschaft und die nachhaltige Beschaffung von Rohstoffen in der Europäischen Union insbesondere im Fokus. Industrierückstände, die mit hochwertigen Technologiemetallen angereichert sein können, sind daher potenzielle Sekundärressourcen. Das Technologiemetall Scandium (Sc) ist eines dieser hochwertigen Elemente, welches Untersuchungen zufolge weltweit in einer Vielzahl verschiedener metallurgischer Rückstände deutlich angereichert ist. Obwohl erhöhte Sc-Gehalte in der Literatur bereits für mehrere Rückstände beschrieben wurden, gibt es keinen umfassenden Überblick und keine Bewertung der möglichen sekundären Sc-Ressourcen in Europa.

Zu den am häufigsten untersuchten sekundären Sc-Quellen gehören Rotschlämme (RS). Diese Rückstände fallen beim Bayer-Prozess an, bei dem Aluminiumoxid aus dem Bauxiterz gewonnen wird. Einige dieser RS können Untersuchungen zufolge mit Sc angereichert sein. Obwohl diese Anreicherungen bereits in den frühen 90er Jahren entdeckt wurden, sind die Sc-Assoziation und -Verteilung sowie der Zusammenhang zwischen dem Sc-Vorkommen im Bauxit und im RS noch weitgehend ungeklärt. In dieser Arbeit wird daher zunächst eine Bewertung verschiedener metallurgischer Industrierückstände in Europa und darüber hinaus vorgenommen und ihr Potenzial als sekundäre Sc-Ressourcen evaluiert. In einem zweiten Schritt werden die geochemischen und mineralogischen Eigenschaften des Sc in dem ausgewählten Rückstand – Rotschlamm – bestimmt.

Metallurgische Rückstände, die bei der Herstellung von Aluminiumoxid, Titandioxid, Nickel, Zinn, Stahl, Düngemitteln und Al-Sc Legierungen anfallen, wurden auf ihre Sc-Massenanteile und ihre allgemeine Mineralogie und Chemie hin untersucht. Es wurden Daten über die jährliche Sc-Anhäufung und die in Halden vorhandene Sc-Menge gesammelt, um die theoretischen Sc-Mengen zu berechnen, die in diesen Rückständen enthalten sind. Der monetäre Wert des enthaltenen Sc wurde mit dem Wert anderer Seltenerdelemente verglichen.

Die detaillierte Untersuchung der Sc-Assoziation und -Verteilung in verschiedenen RS wurde mit nasschemischen und mineralogischen Methoden durchgeführt, die sowohl mikrotexturelle und strukturanalytische Untersuchungen beinhalteten. Die Rückgewinnung des Sc wurde durch Auslaugung und darauffolgende Phasenanalyse untersucht. Die Faktoren, die den Auslaugungsprozess maßgeblich beeinflussen, wurden mittels "Design of experiments", einer Methode der angewandten Statistik, herausgearbeitet. Darüber hinaus wurde der übergeordnete Zusammenhang zwischen der Sc-Assoziation im RS und seinem

jeweiligen Ausgangsgestein durch den Vergleich von RS und Bauxiten verschiedenen geologischen Ursprungs erforscht.

Flüssige, saure Abfälle aus der Titandioxidproduktion sowie RS konnten als die vielversprechendsten Sekundärressourcen für Sc in Europa identifiziert werden. Die Sc-Rückgewinnung aus RS kann allerdings höchstwahrscheinlich nur in Kombination mit anderen Rückgewinnungstechnologien realisiert werden, welche die Wiederverwertung größerer Mengen RS ermöglichen. Die aus lateritischen Bauxiten gewonnenen RS weisen eine geringere Sc-Anreicherung auf als die aus Karstbauxiten gewonnenen RS. Darüber hinaus beeinflussen die physikochemischen Umgebungsbedingungen während der Bauxitisierung die Verteilung von Sc zwischen den verschiedenen Mineralphasen. Dies führt dazu, dass das Sc während des Bayer-Prozesses und der anschließenden Laugung entweder in leicht oder in schwer auslaugbare Phasen eingebaut wird. Die aus Karstbauxiten resultierenden RS, die unter teilweise reduzierenden Bedingungen entstanden sind, weisen einen höheren Anteil an leicht auslaugbarem Sc auf als RS aus Karstbauxiten, die unter vorwiegend oxidierenden Bedingungen entstanden sind. Lateritische Bauxite wiederum weisen tendenziell noch geringere Anteile an leicht auslaugbarem Sc auf.

Zusammenfassend lässt sich sagen, dass die Verteilung und Rückgewinnung von Sc aus RS in engem Zusammenhang mit dem ursprünglichen Bauxiterz stehen. Dieses spielt eine wichtige Rolle bei der Bewertung von RS als sekundäre Sc-Ressource. Da RS eine der beiden möglichen sekundären Sc-Ressourcen in Europa ist, sind diese Zusammenhänge für die Etablierung einer Sc-Lieferkette in Europa von wesentlicher Bedeutung.

Acknowledgements

A good, interdisciplinary team is the strongest foundation for successful research. I would therefore like to take this opportunity to thank my colleagues, friends, and family for without you all, it would have been impossible to write this thesis.

First and foremost, I would like to express my gratitude to my supervisors Christian Adam, Lutz Hecht and Christiane Stephan-Scherb. Christians open, kind and passionate way to tackle new research questions has motivated me throughout the whole process of writing this thesis. He provided an environment where it was possible to discuss problems and develop new ideas at any time. He was not only a supervisor but also someone to laugh and share stories with. Thank you Christian for all the support over the last years. I am grateful that I had the opportunity to carry on working with Lutz Hecht, who has long been someone that inspired me for geosciences and mineralogy. Lutz always brings in new perspectives and I would like to thank him for his dedication and support alongside this work. I am thankful for the ideas, discussions, and exchanges with Christiane-Stephan-Scherb who has helped bringing this thesis together.

Secondly, I would like to thank my close colleagues of division 4.4 at BAM who have grown to become friends. I would like to thank Katharina Schraut and Mareike Taube for sharing so many experiences with me, from Synchrotron nights to unbearable online workshops, from PhD days to running events and through ups and downs of PhD life. Thank you for sharing your knowledge with me on so many things. I would like to express my sincere gratitude to Angela Grabner, who has not only supported me in the lab, but who is also the heart and soul of the kind and supportive environment in division 4.4. I am thankful for the help and motivation provided by Christian Vogel, who has introduced me to the wonderful world of synchrotron measurements and has made it so much fun. I am grateful for the support of my other colleagues Karin Weimann, Hannes Herzel, Antje Bühlmann, Burkart Adamczyk, Theresa Sichler, Florian Loose, Eric Weingart, Juan Serrano, Patrick Piehl and Adib Hanna. They always had an open ear for me. Sharing an office with Dirk Stolle was relaxed and comfortable and I especially thank Dirk for his calm and kind nature that accompanied me on the way towards the doctorate.

Many other colleagues have helped bringing this thesis together. Katja Nordhauß, who has introduced me to Karlchen and Käthe, her dearest analytical devices, has helped me on countless occasions. Thank you Katja for all your time. I would also like to thank my XRD friends Dominik Al-Sabbagh and Torvid Feiler and I am furthermore grateful for the support of the SCALE partners. A vital point of writing a thesis comes down to motivation. I am therefore grateful to have written this thesis alongside Marieke Voight, Maximilian Sprengel and Desirée Hoehnel as they brought inspiration and so much joy to our “shut up and write” sessions.

My whole way towards becoming a researcher has been accompanied by my most amazing friends. Even though the list would be too long I would like to mention Friederike and Clara Körting, who have been my companions and my inspiration on so many occasions, thank you for always being there.

My sincerest gratitude goes to my wonderful parents as they have never doubted anything I did and they have shown their unconditional support, always. I cannot thank you enough.

Finally, one person has been there for me, throughout the whole journey, has overcome all challenges with me and has brought laughter, joy, and happiness whenever I needed it most. Thank you, Robert, my love, I will always be grateful.

Content

Personal contribution and structure

The dissertation comprises two peer reviewed articles, of which one is published and one is submitted and under review at the time of submission of this thesis. Additionally, the thesis contains work conducted for the H2020 Project SCALE under deliverable 6.1 “European inventory of Scandium containing by-products”. The SCALE Project Framework and its aims are explained in the next chapter of this thesis. The SCALE deliverable 6.1 (D 6.1) was published in an open access report in the Community Research and Development Information Service (CORDIS) for research data in the European Union (EU). The research work conducted for this deliverable will be integrated in chapter 2, the content of the peer reviewed publications will be integrated in chapter 3.1 and 3.2. Both chapters 2 and 3 represent collaborative work between several co-authors and the respective contributions are outlined below. The parts of this thesis that are taken from the original report and publications will be briefly described in the footnotes.

Chapter 2

Chapter 2 contains research work and results from the SCALE deliverable 6.1 (D 6.1) published as:

> *Hoffmann, M., V. Emese, U. Éva, I. Fekete-Kertész, M. Molnár, V. Feigl, and C. Adam, 2019: European inventory of Scandium containing by-products. SCALE Deliverable 6.1, Community Research and Development Information Service, 69 pp. [Available online at https://cordis.europa.eu/project/id/730105/results.]*

The chemical and mineralogical analyses were performed and evaluated by M.C. Gentzmann. The inventory and maps were prepared by M.C. Gentzmann, and data was provided by the SCALE consortium and Prof. John Grandfield. The manuscript for the final report was prepared by M.C. Gentzmann. C. Adam supervised the research work, revised and edited the manuscript. D 6.1 includes information about an environmental database which will not be discussed in this thesis. The co-authors É. Ujaczki, I. Fekete-Kertész, M. Molnár, V. Feigl are responsible for the preparation and description of this database in D 6.1.

Chapter 3.1

Chapter 3.1 contains the peer reviewed publication:

> *Gentzmann, M. C., K. Schraut, C. Vogel, H.-E. Gäbler, T. Huthwelker, and C. Adam, 2021: Investigation of scandium in bauxite residues of different origin. Applied Geochemistry, **126,** 104898.https://doi.org/10.1016/j.apgeochem.2021.104898*

The deliverable 6.1 was published as Marie C. Hoffmann (maiden name), the peer reviewed publications were submitted and published later as Marie C. Gentzmann.

M.C. Gentzmann conducted and evaluated geochemical and mineralogical measurements including ICP-MS, ICP-OES, Raman, Electron-Microprobe, XRD and XANES measurements. M.C. Gentzmann wrote the initial and final manuscript. Thomas Huthwelker, K. Schraut and C. Vogel helped with the XANES measurements and supported with editing the initial and the revised manuscript. T. Huthwelker was the supervising beamline scientist for XANES measurement conduction. E. Gäbler performed and evaluated the LA-ICP-MS measurements and participated in writing the specific parts about these measurements. C. Adam provided oversight and leadership of the research. All co-authors contributed to the discussions and helped with the revision and hence preparation of the final manuscript.

Chapter 3.2

Chapter 3.1 contains the peer reviewed publication:

> *M. C. Gentzmann, A. Paul, J. Serrano, C. Adam, 2022: Understanding scandium leaching from bauxite residues of different geological backgrounds using statistical design of experiments. Journal of Geochemical Exploration, Volume 240, 2022, 107041, https://doi.org/10.1016/j.gexplo.2022.107041*

M.C. Gentzmann conceptualized the research, performed the experiments, conducted chemical and mineralogical measurements, and evaluated the results of those measurements. She prepared the initial draft of the manuscript. A. Paul developed the experimental setup and evaluated the outcome of the statistical analyses. She participated in writing the parts concerned with the design of experiments. J. Serrano helped with the experiments. C. Adam supervised the research. All co-authors contributed to editing and discussion of the final manuscript.

The deliverable 6.1 was published as Marie C. Hoffmann (maiden name), the peer reviewed publications were submitted and published later as Marie C. Gentzmann.

The SCALE Project framework

The research presented in this thesis was conducted within the SCALE project (**Sc**andium **Al**uminium **E**urope) funded by the EU Horizon 2020 research and innovation program under Grant Agreement No. 730105. The aim of the SCALE project was to develop a secure supply of scandium (Sc) by recovery of Sc from certain industrial by-products such as bauxite residue (BR) and acid waste streams from Titanium dioxide production. Research and development within the project framework aim to provide in-depth knowledge about Sc resources to enable the future establishment of a European Sc industry. The project consortium consisted of 18 different partners from several European countries including industry, research institutes, universities, and consulting companies. The whole value chain of Sc was addressed within the different technical and non-technical work packages including extraction, refining and production of Sc compounds and Aluminum-Scandium (Al-Sc) alloy as well as life cycle assessment, ecotoxicity, sustainability and public relations.

The research at the Federal Institute of Materials Research and Testing (german: Bundesanstalt für Materialforschung und -prüfung, BAM) included the (geo)chemical analyses of potential secondary raw materials for a European Sc supply and the development of a European Sc inventory in addition to clustering and networking actions for public relations. The project was finalized in autumn 2021 and the data obtained during this thesis was used in the public deliverable report 6.1 of EU H2020 SCALE Project.

1. Introduction

1.1 The technology metal Scandium – current applications and future developments

In the last decades technologies of increased complexity started to gain more and more importance for our future and the supply of many different raw materials is of highest priority. Raw materials considered as especially important can be evaluated in terms of, e.g., supply risk, substitutability, environmental implications and economic importance and can be ranked in "criticality" (Graedel et al. 2012). According to such a criticality assessment every three years (starting in 2011) the European commission publishes a list of critical raw materials, and many other regions and countries evaluate resources in a similar manner (Schrijvers et al. 2020). Many of the materials or elements considered critical in the European Union, United States or other regions are technology metals (TM), hence "rare" metals of high demand promoting the development of future technologies in areas like consumer electronics, automotive industry, or alternative and sustainable energy solutions (Gunn 2014). Scandium (Sc) is one of those TMs and considered critical in the EU and US since 2017/2018 (European Commission 2017; Fortier et al. 2018). Even though the global supply and consumption is currently small, with < 30 t/a (U.S. Geological Survey 2019, 2021), Sc is considered to be a key enabler for certain technologies such as solid oxide fuel cells (SOFCs) and lightweight aluminum alloys.

Currently, ~90% of Sc produced is used in SOFCs (Grandfield 2021). In these devices, electricity is produced by the conversion of the chemical energy of a fuel gas (Stambouli and Traversa 2002). An ion conducting solid electrolyte, often a ceramic, enables the transport of ions from cathode to anode. The most widely used electrolyte amongst commercially available SOFCs is yttria (Y_2O_3) stabilized zirconia (ZrO_2) (Singhal 2007). However, the use of Sc instead of Yttrium (Y) for stabilization of the zirconia has many benefits for the technology since it increases the ionic conductivity of the electrolyte, it is more stable within the SOFC environment and has a higher long-term stability (Ivers-Tiffée et al. 2001). Due to their environmentally friendly energy production the use of SOFCs is considered to grow in the future and with it the demand for high purity Sc-compounds (Grandfield 2018).

Another application of Sc is the use in lightweight aluminum (Al) alloys. When Sc is used as an alloying element to Al, even small mass fractions of Sc can significantly influence the properties of the alloy. In fact, as a microalloying element it strengthens the material, makes it more resistant to recrystallization and hot cracking and reduces the grain size. Sc is therefore considered to be the most effective strengthener of that kind in Al alloys (Dorin et al. 2018). The beneficial effect of Sc in these alloys was first patented in 1971 (Willey 1971), and since then a lot of research has been conducted especially in Russia. The Western world only started reinvestigating the large potential of Al-Sc alloys in the early 2000s increasing the interest in

the use of Al-Sc alloys especially in the aerospace sector which is currently the second largest consumer of Sc (Grandfield 2021).

Apart from the use in SOFCs and Al-Sc alloys for aerospace industry, a small portion of Sc (~2 – 3%) is used in other metallic components e.g., for sporting goods and in special applications like lasers and metal halide lamps (Grandfield 2021).

Even though Sc has several promising applications, and its use certainly proved to be beneficial from a scientific point of view, a large-scale utilization has yet to be established. A major hurdle on the way to large-scale utilization so far has been the insecurity of both Sc supply and demand as well as high, non-transparent prices for Sc compounds. However, in recent years several projects around the world addressed this problem, and large companies such as Rio Tinto and RUSAL have entered the market and pushed forward research and development (RioTinto 2021; RUSAL 2021).

In addition, scandium oxide prices are lower than they have been for 30 years (Grandfield 2021). Sc demand is forecast to show a strong increase as more companies on the market are likely to decide on using Sc in the future, therefore supply options are developed in many regions worldwide.

1.2 Sc in natural rocks and soils

Scandium is a transition metal, which per definition belongs to the rare earth elements (REE). In terms of geochemical considerations, it is however often regarded separately from the REE which is likely due to the differences in behavior and properties (Horovitz 1975). In fact the ionic radius and ionic potential strongly differ from those of the REE (Siegfried and Wall 2018) and the physicochemical properties of Sc are more related to Mg^{2+}, Fe^{2+}/Fe^{3+} and Al^{3+}. Additionally, affinities to high field strength elements such as Ti, Zr and W have been noticed (Wang et al. 2021). Sc exhibits much higher incompatibilities in rock forming minerals than Mg, Fe and Al which results in generally low concentrations of Sc in those minerals (Samson and Chassé 2016). Compared to the other REE, Sc has a higher compatibility in rock forming minerals which is why other REE are predominantly incorporated in REE minerals, and Sc is not (Williams-Jones and Vasyukova 2018).

The average mass fraction of Sc in the Earth's continental crust is 14 – 31 mg/kg (Rudnick and Gao 2014) and rock forming minerals that incorporate Sc are mostly ferromagnesian minerals such as clinopyroxenes and amphiboles (Williams-Jones and Vasyukova 2018). Weathering processes liberate and redistribute Sc through transport in solution, reprecipitation, incorporation in new phases and adsorption onto mineral surfaces (Horovitz 1975). In the following sections some general characteristics of Sc occurrences in igneous and sedimentary rocks and soils will be presented with a special focus on bauxites and laterites. Table 1 gives an overview of average Sc mass fractions in different rock types.

Table 1 Sc mass fractions or grades in different rock types and selected Sc enriched localities with their respective reference. For selected localities, the major Sc bearing phase is given in brackets.

Classification	Rock type	avg. Sc mass fraction or reported ore grade (*) in mg/kg, major Sc bearing mineral in brackets	Reference
igneous	avg. Continental crust	14 – 31	Rudnick and Gao (2014)
	Granites	1-10	Horovitz (1975) and the references therein
	Granodiorite	5-7	Horovitz (1975) and the references therein
	Diorite	28	Horovitz (1975) and the references therein
	Gabbro	35	Horovitz (1975) and the references therein
	Rhyolites	5-9	Horovitz (1975) and the references therein
	Dacite	21	Horovitz (1975) and the references therein
	Andesite	13-34	Horovitz (1975) and the references therein
	Basalts	30-40	Horovitz (1975) and the references therein
	Pyroxenites	35-82	Horovitz (1975) and the references therein
	Peridotites	7-20	Horovitz (1975) and the references therein
sedimentary	Limestones	<1-25	Horovitz (1975) and the references therein
	Sandstones	<1	Horovitz (1975) and the references therein
	Shales	10-15	Horovitz (1975) and the references therein
	Clays	10-25	Horovitz (1975) and the references therein
	Bauxites	7-58	Horovitz (1975) and the references therein
metamorphic	Marble	>1	Horovitz (1975) and the references therein
	Quartzite	1-12	Horovitz (1975) and the references therein
	Schists	6-45	Horovitz (1975) and the references therein
	Greenschists	26	Horovitz (1975) and the references therein
	Gneisses	<1-30	Horovitz (1975) and the references therein
	Amphibolites	31-57	Horovitz (1975) and the references therein
selected carbonatites and alkaline rock complexes	Kovdor	800* (Baddeleyite)	Ivanyuk et al. (2016); Kalashnikov et al. (2016)
	Tomtor	390* (Clinopyroxene)	Williams-Jones and Vasyukova (2018)
	Elk Creek	71* (Xenotime)	Carlson and Treves (2005); Verbaan et al. (2018)
	Crater Lake (Also Misery Syenite)	>150* (Clinopyroxene)	Wang et al. (2021)
selected pegmatite	Kumir	50-2400* (Thortveitite)	Wang et al (2021)
selected Alaskan type mafic-ultramafic intrusions	Ural Mountains	75-135* (Amphibole, Clinopyroxene)	Wang et al (2021)
	Duke Island	54-110* (Amphibole, Clinopyroxene)	Wang et al (2021)
	Dongwanzi	65-99* (Amphibole, Clinopyroxene)	Wang et al (2021)

1.2.1 Sc occurrences in igneous and metamorphic rocks

Due to the dispersive and rather incompatible nature of Sc, enrichments in igneous rocks are rare. Nevertheless, there are environments such as some alkaline igneous rocks (including carbonatites), granitic pegmatites and hydrothermal veins in which significant Sc enrichment was observed (Samson and Chassé 2016). A general comparison of different igneous rocks presented by Wang et al. (2021) shows that ultramafic and mafic rocks tend to have higher bulk rock mass factions of Sc than intermediate, alkaline and acidic rocks. The authors state that the melt composition and origin of the melt is a crucial factor which determines the Sc mass fractions in igneous rocks. As Sc is more compatible in garnet then in spinel (Chassé et al. 2018a), partial melting of garnet peridotite is likely to produce less Sc enriched melts then spinel peridotites. By comparative modeling of different source lithologies Wang et al. (2021) conclude that the best source to produce Sc rich magmas (with 64 ± 7.6 ppm) is fertile spinel lherzolite. During crystallization, Sc is mostly concentrated in clinopyroxene and amphibole (hornblende), whereas the presence of water during crystallization may promote the formation of Sc-rich clinopyroxene. Post-magmatic processes can mobilize, preconcentrate and precipitate Sc bearing minerals. This can cause a further enrichment of Sc in special lithologies such as pegmatites and aplites where Sc is found in actual Sc-minerals like thortveitite ($(Sc,Y)_2Si_2O_7$). The physicochemical environment during mobilization has a major influence on the effectiveness of transport and the formation of Sc-bearing minerals. For example, in phosphate (PO_4^{3-}) rich environments, Sc can be incorporated into phosphates, whereas the presence of fluoride (F^-) can cause Sc incorporation into fluorites or fluorite rich minerals like mica or fluorapatite. For the enrichment observed in some alkaline igneous rocks Williams-Jones and Vasyukova (2018) and references therein also suggest fluoride-liquid-immiscibility as a possible mechanism. In this case Sc behaves similarly to the REE by partitioning strongly into the fluoride liquid. Additionally, Sc is found enriched in some carbonatitic environments where extreme fractional crystallization and silicate-carbonate liquid immiscibility may act as an enrichment process. In carbonatites, Sc is incorporated into zirconium and phosphate minerals like baddeleyite and xenotime that crystallize early during cooling and solidification (Ivanyuk et al. 2016; Kalashnikov et al. 2016).

There are several localities where the enrichment of Sc in igneous or metamorphic rocks reaches potentially exploitable values. Some of these localities were mined in the past, others are actively mined, and some are currently investigated for future mining operations (Williams-Jones and Vasyukova 2018 and references therein).

Some of the most important examples are:

- the Bayan Obo deposit in China
- the Tomotor, Kovdor and Kumir deposits in Russia,
- the Zhvoti Vody deposit in Ukraine
- the Crater Lake deposit (also Misery Syenite) in Canada
- the Crystal Mountain fluorite, Round Top Mountain and Elk Creek deposit in the U.S.
- the Evje-Iveland Pegmatite in Norway
- the Befanamo and Berere pegmatites in Madagascar
- the Kiviniemi deposit in Finland

The Bayan Obo deposit in China is a REE-Nb-Fe deposit hosted in massive dolomites containing numerous and different types of carbonatite dykes (Fan et al. 2016). It is the largest REE deposit in the world and was one of the largest producers of Sc. The Sc in Bayan Obo is hosted mainly in aegirine. Significant amounts of Sc can also be found in bastnaesite, monazite, and fluorite. Mine tailings contain ca. 200 mg/kg of Sc and the Sc resource was estimated to be 140.000 t (Williams-Jones and Vasyukova 2018).

The Tomtor deposit in Yakutia, northern Siberia is one of the largest carbonatite complexes in the world (300km^2) and just as Kovdor one of the two main Sc sources in Russia. The complex contains significant enrichments in niobium, yttrium, REE and Sc within and above the central carbonatite stock (Kravchenko and Pokrovsky 1995). Lapin et al. (2016) suggests xenotime to be the major Sc bearing phase but other Sc bearing minerals such as monazite, rhabdophane (0.95wt% Sc), crandallite group minerals, rutile and precipitated $Sc(OH)_3$ on phosphates were described in the earlier publications by Kravchenko and Pokrovsky (1995).

The Kovdor deposit in the Murmansk region in Russia is a baddeleyite-magnetite-apatite deposit. Here Sc mainly occurs enriched in baddeleyite found in phoscorite-carbonatite pipes. The baddeleyite has an average concentration of 780 mg/kg Sc and the total inferred resource of the Kovdor deposit is 420 t Sc_2O_3 (Ivanyuk et al. 2016; Kalashnikov et al. 2016). Currently baddeleyite is mined for production of ZrO_2 and the recovery of Sc is considered to be incorporable into the zirconium recovery flowsheet (Kalashnikov et al. 2016).

The Kumir deposit in the Altai region could become an important source for future Sc supply (Gusev et al. 2009). In this deposit so called exo- and endosubzones can be distinguished and mineralization is developed at the contact between clastic sediments and porphyritic granite (Williams-Jones and Vasyukova 2018). Exosubzones can contain significant amounts of thortveitite while the endosubzone concentrates Sc mainly in tourmaline. According to Williams-Jones and Vasyukova (2018) most of the Sc (>60%) is concentrated in

thortveitite. Less than 30% is concentrated in tourmaline and minor amounts can be found distributed in micas, feldspars and Fe-oxides.

In the Fe-U deposit Zhvoti Vody in Ukraine, the main Sc bearing mineral is aegirine of metasomatic origin. In this deposit high grade ores with significant amounts of Sc and vanadium but lower concentrations of other REE coexist with low grade ores containing less Sc but higher concentration of other REE and uranium. A total of 7.4 million tons of Sc-resource was described with an average ore grade of 105 ppm Sc. Together with iron-ore and uranium Sc was mined until 2003. At that time the Zhvoti Vody deposit delivered the predominant share of Sc worldwide. (Williams-Jones and Vasyukova 2018)

The Crater Lake deposit (also formerly Misery Syenitic intrusion) is an intrusive complex emplaced within the Mistastin Batholith in Quebec, Canada. Here syenites and ferrosyenites intruded the granitic to monzonitic, pyroxene bearing lithologies of the batholith (Petrella et al. 2014). The ferrosyenitic zone contains high amounts of ferromagnesian minerals where Sc is enriched in hedenbergite (clinopyroxene). Investigations on drillcores yielded Sc grades as high as 0.0506 wt% and an indicated resource of 7.3 million tonnes grading 282 g/t Sc_2O_3 (Cashin 2018; Imperial Mining Group Ltd. 2021; Siegfried and Wall 2018).

The Crystal Mountain fluorite deposit in Montana, U.S. comprises massive fluorite pegmatites emplaced in a biotite granodiorite pluton. Grondin (2019) suggests that the deposit crystallized from a fluorite-silicate melt which separated from a granitic melt. In this deposit thortveitite is one of the major Sc-minerals but elevated mass fractions of Sc were also found in other minerals (Foord et al. 1993). In the past this deposit was mined for fluorite and small amounts of Sc were produced from fluorite tailings (U.S. Geological Survey 1996).

The Round top deposit in Texas, U.S. is a heavy REE, and Sc enriched rhyolitic intrusion, where highest enrichments in heavy REE are reported from yttrofluorite, yttrocerite and bastnaesite. Additionally, many other REE bearing minerals were reported (Pingitore et al. 2014). The enrichment of incompatible REE in this deposit is attributed to a highly evolved magma system, where compatible elements were removed from the source magma chamber over a long period of time. Furthermore, a high temperature, F-rich mineral-vapor phase enabled the formation of late-stage F-complexing minerals, with exceptionally high REE mass fractions (O'Neill et al. 2017). According to the information provided by Texas Mineral Resources Corp. (http://tmrcorp.com/projects/rare_earths/) pre-construction operations at Round Top are currently undertaken and mining of heavy REE, Sc and other accompanying elements is planned.

Another project currently under development in the U.S. is the Elk Creek deposit in Nebraska. Here, Sc and niobium are the main target elements. The Elk Creek deposit is a carbonatite mainly consisting of dolomite, calcite and ankerite. Dolomite was described as the

major Sc bearing mineral. The probable reserve was estimated to have 71 g/t Sc (Carlson and Treves 2005; Verbaan et al. 2018).

The Evje-Iveland Pegmatite in the West-Agder Province in Norway, is one of the most important Sc localities since the mineral thortveitite was first described here by Schetelig (1911). It was likely also the first place where small amounts of thortveitite were mined for Sc production (Webminerals 2002). The REE or Niobium-Yttrium Fluorine pegmatites are thought to have formed from partial melting of rocks of the layered, mafic to ultramafic Iveland-Gautestad Complex. It was furthermore proposed that metamorphic fluids caused the partial melting of the complex where Sc was released from clinopyroxenite. (Williams-Jones and Vasyukova 2018).

The pegmatites in Befanamo and Berere, Madagascar are hosted in amphibolitic rocks and are known for their occurrences of thortveitite that was mined in the 1950's (Williams-Jones and Vasyukova 2018). Unfortunately, research on the Madagascan pegmatites, and their mineral occurrence is extremely rare and more detailed information on the nature of these pegmatites is lacking.

Finally, the Kiviniemi deposit in Finland is a garnet bearing ferrodioritic intrusion within the Central Finland Granitoid complex. In comparison to the other intrusions in this complex, the Kiviniemi ferrodiorite is characterized by a protruding geochemistry i.e., it shows high enrichments in Sc (51 – 281 mg/kg). The main Sc-bearing minerals are amphibole, clinopyroxene and apatite which implies a magmatic enrichment of Sc (Halkoaho et al. 2020).

There are certainly more localities where Sc enrichments in magmatic or metamorphic rocks can be found. The deposits compiled here (as of July 2021) represent a selection of the most established examples in literature including the ones of historical importance. More examples are compiled in the recent publication by Wang et al. (2021) or in the communication by Grandfield (2021).

1.2.2 Sc occurrences in sedimentary rocks and soils

Generally, the reported Sc mass fractions in most sedimentary rocks (excluding bauxites and laterites) are low (≤ crustal abundance of 14 – 31 mg/kg) and summarizing literature on Sc in these rocks is scarce. There are some occurrences of placer sands, where higher mass fractions of Sc are associated with weathering-resistant mineral phases such as zircon, xenotime or cassiterite (Horovitz 1975; Khan et al. 2019). Mineral sands from Namakwa, South Africa for example can contain up to 304 ppm of Sc (Philander and Rozendaal 2009). Limestones and carbonate sediments usually contain very little Sc (Myers et al. 1970). It was found that Sc contents in sediments can be positively correlated to the amount of clay minerals and the specific surface area of the sediment (Das et al. 1971; Horovitz 1975). A higher amount of clay minerals results in a higher specific surface area of the sediment and a higher sorption capacity. When weathering processes release Sc from ferromagnesian rock forming minerals,

it can be transported in solution and adsorb onto the surface of the clay minerals. According to Horovitz (1975) clays and shales have higher mass fractions of Sc compared to other common sedimentary rocks. Sc concentrations reported from soils are also low, but again recent literature is very scarce. According to Jeske and Gworek (2013) Sc contents in soils range between 2-12 mg/kg on average. With the exclusion of the special case of bauxites and laterites, which will be described in the next chapter, it can be inferred that sediments and soils are rarely enriched in Sc. However, there is a lack of literature on the Sc mass fractions in these rocks, so that a more detailed overview cannot be provided.

1.2.3 Sc occurrences in bauxites and laterites

Bauxites and laterites are sedimentary rocks, which form due to strong chemical weathering of the bedrock. These weathering processes mostly take place in tropical or subtropical humid climates with good drainage conditions. The weathering process causes a considerable enrichment of aluminum and/or iron due to the leaching of alkalis and silica (Bardossy and Aleva 1990). In fact, bauxites and laterites are distinguished by their iron and aluminum contents. Bauxites are generally strongly enriched in aluminum (>45%) with lesser enrichments of iron (<20%), in contrast, laterites are significantly enriched in iron (>20%). Bauxites form under even stronger leaching conditions than laterites when gibbsite (γ-$Al_2(OH)_3$) instead of kaolinite stability is favored due to lower concentration of dissolved silica. There are many subdivisions in the nomenclature of bauxites and laterites and many cases where a deposit might exhibit both lateritic and bauxitic horizons. In fact, most bauxites are overlain by a layer of lateritic material (Bardossy and Aleva 1990). It should therefore be noted that a very strict subdivision is not always applicable as transitions are gradual (Retallack 2010). Lateritic and bauxitic deposits are furthermore often subject to substantial transport and redeposition mechanisms and their source areas are not always easily identifiable. Bauxites can additionally be subdivided into lateritic and karstic bauxites. Lateritic bauxites are mostly derived from the underlying alumosilicate rocks. In contrast, karstic bauxites derive from alumosilicate rocks that were bauxitized after erosion, transported and redeposited on karstified relief (Bárdossy 1982).

Lateritic and bauxitic weathering processes that lead to enrichment or depletion of elements are strongly connected to the mobility of the respective element. The enrichment patterns for major and trace elements can be very complex as they are dependent on many factors. These include pH and Eh, drainage conditions, ground water table fluctuations atmospheric conditions, source rocks and underlying lithology (Valeton 1962; 1972). There are several elements which are considered to be highly mobile whereas other elements are moderately mobile or rather immobile. In fact, aluminum is highly immobile and therefore enriched during weathering. Silicon and alkalis are very mobile, and they are easily leached and transported away from the system during weathering i.e., depleted. There are also

elements, such as Fe, which can be either mobile or immobile and their behavior can change with variations of the surrounding physicochemical conditions. Sc is generally considered to be immobile, whereas REE are immobile during moderate weathering but can be mobilized under certain conditions. Bauxitic and lateritic weathering processes are therefore prone to enrich Sc and REE.

Recent studies have shown that laterites and bauxites can be relatively enriched in Sc by a factor of up to 10 compared to the original source rock (e.g.Teitler et al. 2019; Vind et al. 2018). Since ultramafic and mafic rocks tend to have higher mass fractions of Sc, deposits developed on or from such basements are more prone to show an enrichment of Sc. Especially Ni-Co laterites are nowadays often investigated as a potential Sc resource (Ulrich et al. 2019). In Table 2 different examples of bauxitic and lateritic deposits are listed with their respective reported Sc mass fractions and their reference.

The behavior of Sc during bauxitic and lateritic weathering has been investigated in a few recent studies by Chassé et al. (2019); Deady et al. (2014); Qin et al. (2020, 2021); Teitler et al. (2019) and (Vind et al. 2018). In the case of laterites, the authors agree that formation, dissolution and reprecipitation of iron hydroxides and oxides, especially goethite, plays a major role for the Sc distribution. According to their findings Sc is released from the weathering minerals of the protolith and immobilized by surface adsorption onto clay minerals such as smectites and later goethite (after clay dissolution).

Table 2 Sc mass fractions in different types of bauxites and laterites reported in literature and determined for the SCALE project deliverable 6.1 (SCALE D 6.1)

Country	Deposit/Area	Type	Sc [mg/kg]	reference
Bauxites				
Greece	Parnassos-Ghiona bauxite deposit	Karst bauxite	42 - 53	Vind et al. (2018)
Ghana	Awaso Bauxite	Lateritic bauxite	8,6	Vind et al. (2018)
Brazil	Porto Trombetas Bauxite	Lateritic bauxite	7	Vind et al. (2018)
Jamaica	Jamaican Bauxite	Karst bauxite	87-113	Wagh and Pinnock (1987)
Russia	Schugorsk deposit	Both types occur	12-307	Mordberg et al. (2001)
Russia	North Ural	Karst bauxite	32	SCALE D 6.1
Russia	North Timan	Likely lateritic	12	SCALE D 6.1
Italy	Apulian karst bauxite	Karst bauxite	35-73	Mongelli et al. (2017)
Italy	Campania karst bauxite	Karst bauxite	27-110	Mongelli et al. (2017)
Italy	Abruzzi karst bauxite	Karst bauxite	53-61	Mongelli et al. (2017)
Italy	Sardinia karst bauxite	Karst bauxite	16-81	Mongelli et al. (2017)
Guinea	Boké Bauxite	Lateritic bauxite	5-6	SCALE D 6.1
Spain	Catalan Coastal Range	Karst bauxite	28,5-64	Reinhardt et al. (2018)
Montenegro	Bauxites in the Dinaric metallogenetic province	Karst bauxite	28-59	Radusinović and Papadopoulos (2021)
Bosnia	Jajce deposit	Karst bauxite	63	Gamaletsos et al. (2019)
Suriname	unknown	Lateritic bauxite	8	Grant et al. (2005)

Table 2 continued

Country	Deposit/Area	Type	Sc [mg/kg]	reference
Laterites				
Australia	New South Wales deposits (Syerston–Flemington, Hylea, Owendale, Nyngan, Sconi, Pacific Express)	Laterite derived from mafic–ultramafic intrusions	50-600	Chassé et al. (2019)
Greece	Kastoria, Agios Ioannis, Evia	reworked and redeposited laterites derived from different source rocks	30-50	SCALE D.6,1
New Caledonia	Koniambo massif & Bien Sûr mine (Massif du Sud)	Laterite derived from ophiolite (upper mantle peridotites and mafic to ultramafic rocks)	51-67	Ulrich et al. (2019)
Philippines	Eramen Ni Mine Zambales Province, Berong Ni Mine Plawan Province	Laterite derived from serpentinized peridotite	14.9-82.5	Qin et al. (2020)
Cuba	Moa Bay mining area	Laterite derived from ophiolite	8-98	Aiglsperger et al. (2016)
Dominican Republic	Falcondo mining area	Laterite derived from ophiolite	21-121	Aiglsperger et al. (2016)
Laos	Bolaven Plateau	Laterite derived from basalt	22-48	Sanematsu et al. 2011
Brazil	Morro dos Seis Lagos (Amazonas)	Laterite derived from siderite carbonatite	146-482	Giovannini et al. (2017)

In the presence of aqueous Fe^{2+}, Sc can be substituted for Fe into goethite and incorporated into the crystal lattice of goethite. Because hematite has a lower capacity to incorporate Sc the recrystallization of goethite as well as hematite formation can lead to a sequence of Sc release and recapture. These effects can cause significant redistribution within a lateritic weathering profile. The same processes have been inferred for bauxites even though there is additional evidence that significant amounts of Sc can be incorporated into aluminum hydroxides (Suss et al. 2018). It has also been suggested that in the special case of karstic bauxites, the underlying karst relief and the associated physicochemical conditions might influence the Sc (and REE) enrichment. The karstic relief provides very good drainage conditions coupled with an increase in pH due to the alkalinity of the limestone so that REE and Sc could be stabilized as carbonate complexes or by adsorption (Deady et al. 2014; Lozano et al. 2020b). This effect will be evaluated in more detail in chapter 3.1.3.4.2.

1.3 Secondary sources of Sc and the potential of TiO_2-acid waste and bauxite residues

Since the interest and demand in Sc has only recently increased, Sc has never had a large and established supply chain as is common for other metals. In contrast, the production of Sc compounds is to a large extent connected to co-production as a by-product of other larger supply chains. Hence, there are several industrial by-products that can serve as secondary sources for Sc.

Those include:

- Rare earth element mine tailings
- Uranium leach liquors
- Residues from tin and tungsten processing
- Drosses and scraps from Al-Sc alloy production
- Coal mining wastes
- TiO_2-acid waste
- Zirconia oxychloride liquor
- Bauxite residues

Sc can be recovered as a by-product from primary mining operations as was the case in the Bayan-Obo deposit. Here Sc_2O_3 was produced from the rare earth tailings of the mine (Wang et al. 2020). Sc compounds are also produced as by-products of uranium mining where Sc is recovered from uranium leach liquors (Rychkov et al. 2016; Semenishchev 2018; Smirnov et al. 2017; Wang et al. 2011). The residues that accumulate during processing of tungsten and tin ores (i.e. wolframite and cassiterite residue/tin slag) can contain significant mass fractions of Sc (Wang et al. 2011). These enrichments can be attributed to the anomalous enrichment of Sc in some tin-tungsten deposits as for example reported in Kempe and Wolf (2006) in the Erzgebirge in Germany, Central Kazakhstan or Mongolian Altai region. The digestion of tungsten by an alkali medium leaves behind a precipitate rich in calcium, iron, manganese and up to 0.06 wt% Sc in the form of scandium hydroxide (Vanderpool et al. 1986). This residue can be treated by high temperature acid leaching and solvent extraction to recover the Sc (Wang et al. 2011). Tin slags from smelting of cassiterite can be treated in a similar manner (Wakui et al. 1989).

During the production of Sc containing alloys and master alloys, significant amounts of Sc can accumulate in the salty wastes and in metallic dross. The Sc from these materials can be recovered by leaching and solvent extraction. This process is very effective and nearly 100% of Sc can be recovered (Ditze and Kongolo 1997). However, since only small amounts of these alloys are currently produced, there is naturally only a small amount of Sc which can be provided by this recovery scheme.

Another potential secondary resource for Sc (and other REE) is coal fly ash and coal mining waste material. The material contains 20-40 mg/kg of Sc and also elevated contents of other REE (Alipanah et al. 2020; Stoy et al. 2021; Taggart et al. 2016). Some materials with higher enrichments of Sc have also been reported (Botelho Junior et al. 2021). Stoy et al. (2021) suggests that efficient and sustainable recovery techniques will involve the use of ionic liquids for concentration of the REE, since more conventional leaching and solvent extraction methods require strong leaching conditions connected to high consumption of chemicals. The company

Texas Mineral Resources Corp. currently performs pilot plant tests on Pennsylvania coal wastes and plans to recover Sc and other REE from those wastes in the near future (Texas Mineral Resources 2021).

The waste that is produced during the production of TiO_2 (white pigment) is a very important source for Sc. Sc is enriched in the liquid acid waste and the solid waste of both white pigment processing routes i.e., the sulfate and chloride route and stems from the feedstock of the process. For the chloride route mainly synthetic and natural rutile as well as chloride slag is used. For the sulfate route ilmenite can be used as a feedstock together with sulfate slag. Both chloride and sulfate slag are materials that result from smelting of ilmenite in an electric arc furnace (EAF) whereas chloride slag generally has a higher grade than sulfate slag (Filippou and Hudon 2020). Due to the affinity of Sc to high field strength elements such as Ti, the feedstock for the white pigment production contains Sc. It is relatively enriched in the process and accumulates in the liquid acid waste stream as well as in the solid filter cake. In fact, according to Grandfield (2021), the majority of Sc produced in 2021 stems from processing of this liquid acid waste stream. In the last 5 years, several pigment producing companies in China as well as in Canada have started using parts of their acid waste for Sc-compound production and the capacity of these suppliers is expected to grow substantially. TiO_2 pigment waste therefore has a very high potential to remain one of the main industrial by-products used for Sc production.

In addition to white pigment acid waste, the oxychloride liquor from zirconia production is also enriched in Sc due to its affinity to the minerals used in the feedstock. The recovery of Sc from this waste therefore also represents a possible source and it was reported that small amounts of Sc are currently supplied through this processing route (Grandfield 2021; Zhong and Wu 2012). Generally, the association of Sc with Zr naturally causes the enrichment of Sc in many processing routes that involve Zr so that several recovery and co-production schemes have been reported in the literature (Feuling 1991b; Lebedev 2007).

Finally, another waste stream that was found to contain enriched amounts of Sc is bauxite residue (in the following abbreviated as BR). This residue accumulates during conventional Bayer processing of bauxites for production of alumina (Al_2O_3). The material is an industrial waste stream of enormous mass since > 160 million metric tons accumulate worldwide each year (Habashi 2016; The International Aluminium Institute 2020). Various approaches for reuse and recycling are currently investigated and the proposed environmental applications are manifold (Klauber et al. 2011; Snars and Gilkes 2009; Sutar et al. 2014). Enrichment of Sc has already been described more than 25 years ago for example by Wagh and Pinnock (1987) for Jamaican BR and by Ochsenkühn-Petropulu et al. (1994) for Greek BR. This relative enrichment can be explained by means of mass balance, since the Bayer process dissolves approximately half of the original bauxite ore. The undissolved ore and newly formed

precipitates make up the residual waste stream called BR. The largest fraction of Sc is partitioning to the BR and is enriched (relatively) by a factor of ~2 (Vind et al. 2018). The enrichment factor can however vary because it depends on the mineralogy of the primary bauxitic raw material, other input materials and the process flow sheet of the alumina plant. As BR is one of the largest industrial waste streams, the need to reutilize it is strong. Many alumina refining companies are willing to approach this topic, but economic benefits must be considered as well. Due to the high value of Sc, its recovery could play an important role for the development of economic recycling and reutilization schemes for BR. Therefore, this residue has a high potential to become one of the main sources for future Sc supply.

1.4 Sc recovery and purification methods

The recovery of Sc from the different sources introduced in the previous chapter is generally connected to a complex multilevel flowsheet. In all cases Sc is either recovered as a by-product (e.g., TiO_2 acid waste) or recovered from a residue that was previously exploited for another raw material (e.g., BR). Therefore, the Sc recovery and production technologies have to be implemented into other processing schemes. Since the sources can differ strongly in their nature as they comprise e.g., solutions, slags, precipitates and muds, various different technologies were developed. All of these technologies combine leaching with ion exchange or solvent extraction methodologies to first form crude Sc concentrates (Molchanova et al. 2017). These crude concentrates have to be processed further to produce pure Sc compounds such as ScF_3 and Sc_2O_3.

In nearly all Sc recovery schemes, Sc is either brought into acidic solution by leaching or is already present in an acidic solution. The latter is the case in uranium leach liquors, TiO_2 liquid acid waste or Zirconia oxychloride liquors. It was described by Yagmurlu et al. (2018) that Sc can be concentrated by solvent extraction with acidic or neutral organophosphorus extractants. Examples for those extractants are DEHPA, lonquest 801, TBP or Cyanex 272, 302 or 923 (DEHPA: Di-(2-ethylhexyl) phosphoric acid, lonquest 801: 2-ethyhexyl phosphonic acid mono-2-ethylhexyl ester, TBP: tri-butyl-phosphate, Cyanex: different phosphinic acid-based extractants). All these extractants have advantages and disadvantages with regard to extraction yield, stripping behavior, cost of chemicals and selectivity over other impurities.

Instead of solvent extraction, ion exchange methods can also be used to concentrate the Sc. In contrast to solvent extraction, ion exchange methods generally do not need multiple stages of the different operation steps and can be advantageous in terms of extractant consumption. However, the process is often more time consuming and has a lower efficiency when impure solutions need to be treated. Furthermore, the costs for ion exchange resins are generally quite high.

Another hydrometallurgical approach of high potential is the use of ionic liquids for selective recovery of Sc. Ionic liquids are highly selective for REE, but they are expensive and highly viscous which can complicate their use.

When using solvent extraction and ion-exchange methods, the concentrated solution will contain impurities which makes intense purification steps necessary. Certain elements, especially Fe^{3+}, behave similar to Sc^{3+} in aqueous solution so that advanced purification methods with several stages are needed for trace element recovery. The Fe can be removed from the solution by precipitation, or it can be reduced to $Fe^{2+}$to change its interfering behavior and facilitate separation. Fe-Sc separation can for example be achieved by selective precipitation with aqueous ammonia. After Fe removal Sc can be precipitated as phosphate.
The production of Sc compounds therefore needs many processing steps. Often a combination of solvent extraction, ion exchange and precipitation methods is used to purify the end products according to the requirements of the application.

1.4.1 Recovery from TiO_2 production wastes

As stated in chapter 1.3, the majority of Sc produced currently (as of July 2021) stems from processing of TiO_2 liquid acid waste in China (Grandfield 2021). According to a recent publication by Zhang et al. (2021) most of this production is associated with the sulfuric acid process for TiO_2 production. Studies that involve the Sc recovery from acid waste of TiO_2 chloride route are rare and mainly demonstrate the proof of concept (Remmen et al. 2019). To recover the Sc, the liquid acidic wastes are generally treated by solvent extraction with an organic extractant such as DEHPA and TBP. The loaded organic phase is subsequently scrubbed with a solution of H_2SO_4 and H_2O_2 and is then stripped e.g., with an NaOH or NH_4F solution. Sc is recovered in the strip liquor from which $ScOH_3$ can be precipitated (Peters et al. 2019; Zhang et al. 2021). Apart from this general approach, there are several studies that investigate the use of other extractants, scrubbing solutions or the pretreatment methods with nanofiltration to enhance selectivity of the solvent extraction process (Li and Wang 1998; Remmen et al. 2019; Zhang et al. 2021).
In addition to the liquid acidic waste, the solid waste accumulating during TiO_2 pigment production can also contain high mass fractions of Sc. However, to my knowledge, investigations on the recovery of Sc from these solid residues have not been published.

1.4.2 Recovery from bauxite residues

As stated in the previous chapter, Sc is often brought into solution by leaching. In fact, leaching is also the first major step for the recovery of Sc from BR. Various leaching procedures have been studied in much detail with a strong focus on metallurgical and technical aspects. The review by Borra et al. (2016) gives an overview over the different approaches. There are many different factors that can influence the leaching behavior of Sc and the efficiency of the

subsequent concentration methods (introduced in the previous chapter). Generally, one can distinguish between acid leaching with either organic or inorganic acids, alkaline leaching (also carbonate leaching), bioleaching and leaching with ionic liquids. The parameters that were mainly studied include temperature, time, liquid to solid ratio, concentration of leaching agent, pH value, stirring rate and pressure. It is also possible to combine the leaching with precursor reductive roasting or smelting, which can enable the recovery of other valuable metals like Fe or Ti (Alkan et al. 2017; Borra et al. 2016; Zinoveev et al. 2021). In addition to those parameters the BR itself and its primary bauxite will play an important role, since the Sc species can vary significantly between materials of different origin (Suss et al. 2018; Vind et al. 2018). Understanding the influence of the primary raw material bauxite on Sc species and leaching behavior is therefore the major focus of this thesis as is explained in chapter 1.5. In Figure 1, the ranges of possible Sc recovery achieved by leaching of BR with different approaches is presented and the underlying data from literature can be found in appendix Table A 1. The Figure illustrates that acidic leaching, bioleaching and ionic liquid leaching can recover large parts of the Sc whereas acidic leaching with inorganic acids can achieve the highest recovery. It is important to mention that inorganic acid leaching is by far the most widely investigated method and there is a large amount of literature and data available. Hence the other approaches are relatively underrepresented. To the best of my knowledge, alkaline leaching has only been reported for Russian BR (Petrakova et al. 2015; Rychkov et al. 2021).

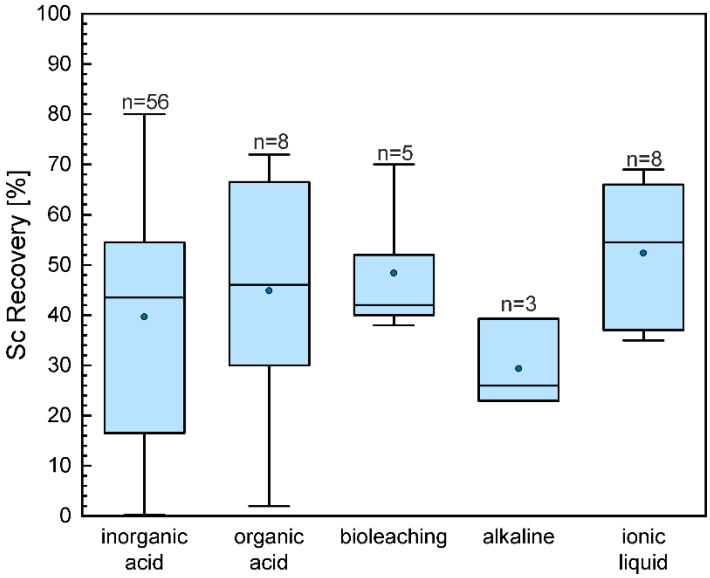

Figure 1 Box and whisker plot representing the range, upper and lower quartile, median and mean values (blue dot) reported for Sc recovery from bauxite residues by leaching with different approaches. N is the number of data points.

Leaching studies with inorganic acids (Borra et al. 2015; Ochsenkuehn-Petropoulou et al. 2018; Ochsenkühn-Petropoulou et al. 2002; Ochsenkühn-Petropulu et al. 1996; Sugita et al. 2015; Ujaczki et al. 2017; Wang et al. 2013) often conclude that a low pH value is key to efficient and maximum recovery of Sc. The tested mineral acids comprise HCl, H_2SO_4, HNO_3

and H_3PO_4, whereas in depth studies were mainly performed for the first three and mainly on Greek BR. Several aspects were investigated and compared, and the following effects were generally observed. HNO_3, HCl, and H_2SO_4 perform similarly but in descending order whereas HNO_3 provides better selectivity over Fe than HCl. Lower pulp densities (i.e., higher liquid to solid ratios) increase the recovery and several leaching stages can increase the Sc concentration in solution so that subsequent concentration of Sc can be improved. An increase in acid concentration is only beneficial up to a certain point after which there is no further increase in Sc recovery. The most desired inorganic acid must be evaluated in terms of recovery, selectivity, acid consumption and leaching residue characteristics. Hence, it will differ for different BRs and processing scenarios.

Studies that evaluate the leaching with organic acids are not as numerous but still deliver insights into the general aspects. Here, the effects of citric ($C_6H_8O_7$), acetic ($C_2H_4O_2$), formic (CH_2O_2), methanosulfonic (CH_4O_3S), oxalic ($C_2H_2O_4$) and succinic acid ($C_4H_6O_4$) have been investigated (Bogomazov and Senyuta 2017; Borra et al. 2015; Oqilov et al. 2020; Ujaczki et al. 2017). When compared at the same conditions, most organic acids are not able to achieve as high a Sc recovery as inorganic acids. They are not as effective in lowering the pH-value of the BR-acid slurry which causes this lower recovery. In fact, Borra et al. (2015) found that acetic acid, citric acid and methanosulfonic acid lower the pH of the slurry in ascending order, whereas the latter performs similarly to nitric or hydrochloric acid. However, increasing temperatures can significantly improve the performance of organic acids. In addition, the use of these acids often achieves better selectivity over Fe. Studies with acetic and formic acids (Bogomazov and Senyuta 2017) achieved a high Sc recovery (~70%) for Russian BR. The use of those acids was furthermore described as advantageous since leaching approaches with sulfuric acid hinders the effective filtering and separation of leachate and solid residue. The leaching with succinic acid, which was also performed on Russian BR, could achieve a recovery of >50%. However, a high acid concentration and several leaching stages at high liquid to solid ratios were required.

Studies on bioleaching are rare but several different microorganisms including fungi, bacteria and microalgae have been tested to leach or accumulate Sc and/or REE from BR (Čížková et al. 2019). In the case of bacteria and fungi, the leaching effect is caused by the organic acids produced by the microorganisms. Different procedures can be distinguished depending on whether the BR is treated together with the bacteria or whether there is a pretreatment of the bacterial culture. Kiskira et al. (2021) and Qu et al. (2019) studied the leaching of Sc by chemoheterotrophic bacterial strains such as acetobacter tropicalis and acetobacter sp., the latter was isolated from Chinese BR. In their experiments, the one-step leaching process achieved 38-50% Sc recovery. The main acids that were produced by the bacteria included acetic, oxalic, citric and malic acid. In addition, the fungi Penicillium tricolor was also isolated

from BR and leaching studies were performed (Qu and Lian 2013). Here up to 70% of Sc could be leached in a two-step process and the most significant acids involved were citric and oxalic acid. Even though it was illustrated in these studies that a high recovery is possible with bioleaching, there are several aspects such as the handling of the treated BR and long treatment times that can be challenging with this approach.

As already stated above, alkali and carbonate leaching are special cases that have mainly been studied on Russian BRs. According to Petrakova et al. (2015), this method is based on the ability of Sc to dissolve in presence of excess alkali carbonates and hydro carbonates. The BR is leached with carbonate and bicarbonate liquors (e.g., $NaHCO_3$ and Na_2CO_3) and CO_2 gas is used to intensify the carbonization leaching. With up to ~40%, the Sc recovery achieved is generally lower than for acid and bioleaching. However, the formation of another acidic and in cases toxic sludge can be avoided and separation and selective extraction are simplified due to lower amounts of salt products (Rychkov et al. 2021).

Finally, BR can also be leached with ionic liquids (ILs), i.e., liquids that only consist of ions which are essentially room temperature molten salts (Bonomi et al. 2018). The ILs can be tuned to meet the requirements of a specific method, which makes them superior to other organic solvents (Davris et al. 2018). Therefore, ILs can be used for metal recovery by leaching to increase the selectivity of the process and avoid high concentrations of interfering elements. In BR-leaching for example, the dissolution of Fe-containing minerals can be avoided, while Sc can be selectively leached from the material. Studies by Davris et al. (2018) showed that ~45% of Sc can be leached with the IL betainium bis(trifluoromethylsulfonyl)imide (abbreviated: [Hbet] [Tf2N]) at a temperature of 180°C, while dissolution of Fe is low. In another study performed by Bonomi et al. (2018) another IL, 1-ethyl-3-methylimidazolium hydrogensulfate (abbreviated: $[Emim][HSO_4]$), was tested and a Sc recovery of ~80% was achieved at 200°C. Since the IL used here was not selective over Fe and greatly dissolved Fe oxides and hydroxides, nearly all Fe was recovered alongside Sc. Generally, the use of ILs is beneficial when Sc concentrations in the leachate are high while Fe concentrations remain low (Mikeli et al. 2021). However, the high prices of these solvents as well as high IL losses during the leaching procedure remain drawbacks of this method.

In conclusion, there are many studies that deal with the recovery of Sc from BR by leaching and various set ups and parameters were studied for different BRs. A high recovery of Sc is generally possible, but it is always at the cost of selectivity over other elements, predominantly Fe. It is therefore of high importance to increase the understanding of Sc species and association in bauxite residues and their precursor rocks to be able to draw conclusions from the primary ore towards Sc recovery possibilities.

1.5 Motivation and aim of this thesis

As the demand for Sc in Europe increases with the development of promising technologies for a more sustainable future, potential raw materials need to be identified and evaluated. Since Sc is rarely enriched to exploitable grades in natural ore deposits, metallurgical wastes and residues have a high potential to become major sources of Sc supply in European countries. However, Sc has long been the "forgotten" rare earth element and has often been omitted in geochemical and mineralogical studies of primary and secondary raw materials (SRMs). Even though the increase in Sc demand sparked research in the fields of metal recovery and chemical engineering there is a knowledge gap in linking Sc geochemistry to ore processing and metallurgy. It is the aim of this thesis to evaluate the Sc recovery potential of selected metallurgical wastes and residues in Europe and increase knowledge about Sc species and association in one of the most promising SRMs for Sc recovery – bauxite residues (BRs). The comparative investigations provide insights into significant similarities and differences between BRs of various geological backgrounds. The findings furthermore provide an understanding of how and why the BRs behave differently during leaching.

As the leaching technology and the chemicals used are subject to constant innovation and change, this work provides basic knowledge about possible Sc containing minerals, adsorption phenomena, the stability of those minerals in BRs and how these depend on the bauxitic material that was subjected to alumina processing. It is furthermore considered, how different conditions during leaching influence the changes in mineralogy and how these changes correspond to the liberation of Sc into the leachate. As the influence of physicochemical environments of bauxite formation on Sc association in the resulting residue are determined, Sc recovery schemes will be easier to implement and assess.

The major questions that need to be answered are:

- ⇒ ***Which industrial residues in Europe contain Scandium and what is their potential resource?***
- ⇒ ***How does Scandium associate in bauxite residues – from ore to waste?***
- ⇒ ***How is Scandium released under variable leaching conditions?***
- ⇒ ***Can we draw conclusions on the recovery potential of Sc from a bauxite residue by assessing its geologic history?***

Answering those questions will help to fulfill the prime objective of this work, which is to provide an overall understanding of the Sc mineralogy and geochemistry in BRs to enable the development of effective leaching procedures.

2. An inventory of Sc containing metallurgical residues

Sc enrichments are rare in natural rocks, while relative enrichment of Sc in metallurgical wastes and residues has been observed for a range of different materials (comp. chapter 1.2 and 1.3). However, comprehensive literature on Sc contents in these wastes and residues is scarce and often outdated. In this chapter, the results of chemical and mineralogical analyses on metallurgical residues that accumulate during the production processes of Al_2O_3, TiO_2, Ni, phosphoric acid (for phosphate fertilizer), steel, Sn and Al-Sc alloy are presented. The Sc and REE mass fractions were determined by inductively coupled plasma mass spectrometry (ICP-MS) and inductively coupled plasma optical emission spectrometry (ICP-OES). Mineral phase assemblages were determined by X-ray diffraction (XRD) and mass fractions of major elements were determined by X-ray fluorescence (XRF). Data on accumulation of respective industrial residues was collected from the sample-providing companies and taken from literature to calculate a European inventory of Sc containing metallurgical wastes and residues. From the review of existing literature and investigations presented in this chapter, a Sc inventory world map was compiled providing an overview of the global localities currently involved in Sc mining, exploration and recovery.

The content of the chapters 2.1, 2.2, 2.3.1, 2.3.3 & 2.3.4 are based on the project deliverable: *Hoffmann, M., V. Emese, U. Éva, I. Fekete-Kertész, M. Molnár, V. Feigl, and C. Adam, 2019: European inventory of Scandium containing by-products. SCALE Deliverable 6.1, Community Research and Development Information Service, 69 pp.*

2.1 Materials and sample preparation

The materials, that were collected and analyzed in this work were provided by companies and institutes both within and beyond the project consortium of the H2020 project SCALE. The samples comprised BRs, TiO_2 liquid acid waste and solid waste, phosphogypsum, tin slag, electric arc furnace slag from Ni production, electric arc furnace dust and blast furnace sludge from steel production and dross from Al-Sc alloy production. Some selected materials including BR are shown in Figure 2 A and B.

2.1.1 Bauxite residues

BR samples from four different countries including Greece (n=2), Germany (n=3), Russia (n=2) and Hungary (n=2) were investigated. Greek, German and Russian samples were kindly provided by the active alumina plants of MYTILINEOS AOG, Aluminium Oxid Stade and RUSAL respectively. Both the Greek and German processing plants provided samples taken on two - three different dates approximately six months apart. The BRs from Russia originate from two different plants. One of the BR samples from Hungary comes from the closed down pond near Ajka Alumina plant which was operated by the Hungarian Alumina Production company MAL. In 2010, the large BR containment reservoir broke causing an accident with very dramatic aftermath. After the accident this reservoir was no longer used. A second sample of Hungarian BR stems from a dry disposal area installed after 2010. Generally, bauxite processing in the Hungarian facility mentioned here has stopped in 2014. A general description of BR can be found in the introduction in chapter 1.3. Furthermore, the subsequent chapter 3 of this thesis, focuses on more detailed investigations of BRs and provides further background knowledge on the samples.

2.1.2 TiO_2 production waste materials

The samples of TiO_2 liquid acid waste (with a bottom sediment) and solid waste were provided by TRONOX TiO_2 production plant in Botlek, the Netherlands. Both samples are derived from the chloride route where the production of highly pure TiO_2 is realized by chlorination of feedstock in presence of carbon at high temperatures of about 1000°C (McNulty 2007). As explained by McNulty (2007) this results in a gas stream containing titanium chloride ($TiCl_4$), impurity metal chlorides and carbon oxides. The impurity metal chlorides are separated from the $TiCl_4$ after condensation by cooling, whereas the $TiCl_4$ remains gaseous. It is then liquified by cooling and condensation and sent to a high temperature oxidation reactor where $TiCl_4$ reacts to TiO_2 under formation of chlorine which is recycled in the process. This process yields a very pure product that is generally known as titania or titanium white. During the process, two different waste streams can accumulate. Metal chlorides unreacted ore and coke dusts are mixed and dissolved in water and form an acidic, liquid waste stream with a certain amount of solid bottom sediment. This bottom sediment will further be referred to as acid slurry (AS).

The AS can be treated with lime whereby it is neutralized and metals precipitate mainly as hydroxides. The precipitates and the undissolved solids are filtered, and filter pressed, resulting in a second waste stream, the filter cake (FC). The input materials used are natural rutile from operations in Empangeni, KwaZulu-Natal and Brand-se-Baai, Western Cape (Namakwa Sands), South Africa as well as from Perth, Western Australia. Additionally, titanium slag from Namakwa Sands and synthetic rutile from Western Australia are used as feedstock and make up > 75% of the input (status 2018). In the TRONOX facility in the Netherlands, only small amounts of the AS and FC are currently stored on-site. Most of the AS is converted to FC and then landfilled offsite. AS and consequently the FC are prone to changes in the original feedstock which can influence the general chemical composition specifically with regard to trace elements.

2.1.3 Phosphogypsum

Phosphogypsum (PG) samples from three different localities were investigated: South Africa, Greece and Lithuania. The samples from South Africa originate from the mines that mine phosphate rock in the carbonatite complex at Phalaborwa, Limpopo province South Africa. The Greek sample was provided by a company that develops processes for utilization of industrial by-products and wastes for production of functional materials (company name remains confidential). The original source of the PG is unknown. Lithuanian samples derive from processing of Russian apatite (old sample) and processing of a mixture of Russian and Moroccan apatite (new sample), the processing company here also remains unknown.

PG is a waste that is generated during processing of phosphate ore such as apatite (mostly fluorapatite) to produce phosphoric acid (Tayibi et al. 2009), which is mainly used for the production of phosphate fertilizer. In the wet process of phosphoric acid production, the ore is treated with sulfuric acid and forms phosphoric acid, gypsum and hydrofluoric acid. The gypsum, called PG, can have highly variable characteristics that are very much dependent on the processed ore feed. It can contain different residues of calcium phosphates, hydrogen phosphates, fluorides and trace metals such as REE, naturally occurring radionuclides and organic matter. Due to the environmentally harmful properties, the material is mostly dumped on large stockpiles and only little amounts are reutilized for other processes (Tayibi et al. 2009).

2.1.4 Tin slag

The tin slag is of unknown origin and was sampled in the context of another project investigating the optimization of the Nb-Ta production process. It results from smelting of Sn ores such as cassiterite. Tin slags are widely used as an aggregate for Nb-Ta production due to their high contents in those refractory metals (Odo et al. 2014). Most of the Sn worldwide is produced in China and Southeast Asia, but there is also production in countries in South America, Africa and Europe (Elsner 2014).

2.1.5 Slag from Ni production

The electric arc furnace (EAF) slag from Ni production was kindly provided by the company LARCO from Greece and results from production of Ni. The company processes different lateritic ores from their mines at Kastoria, Evia and Agios Ioannis and produces ferronickel (alloy of Ni and Fe). In the third processing step, the pre-heated/ pre-reduced feedstock is fed to an EAF where it is reduced at 1600°C. During this process, a slag phase is separated from the metallic phase. This so-called EAF slag is granulated with seawater and is either dumped or exploited in further steps. The slag is also sold by LARCO for applications like sand blasting or utilization in cement production (LARCO 2022).

2.1.6 Wastes and residues from steel industry

The samples that originate from steel production comprise blast furnace sludge (BFS) and EAF dust. The BFS originates from a large German steel mill. It is a material that accumulates during production of iron which is an intermediate product for steel production. During production of iron in large blast furnaces a preheated air flow is introduced into the lower part of the furnace. The air that leaves the furnace at the top is a dusty gas flow, which can contain N_2, CO_2, CO and H_2 as well as high amounts of fine solids (dust). The material is first dry cleaned and subsequently washed so that a wet, muddy waste is generated, the so-called BFS. Generally, the material consists of iron ores, metallurgical coke and flux and is enriched in volatile elements like Na, K, and Zn (Mansfeldt and Dohrmann 2004).

The EAF dust originates from a German steel mill. During the production of steel in EAFs, a dust formation occurs, whereby about 15-25 kg of this dust accumulate per 1 t of steel (Guézennec et al. 2005). The process of steel production basically includes the five steps of furnace charging, melting, refining, slag foaming and casting. During those steps, which partly involve addition of coal powder and introduction of CO gas streams, a gaseous phase is being extracted at the top of the furnace. This gas stream is combusted, cooled and cleaned from dust. The dust contains mainly metal oxides (especially iron and zinc oxides), silicates, sulphates and coke and high mass fractions of lead and cadmium (Hagni et al. 1991; Sofilic et al. 2005). It is caught in bag filters and has to be stored in special landfills due to its hazardous properties (Guézennec et al. 2005).

2.1.7 Dross from Al-Sc alloy production

The dross investigated in this work originates from KBM Master Alloys in the Netherlands. According to Das et al. (2007) the formation of a waste product called dross is very common during melting processes for production of metallic Al and Al-alloys. Dross formation happens at the melt-air interface and is caused by oxidation of the metal. Normally, the dross is recovered and remolten and oxidation is minimized by addition of certain salts such as NaCl

and KCl. The main constituents of the remaining dross are therefore aluminum oxide, alloying elements, flux salts and metallic and nonmetallic impurities.

KBM produces various kinds of master alloys such as AlSc, which can further be used for alloying Sc into Al. The alloy produced contains 2% Sc with balance of Al. During production of this alloy, a dross is formed which is stockpiled and not used for other larger scale applications so far.

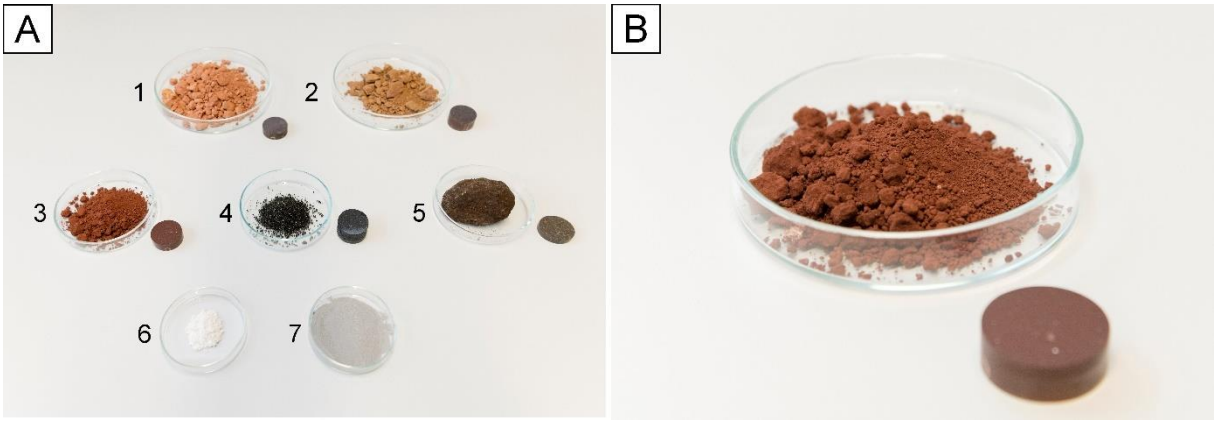

Figure 2 A) Selected primary and secondary raw materials in parts with their respective polished section together with two selected Scandium products: 1 — Bauxite ore, 2 — Laterite ore, 3 — Bauxite residue, 4 — Electric arc furnace slag from Nickel production, 5 — TiO_2 Filter cake, 6 — Scandium Oxide, 7 — Al-Sc Alloy Powder. B) A close-up of the Bauxite residue with a respective polished section.

2.1.8 Sample preparation

For major and trace element analyses all samples except PG samples were dried at 105°C. PG samples were dried at 40°C and all samples were ground in a vibratory disc mill for wet chemical and XRF analyses. The AS was filtered by pressure filtration beforehand to retrieve the solid bottom sediment. Samples for XRF measurements were pressed to powder pellets, whereas some samples were prepared with the addition of wax. Samples from the steel industry were not suited for powder pellet preparation so that XRF analyses were not performed. For wet chemical analyses the samples were digested with revers aqua regia (HNO_3/HCl =3/1) and total digestion ($HClO_4$, HF, HNO_3, complexation with H_3BO_3). To perform reflected light microscopy and electron microscopy, thick sections of original (unground) samples were prepared. The samples were embedded in epoxy-resin and polished to < 1µm surface roughness.

2.2 Methods

The materials that were examined for the Sc inventory were analyzed with different destructive and non-destructive analytical methods to determine their chemical and mineralogical composition. In some cases, the mineral composition of certain phases was analyzed to get further insights into the material characteristics.

Chemical analyses were carried out with three different approaches to obtain reliable and comparable data for the whole range of elements (major, minor and trace-elements). Therefore, the composition was obtained by XRF, ICP-OES, ICP-MS.

Determination of major elements (Al, Si, Fe, Mg, Na, Ca, K, Mn and in certain cases Sc for highly Sc containing samples) was performed by (XRF) executed with a wavelength-dispersive XRF-spectrometer (Panalytical type MagiX-pro). The ground samples were pressed to power pellets of approx. 0.5 cm height and 3 cm diameter. Some samples had to be prepared with the addition of wax. Depending on the investigated materials two different evaluation methods namely the Omnian approach developed by PANalytical and a combination of OMNIAN and a 6-point calibration using ORAES reference materials purchased from ORE Research & Exploration Pty Ltd were used for quantification. It should be noted here that the data are displayed in wt% oxides, even though some of the elements may not actually occur in oxidic form. Due to their sample characteristics the samples from the steel industry (EAF dust, BFS) could not be prepared as powder pellets and XRF analysis was not performed for these two samples.

ICP-OES and ICP-MS measurements were performed to determine concentrations of minor and trace elements. The ICP-OES measurements were performed from undiluted solutions with a Thermo Scientific iCAP 7400. For calibration solutions, highly pure single-element standards were used in reasonable concentrations to obtain a 5-point calibration curve. In case of exceedance of the calibration range, samples were diluted with an acidic solution. Samples and calibration solutions for ICP-OES measurements are spiked with 10 g/L $LiNO_3$ to even out matrix effects. Evaluation of results was performed using the Thermo Scientific software QTEGRA. ICP-MS measurements were performed with a Thermo Scientific iCAP Q starting with a 10-fold dilution of the sample. The Thermo Scientific iCAP Q was equipped with a prepFAST auto dilution system which automatically determines further necessary dilution steps up to 1:400 and independently dilutes the samples with an acidic solution. All elements were measured in kinetic energy discrimination mode (KED) with He as collision gas. 115In, 101Ru, 185Re are used as internal standards. Calibration solutions are made from highly pure single and multi-element standards and a 5-point calibration is used for the analyses. All reagents used within the process are in analytical grade.

Structural analysis and the determination of the general mineral assemblages was carried out with powder X-ray diffraction (PXRD) using a Bruker D8 Advance diffractometer with Bragg-Brentano geometry, a CuKα radiation source (X-ray tube with 40kV, 40mA) and an energy dispersive Lynxeye XE-T detector. XRD patterns were evaluated semi quantitatively with the software MATCH using the COD and PDF 2.0 (2003) databases.

Scanning electron microscopy (SEM) and electron microprobe analyses (EMPA) were carried out for some samples to investigate the mineral chemistry. EMPA measurements were

performed for certain BRs (see chapter 3.1) and AS from TiO_2 production. SEM analysis was used to investigate the general characteristics such as, particle size, habit and nature. Subsequently, EMPA was performed with a field-emission cathode JEOL JSM-6610LV (type 8500F) instrument equipped with five wavelength-dispersive and one energy-dispersive X-ray detector. Astimex and Smithonian standards used for quantitative measurements of iron-oxide and iron-hydroxide phases as well as rutile and aluminum-hydroxide were: hematite (Fe), chromite (Mg,Cr), plagioclase (Na, Si, Al, Ca), ilmenite (Ti), elementary scandium and elementary vanadium. For reliable determination of Sc concentrations and its detection limits, NIST glass standards 610 and 612 were used as reference materials. More information on the Sc determination with EMPA can be found in chapter 3.1 and appendix C A.

2.3 Results

2.3.1 Composition and mineral assemblage of investigated residues and wastes

The analyses of major and minor elements performed by XRF gave insights into the chemical composition of the different materials. XRD and SEM analyses provided further knowledge about the mineral assemblage and the material and particle characteristics. Figure 3 A shows the major element composition (element oxide mass fraction for oxides > 1wt%) of the nine BR samples. Figure 3 B presents the respective composition of the other materials except those from the steel industry. The detailed analyses can be found in the appendix B in Table B1. The X-ray diffractograms of the materials (except for BRs, see chapter 3.1.3.1) are presented in Figures 4 and 5.

The main constituents of BRs are Fe_2O_3 and Al_2O_3. Other constituents are SiO_2, CaO, TiO_2 and Na_2O in variable mass fractions that rarely exceed 10 wt%. In all BRs hematite and goethite are the dominant phases. Aluminum hydroxides (e.g., boehmite, diaspore and gibbsite) are major constituents of the BRs together with desilication products and other phases that form during Bayer processing (e.g., katoite and cancrinite). Russian bauxite residue also contains high amounts of the chlorite group mineral chamosite. Furthermore, titanium dioxides (rutile and anatase) were detected in some of the BRs. The SEM micrograph of a polished section of BR (Fig. 6 A) illustrates that larger mineral particles like hematite and goethite are agglomerated with a fine-grained matrix material. A more detailed mineralogical and chemical investigation of the different BRs is given in chapter **Fehler! Verweisquelle konnte nicht gefunden werden.**. In Figure 11 and Table 6 in chapter 3.1.3.1, the results of XRD measurements and the mineralogical assemblage of BR samples are presented.

The solid AS from TiO_2 production consists of TiO_2, SiO_2, sulfur and carbon. The FC, which results from lime addition to the liquid acid waste, mainly contains Fe_2O_3 and TiO_2 and significant mass fractions of Cl. The crystalline phases detected by XRD in the AS are rutile, cristobalite and quartz (Fig. 4 A). Furthermore, the broad flat signal between ~23-27° 2Θ can

be attributed to amorphous carbon (Manoj and Kunjomana 2012) whereas the small sharp signal at 26.6° 2Θ indicates the existence of crystalline graphite. Investigations by SEM show the existence of large, rounded particles of cristobalite next to numerous smaller rutile grains (Fig. 6 B). In the polished section, some of the rutile particles look highly porous but SEM investigations on AS powder revealed that these porous particles are in fact agglomerates of much smaller rutile particles (Fig. 6 C). EMPA measurements on both rutile agglomerates and larger rutile grains revealed that the Sc mass fraction of those grains is below the limit of detection. The main phases that were detected by XRD in FC samples were rutile, cristobalite, calcite and Fe-oxychloride (Fig. 4 A). The diffractogram also showed the broad carbon signal between ~23-27° 2Θ.

In addition to these crystalline phases, a high mass fraction of FC consists of amorphous precipitation products. These can therefore not be detected by XRD but are visible in the SEM micrograph in Figure 6 D.

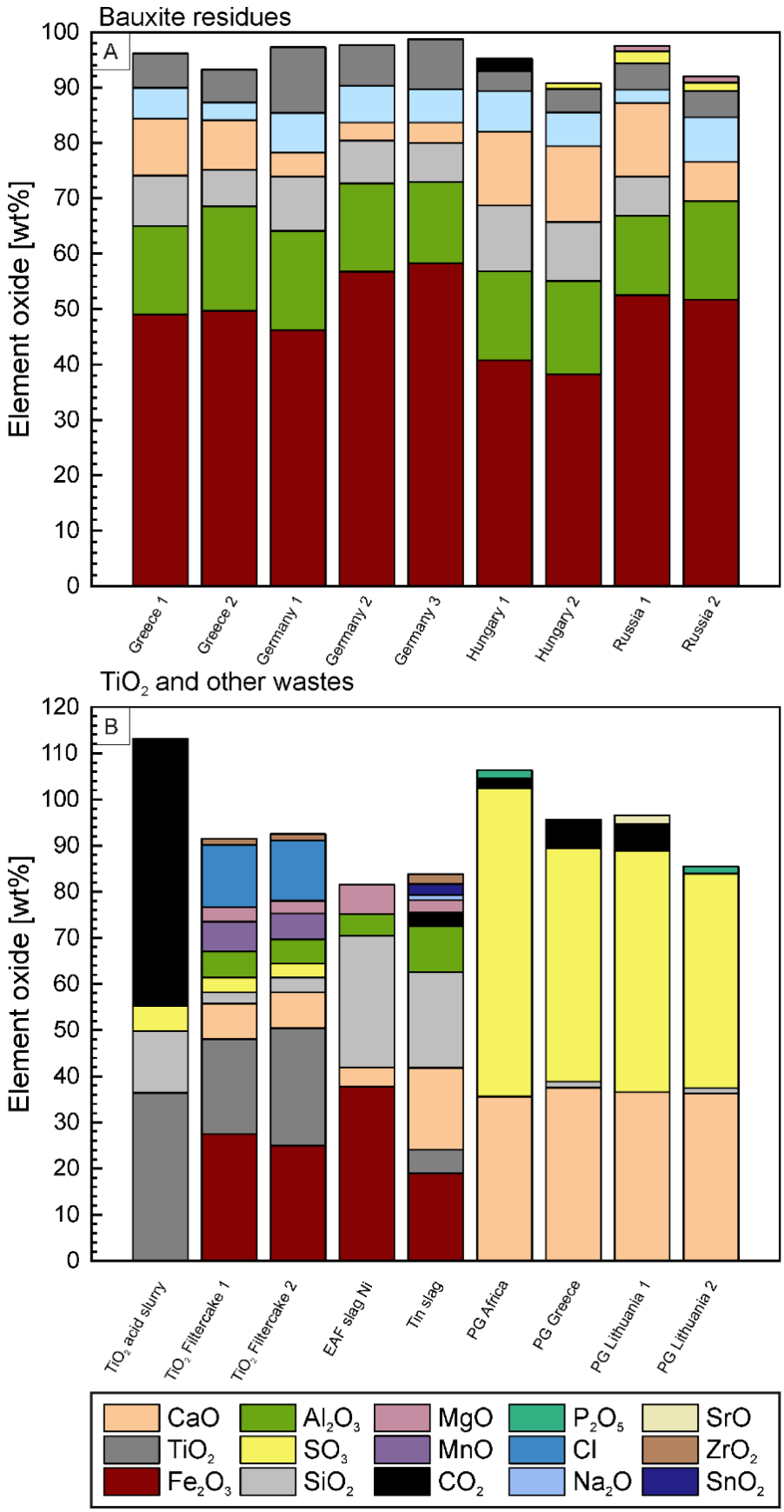

Figure 3 Major element oxide mass fractions as determined by X-ray fluorescence for (A) bauxite residue samples and (B) samples from TiO_2-, Ni-, Sn- and phosphoric acid production (EAF=Electric arc furnace, PG=Phosphogypsum)

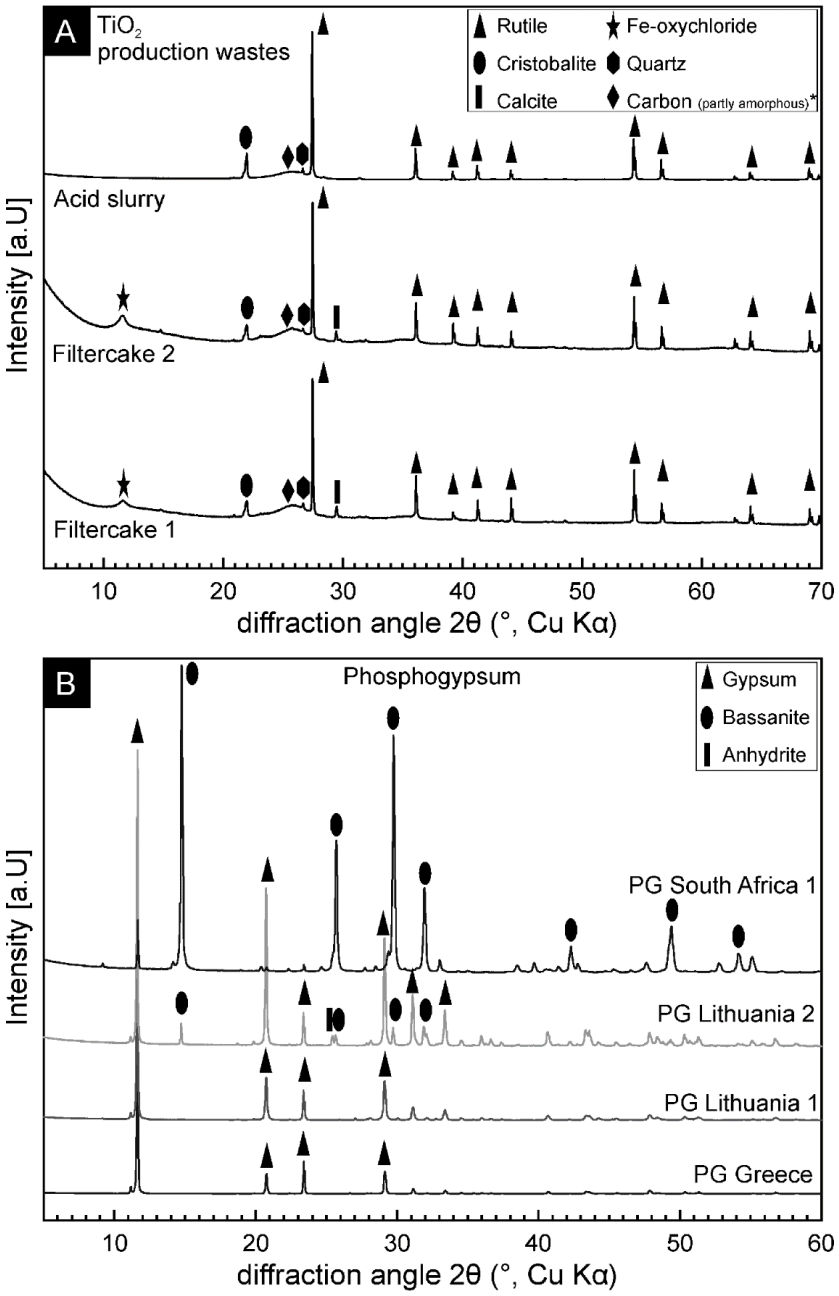

*Figure 4 (A) X-ray diffractograms of wastes and residues from TiO_2 production and (B) of Phosphogypsum (PG) samples. The main peaks are marked according to the assigned phase. *Amorphous carbon exhibits a broad signal between 23-27°2Θ (Manoj and Kunjomana 2012).*

PG samples contain high mass fractions of sulfur and CaO and small mass fractions of carbon, phosphor and SiO_2. The major crystalline phases in PG are gypsum and/or bassanite sometimes associated with small amounts of anhydrite (Fig. 4 B). All these phases are essentially calcium sulfate which can occur in the anhydrous or hydrous form with half a water (bassanite) or one water (gypsum) per $CaSO_4$.

The samples of steel industry wastes were not analyzed by XRF within the scope of the SCALE project (see chapter 2.2) but information on the major element composition was available through research activities within the research group at BAM.

According to Hamann et al. (2019), EAF dust contains high mass fractions of iron and zinc (each ~1/4 of the total mass) as well as smaller mass fractions (< 5%) of Ca, Cl, Pb, Si, C and Mg. Minor constituents are Na, K, P, Mn, Al and Cu.

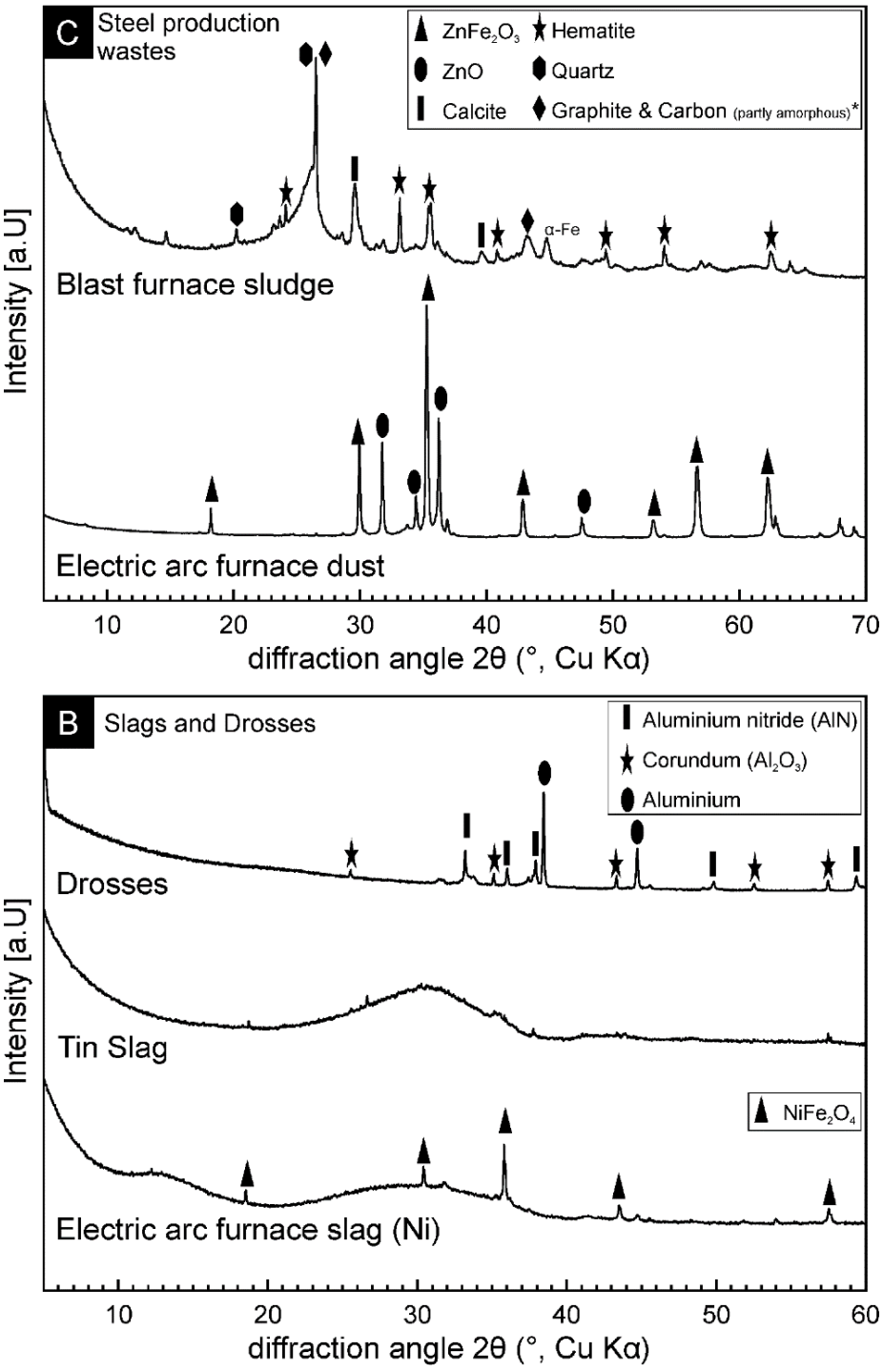

*Figure 5 X-ray diffractograms of wastes and residues from (A) steel production and (B) from Ni-, Sn and Aluminum-Scandium alloy production. The main peaks are marked according to the assigned phase. The tin slag was found to be completely amorphous since the diffractogram does not exhibit any distinct peaks. The electric arc furnace slag from Ni production is also mostly amorphous but contains one crystalline phase that could be identified. *Amorphous carbon exhibits a broad signal between 23-27°2Θ (Manoj and Kunjomana 2012).*

The BFS contains high mass fractions of C and Fe and smaller mass fractions of Ca, Mg, Zn, Pb and other minor constituents (Hamann et al. 2019). The main phases that could be identified in EAF dust are $ZnFe_2O_3$ and ZnO (Fig. 5 A). In BFS carbon and graphite could be identified together with hematite, calcite, quartz and α-iron (Fig. 5 A).

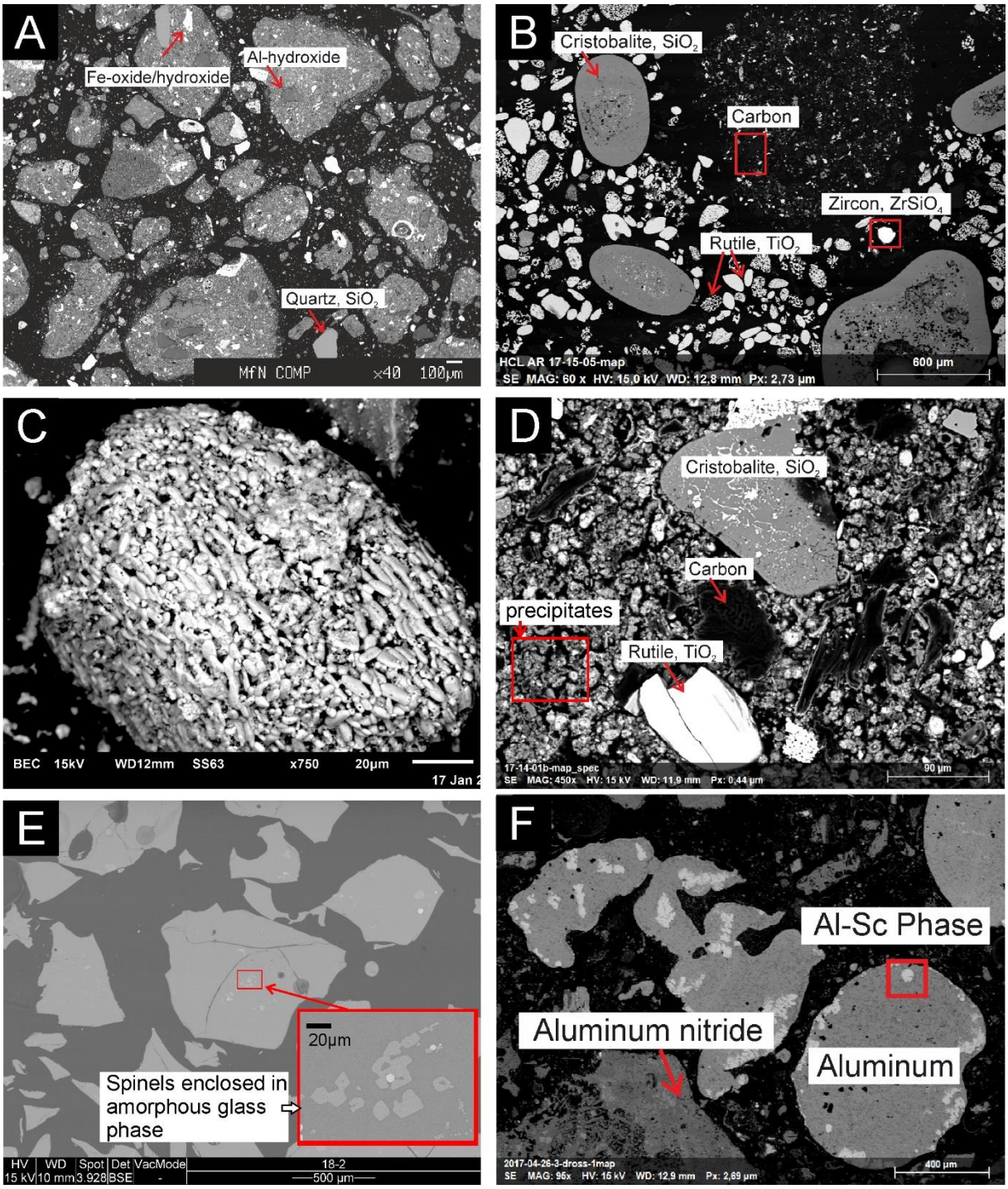

Figure 6 Scanning electron microscopy images of (A) bauxite residue, (B) acid slurry, (C) a rutile particle in acid slurry, (D) filter cake, (E) electric arc furnace slag from Ni production and (F) dross.

The main constituents of slags (Ni production and Sn) are Fe_2O_3 and SiO_2 (Fig.3 B). The Ni production slag additionally contains Al_2O_3, CaO and MgO in mass fractions <10 wt%. Tin slag also contains significant mass fractions of CaO. XRD analyses revealed that both slags are mostly amorphous, which is in accordance with the glassy occurrence of the slags. The SEM investigation on EAF slag from Ni production (Fig. 6 E) showed that two different spinel phases, one containing Ni and Fe (trevorite) and one containing mainly Cr, Fe and small mass fractions of Mg and Al (Mg-Al bearing chromite), are embedded in the amorphous silicon rich glass phase (Fig. 6 E).

The sample of dross resulting from Al-Sc alloy production mainly contains aluminum and approximately 5% Sc_2O_3 were detected by XRF analyses. It should however be noted that, according to the alloy producer, the dross is a material that can be inhomogeneous due to the process of its accumulation. Therefore, other dross charges could have deviating contents of Sc_2O_3. The phases detected by XRD (Fig. 5 B) were aluminum, corundum (Al_2O_3) and aluminum nitride (AlN). In Figure 6 F, the SEM image illustrates the particle characteristics of the dross and shows that large metallic aluminum particles generally enclose an Al-Sc phase. These larger metallic particles coexist with the aluminum nitride.

2.3.2 Concentration of Sc and other REE

The Sc and REE mass fractions were determined by ICP-MS and for Sc, the results for the different materials are illustrated in Figure 7. Table 3 contains the information on the other REE. A list of the average (avg.) proportion of Sc in comparison to the other measured REE and the avg. and minimum proportion of monetary value represented by the respective mass fraction of Sc (Fig. 8 &9) can be found in the appendix in Table B2. The comparison of Sc and REE mass fractions showed, that there are significant differences between the investigated materials. The highest mass fraction by far was found in the sample of Al-Sc alloy dross, which contains > 6000 mg/kg Sc. Since this material is a residue of Al-Sc alloy production it naturally contains much higher mass fractions of Sc than the other investigated materials. Furthermore, it does not contain significant amounts of other REE and >99% of the monetary value of REE is therefore represented by Sc. All the other materials contain < 400 mg/kg Sc (Fig.7). PG samples as well as the BFS exhibit the lowest mass fractions of Sc. With < 20 mg/kg they are depleted in Sc in comparison to the Earth's crust (Rudnick and Gao 2014). While African and Lithuanian PG samples are rich in some of the light rare earth elements (LREE) such as La, Ce, Pr, Nd and Sm, the Greek sample is generally low in REE (Tab. 3). The BFS furthermore exhibits the lowest mass fraction of total REE (Tab. B2).

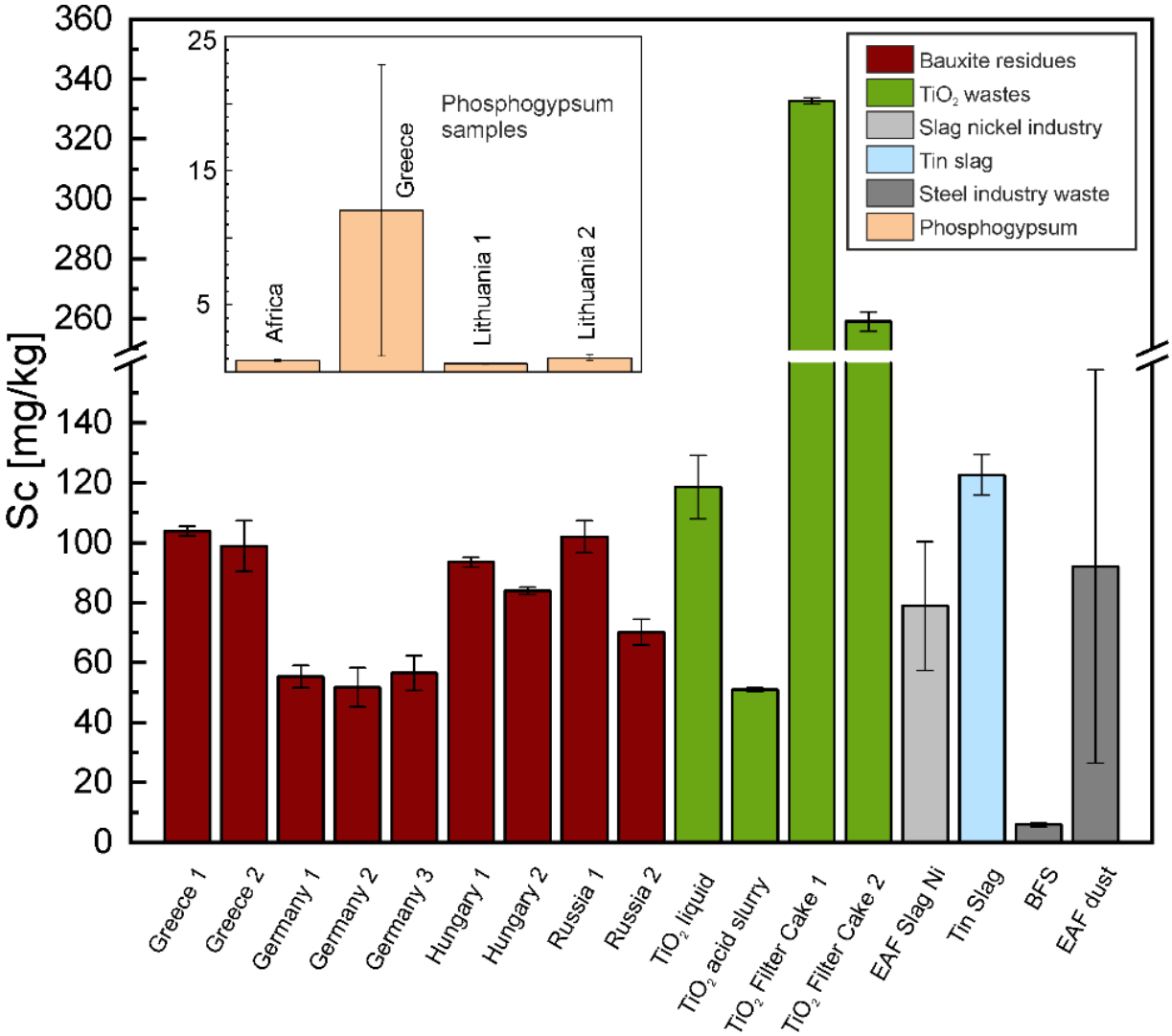

Figure 7 Sc mass fractions of the investigated wastes and residues. Note that Al-Sc alloy dross was excluded due to its very high Sc mass fractions (> 6000 mg/kg) compared to the rest of the materials. Phosphogypsum samples are shown in the separate diagram inserted on the upper left. Electric arc furnace (EAF) residues from Ni and steel production exhibit high uncertainties, due to strong variations between single measurements within one triplet determination. (BFS=Blast furnace sludge)

Table 3 Mass fractions of rare earth elements (REE) determined by ICP-MS for the investigated wastes and residues.

REE in mg/kg	Bauxite residue Greece 1	Bauxite residue Greece 2	Bauxite residue Germany 1	Bauxite residue Germany 2	Bauxite residue Germany 3	Bauxite residue Hungary 1	Bauxite residue Hungary 2	Bauxite residue Russia 1	Bauxite residue Russia 2	TiO_2 liquid	TiO_2 solid
Y	76 ± 1.2	71 ± 5.2	64 ± 9.6	48 ± 1.6	47 ± 1.2	111 ± 1.2	97 ± 1.6	359 ± 6.1	124 ± 3.8	52 ± 6.5	24 ± 0.2
La	83 ± 3.6	99 ± 8.8	94 ± 0.7	88 ± 0.7	97 ± 3.7	211 ± 3.3	164 ± 1.3	252 ± 3.2	212 ± 5	102 ± 9.4	51 ± 1
Ce	361 ± 6.5	420 ± 20.7	187 ± 1.3	159 ± 1.1	188 ± 8.5	433 ± 10.1	415 ± 2.5	409 ± 5.2	471 ± 14	245 ± 23.1	103 ± 1.9
Pr	20 ± 0.9	22 ± 1.2	16 ± 0.1	14 ± 0.1	17 ± 0.1	40 ± 0.6	35 ± 0.3	54 ± 0.9	52 ± 1.2	28 ± 2.7	12 ± 0.1
Nd	74 ± 3	82 ± 3.8	55 ± 0.7	48 ± 0.3	67 ± 2.7	144 ± 2.2	132 ± 0.9	214 ± 3.3	192 ± 5.5	100 ± 9.1	43 ± 0.5
Sm	15 ± 0.3	16 ± 0.7	10 ± 0.1	9 ± 0.1	10 ± 0.1	26 ± 0.4	25 ± 0.2	42 ± 0.7	36 ± 0.9	16 ± 1.6	8 ± 0.1
Eu	3 ± 0.1	4 ± 0.2	2 ± 0.1	2 ± 0.04	2 ± 0.02	6 ± 0.1	6 ± 0.01	11 ± 0.2	7 ± 0.2	2 ± 0.2	2 ± 0.01
Gd	15 ± 0.1	15 ± 0.7	10 ± 0.2	9 ± 0.1	10 ± 0.1	23 ± 0.4	22 ± 0.2	45 ± 0.8	32 ± 1	13 ± 1.2	7 ± 0.1
Tb	3 ± 0.03	3 ± 0.1	2 ± 0.1	2 ± 0.03	1 ± 0.02	4 ± 0.04	4 ± 0.03	7 ± 0.2	5 ± 0.1	2 ± 0.2	3 ± 0.01
Dy	16 ± 0.1	16 ± 0.7	11 ± 0.5	9 ± 0.3	9 ± 0.2	20 ± 0.4	19 ± 0.2	41 ± 0.6	26 ± 0.7	11 ± 1	5 ± 0.04
Ho	3 ± 0.02	4 ± 0.1	3 ± 0.1	2 ± 0.1	2 ± 0.04	4 ± 0.04	4 ± 0.04	10 ± 0.1	6 ± 0.1	2 ± 0.2	3 ± 0.01
Er	10 ± 0.1	10 ± 0.3	7 ± 0.5	6 ± 0.1	6 ± 0.1	12 ± 0.1	11 ± 0.1	27 ± 0.5	15 ± 0.4	6 ± 0.6	3 ± 0.05
Tm	2 ± 0.01	2 ± 0.1	2 ± 0.1	2 ± 0.03	1 ± 0.02	2 ± 0.02	2 ± 0.03	5 ± 0.1	3 ± 0.1	1 ± 0.1	2 ± 0.01
Yb	12 ± 0.1	11 ± 0.5	8 ± 0.3	6 ± 0.2	6 ± 0.1	11 ± 0.2	11 ± 0.1	25 ± 0.7	15 ± 0.2	7 ± 0.8	3 ± 0.01
Lu	2 ± 0.01	2 ± 0.1	2 ± 0.1	2 ± 0.02	1 ± 0.02	2 ± 0.02	2 ± 0.03	4 ± 0.1	3 ± 0.1	1 ± 0.1	2 ± 0.01

REE in mg/kg	TiO_2 Filter-cake 1	TiO_2 Filter-cake 2	Electric arc furnace slag	Tin slag	PG Africa	PG Greece	PG Lithuania 1	PG Lithuania 2	Blast furnace sludge	Electric arc furnace dust	Al-Sc Alloy dross
Y	143 ± 2	151 ± 2.7	9 ± 0.2	1051 ± 81.3	61 ± 1.3	75 ± 1.1	69 ± 0.7	105 ± 2	14 ± 1.6	0.2 ± 0.1	4 ± 1.9
La	316 ± 3	251 ± 4.7	8 ± 0.2	1636 ± 147.6	410 ± 12.1	43 ± 0.6	1120 ± 47.9	686 ± 14.7	17 ± 3.6	6 ± 0.6	0.4 ± 0
Ce	755 ± 6.6	588 ± 10.4	17 ± 0.7	3576 ± 315.4	1060 ± 18.3	39 ± 0.7	1636 ± 70.2	1433 ± 33.2	32 ± 6.9	9 ± 0.5	0 ± 0.1
Pr	86 ± 0.8	67 ± 1.3	2 ± 0.04	397 ± 32.1	140 ± 4.3	9 ± 0.2	155 ± 6.7	179 ± 3.6	4 ± 0.6	1 ± 0.3	0.1 ± 0.005
Nd	312 ± 2.7	249 ± 4.2	7 ± 0.2	1431 ± 113.2	611 ± 8.9	32 ± 1.2	527 ± 23.3	757 ± 17.4	b.d.	b.d.	0.3 ± 0.03
Sm	53 ± 0.5	45 ± 0.7	1 ± 0	245 ± 16.8	105 ± 2.5	7 ± 0.2	61 ± 0.5	126 ± 7.8	3 ± 0.4	0.5 ± 0.1	0.1 ± 0.01
Eu	6 ± 0.1	5 ± 0.1	0 ± 0.01	8 ± 0.5	22 ± 0.3	2 ± 0.1	17 ± 0.2	25 ± 0.4	1 ± 0.1	1 ± 0.2	0.1 ± 0.005
Gd	40 ± 0.4	38 ± 0.5	2 ± 0.1	226 ± 13.4	72 ± 1.3	9 ± 0.3	49 ± 0.6	89 ± 1.7	3 ± 0.4	1 ± 0.2	0.1 ± 0.01
Tb	6 ± 0.05	5 ± 0.1	1 ± 0.03	36 ± 1.9	7 ± 0.1	2 ± 0.1	5 ± 0.03	8 ± 0.1	1 ± 0.03	1 ± 0.3	0.1 ± 0.001
Dy	32 ± 0.3	32 ± 0.4	1 ± 0.1	234 ± 9.6	24 ± 0.7	8 ± 0.2	21 ± 0.2	32 ± 0.4	3 ± 0.3	0.3 ± 0.1	0.2 ± 0.02
Ho	6 ± 0.1	6 ± 0.1	1 ± 0.03	49 ± 2	3 ± 0.05	2 ± 0.1	3 ± 0.03	4 ± 0.1	1 ± 0.05	1 ± 0.3	0.2 ± 0.01
Er	19 ± 0.2	20 ± 0.2	1 ± 0.02	149 ± 5.2	5 ± 0.1	6 ± 0.2	6 ± 0.03	8 ± 0.1	2 ± 0.2	1 ± 0.4	0.2 ± 0.02
Tm	3 ± 0.03	3 ± 0.04	1 ± 0.04	24 ± 0.7	0.5 ± 0.01	2 ± 0.1	0 ± 0.01	1 ± 0.01	1 ± 0.02	1 ± 0.5	0.1 ± 0.004
Yb	23 ± 0.2	24 ± 0.3	1 ± 0.02	159 ± 3.7	2 ± 0	4 ± 0.1	2 ± 0.003	3 ± 0.03	2 ± 0.2	1 ± 0.4	0.2 ± 0.02
Lu	4 ± 0.04	4 ± 0.04	1 ± 0.04	23 ± 0.4	0.3 ± 0.01	1 ± 0.04	0.2 ± 0.004	0.3 ± 0.003	1 ± 0.02	1 ± 0.3	0.3 ± 0.05

The mass fraction of Sc in BRs ranges from 52-104 mg/kg which corresponds to only 6-13% of the total REE mass fraction (Fig. 8). However, due to the high price of Sc_2O_3 (Fig. 9 B) in comparison to the other rare earth oxides (REO), the avg. share of monetary value represented by Sc (Fig. 9 A) is significantly higher and ranges on avg. between 74% and 89%. According to this data, one metric ton of BR that contains at least 80 mg/kg Sc_2O_3, has a value of ca. 72 € worth in Sc_2O_3 (80 mg/kg x 0.906323 €/g)

The TiO_2 production wastes contain on avg. between 51-333 mg/kg Sc, whereas FC exhibits the highest values. Other REE such as Y, La, Ce and Nd also occur in elevated mass fractions and hence the avg. share of Sc lies between 15-17%. However, > 85% of the monetary value is represented by Sc. Both tin slag and EAF slag from Ni production are enriched in Sc with 123 mg/kg and 79 mg/kg Sc respectively. The EAF slag exhibits a very high uncertainty caused by large variations between the single samples within one triplet determination. Nevertheless at least 56% of monetary value is represented by Sc since other valuable REE are scarce within the material. In contrast, tin slag is also rich in many other REE, including highly valuable ones such as Nd and Dy. Therefore, on avg. only 38% of monetary value is represented by Sc. Similarly, to EAF slag, EAF dust from steel production yielded strongly variable results for Sc mass fractions when comparing the three-single measurements. However since other REE are scarce within the material, Sc is likely to represent the largest proportion of monetary value amongst all REE within EAF dust.

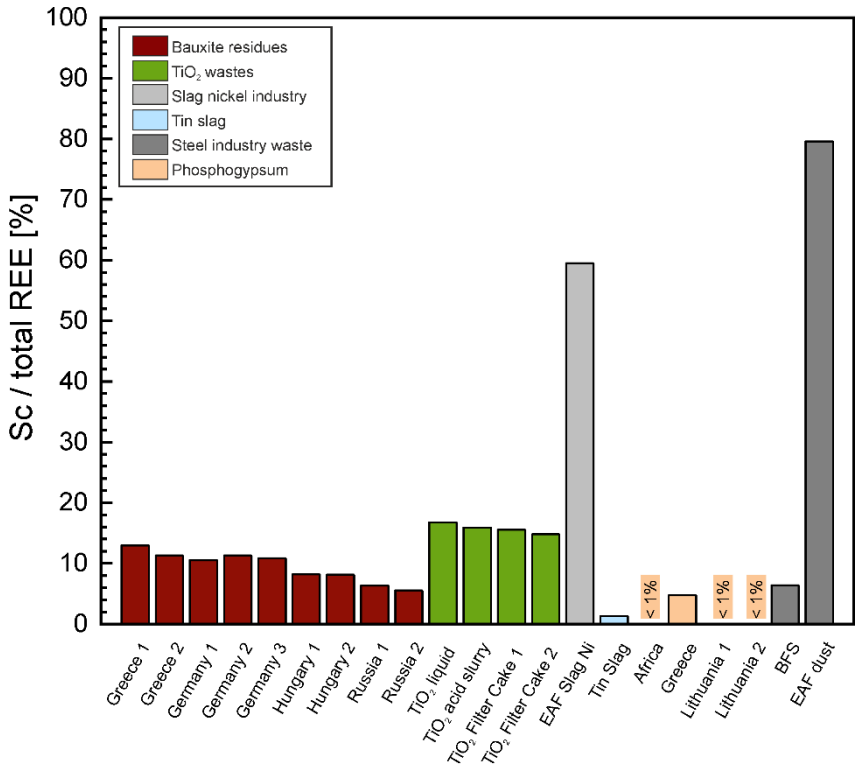

Figure 8 The average share of Sc of the total REE mass fraction. Note that dross was excluded since > 99% of the average REE share is represented by Sc.

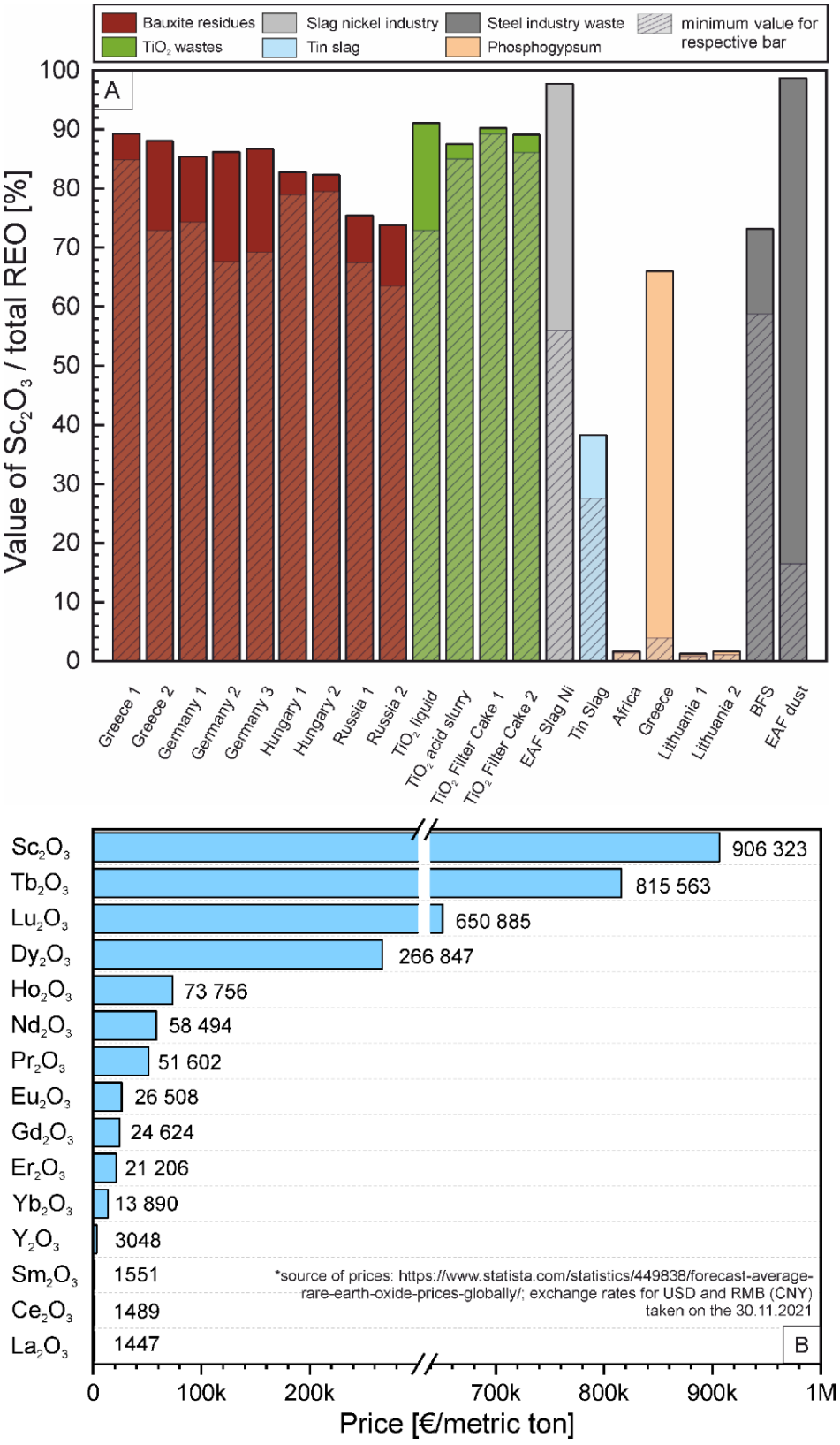

Figure 9 (A) Average monetary value of Sc of the total monetary value of all rare earth oxides (REO) for the investigated residues. Al-Sc alloy dross was excluded as the monetary value of REO is solely represented by Scandium. (B) Prices of REO as of November 2021. Prices were calculated in € per metric ton from original prices in US dollars (USD) or Renminbi (RMB or CNY). (EAF=Electric arc funace, BFS=Blast furnace sludge)

According to the measurements, most of the investigated residues contain significant mass fractions of Sc, which represent a high monetary value. Only the PG and BFS samples investigated in this work exhibit Sc mass fractions that lie even below the crustal abundance of Sc. Hence, they do not represent possible secondary sources for Sc. PG samples however have shown to contain significant mass fractions of other valuable elements and might therefore be interesting for the recovery of e.g., LREE.

Based on these observations it can be concluded that the investigated BRs, TiO_2 production wastes, tin slag, EAF slag and EAF dust can be considered as candidates for secondary Sc resources. Whether Sc recovery would take the primary role during reutilization of these residues or would rather be an additional step within the process (e.g., to increase economic viability of a reutilization scheme) goes beyond the scope of this work. The following chapter 2.3.3 will present a calculation of possible resources of Sc inherited in the investigated European residues, that were identified as possible candidates.

2.3.3 A Sc inventory of metallurgical by-products

To calculate the potential mass of Sc that is currently stored and/or accumulated each year in metallurgical residues in Europe, data on annual production and storage quantities were collected from the industrial partners (Tab. 4). In some cases, the data was inferred from the literature. For BR, AS, FC, EAF slag and dross the data was provided by the partners within and beyond the SCALE consortium.

Data on EAF dust accumulation was deduced from information provided by the World Steel association (2020) and Machado et al. (2006). With ~523 Mio t of steel produced in Europe in 2019 in electric arc furnaces and an average accumulation of 12-14 kg of EAF dust per ton of steel, the annual accumulation of EAF dust amounts to 6.28-7.32 Mio t. According to Antrekowitsch and Rösler (2015) and von Billerbeck et al. (2014), certain amounts (ca. 50%) of EAF dusts are recycled in the so called Waelz Process. However, a certain part is still landfilled. For an approximate calculation it is hence assumed that, for a time period of 10 years, 20% of EAF dust is not recycled but stored.

Comprehensive data on the material flows of Sn production are rare and furthermore the production and refining of Sn in Europe is very low (Raw Materials Information System 2021a). Therefore, an approximation for the Sc resources in tin slags can only be made for the whole world. It is hence assumed here that ~2 Mio t of tin slag are currently landfilled worldwide (Olukotun et al. 2021) but only small quantities are expected to exist in Europe.

The information on annual residue accumulation and storage quantities, as well as the Sc mass fractions determined for the residues, were used to calculate the European Sc inventory. The Sc that accumulates with the residue each year as well as the mass that is currently stored or landfilled was determined and the results are listed in Table 4. It should be noted that these quantities represent the theoretical resource inherited in the material.

Table 4 The Sc inventory of metallurgical residues investigated in this thesis: annual accumulation of residues, quantities in storage facilities and resulting theoretical quantities of Sc based on the average Sc mass fraction that was determined for the respective residues.

Material	Company or Location	annual accumulation [t/a]	amount on storage facilities [t]	avg. Sc content [g/t]	Sc accu-mulating [t/a]	resource of Sc in storage facilities [t]
BR Hungary	MAL Hungarian Aluminium,	prod. stopped in 2014	19 Mio	90	none	1710
BR Germany	Aluminium Oxid Stade	850.000	~ 17 Mio[1]	55	46.75	935
BR Greece	MYTILINEOS	750.000[2]	4.5 Mio	100	75	450
BR Russia 1	Rusal	unknown	~ 60 Mio	100	unknown	6000
BR Russia 2	Rusal	unknown	~ 60 Mio	70	unknown	4620
Acid slurry	Tronox, Rotterdam	120.000	not stored in larger amounts	120	14.4	none
Filter cake	Tronox, Rotterdam	50.000	300[3]	300	15	0.09
EAF slag (Ni-Prod.)	GMM SA LARCO, Greece	1.900.000[4]	unknown	ca. 60	92.4	unknown
Tin slag	Worldwide	unknown	~ 2 Mio	ca. 120	unknown	240
EAF dust	Europe	~7 Mio	~14 Mio[5]	ca. 90	597.6	1260
Dross	KBM	1	3	ca. 6500[5]	0.0065	0.0195

[1]estimation from personal communication, [2]100.000 t/a are reused in other processes, [3]the major amount is landfilled offsite by a third-party landfill owner, [4]360.000t/a reused for other processes, [5]the Sc content of the dross is difficult to average since it is prone to continuous changes, here we have assumed an average of 1% Sc_2O_3, [5]accumulated mass based on the assumption that, for 10 years, 20% of EAF dust is not reutilized in other processes

The inventory illustrated in Table 4 shows that the amounts of BR currently stored in Europe (i.e., Greece, Germany and Hungary) contain high quantities of Sc and represent a very large resource bearing in mind the current low annual supply and consumption of Sc (< 30t/a). The high quantities of steel produced in Europe via the electric furnace route result in high quantities of EAF dust accruing with it. Even though a significant fraction of EAF dust is reutilized in other processes, the remaining quantities theoretically still represent a large Sc resource (>1000 t). The annual accumulation of Sc inherited in TiO_2 residues also represents a significant possible resource. However, since most of the solid material (i.e., the FC) was landfilled and is not stored for possible reutilization this Sc resource presented here is rather

inaccessible. It is nevertheless important to stress that the recovery of Sc from TiO_2 wastes generally happens from the liquid acidic waste stream, where the Sc is largely present in solution. Together with the acid slurry the metal chlorides precipitated from this solution essentially form the FC. The quantities of Sc evident in the liquid acid waste are therefore directly connected to the quantities that were determined for FC. The TiO_2 production wastes hence represent an important Sc resource in Europe. Finally, both the slag from Sn and Ni production have shown to be potentially interesting Sc resources. However, Sn production and refining largely takes place outside Europe so that Tin slag accumulation inside Europe will be at a low level (Raw Materials Information System 2021a).

2.3.4 A worldwide view on Sc activities

The increasing interest in Sc has sparked the development of new projects, research activities and recovery technologies in the past decades (comp. chapter 1). However, a comprehensive updated overview of global activities is lacking, which is why the information collected in the scope of the SCALE project and this thesis were summarized in form of a world map. The map is a compilation of the available information (as of July 2021) showing the localities currently involved in Sc mining, exploration and recovery (Fig. 10) and should serve to provide an overview of the current status of global Sc activities. Additionally, formerly important Sc sources and the locations involved in the SCALE project activities are listed as well. Each point in Figure 10 is supported by additional information about the operating company (if applicable), classification, avg. Sc grade (if available) and a reference. This information can be found in the appendix in Table B3. The Figure illustrates the diversity of Sc projects all over the world including recovery activities from TiO_2 wastes concentrated in China as well potential primary production routes from sedimentary rocks in Australia and igneous rocks in Canada.

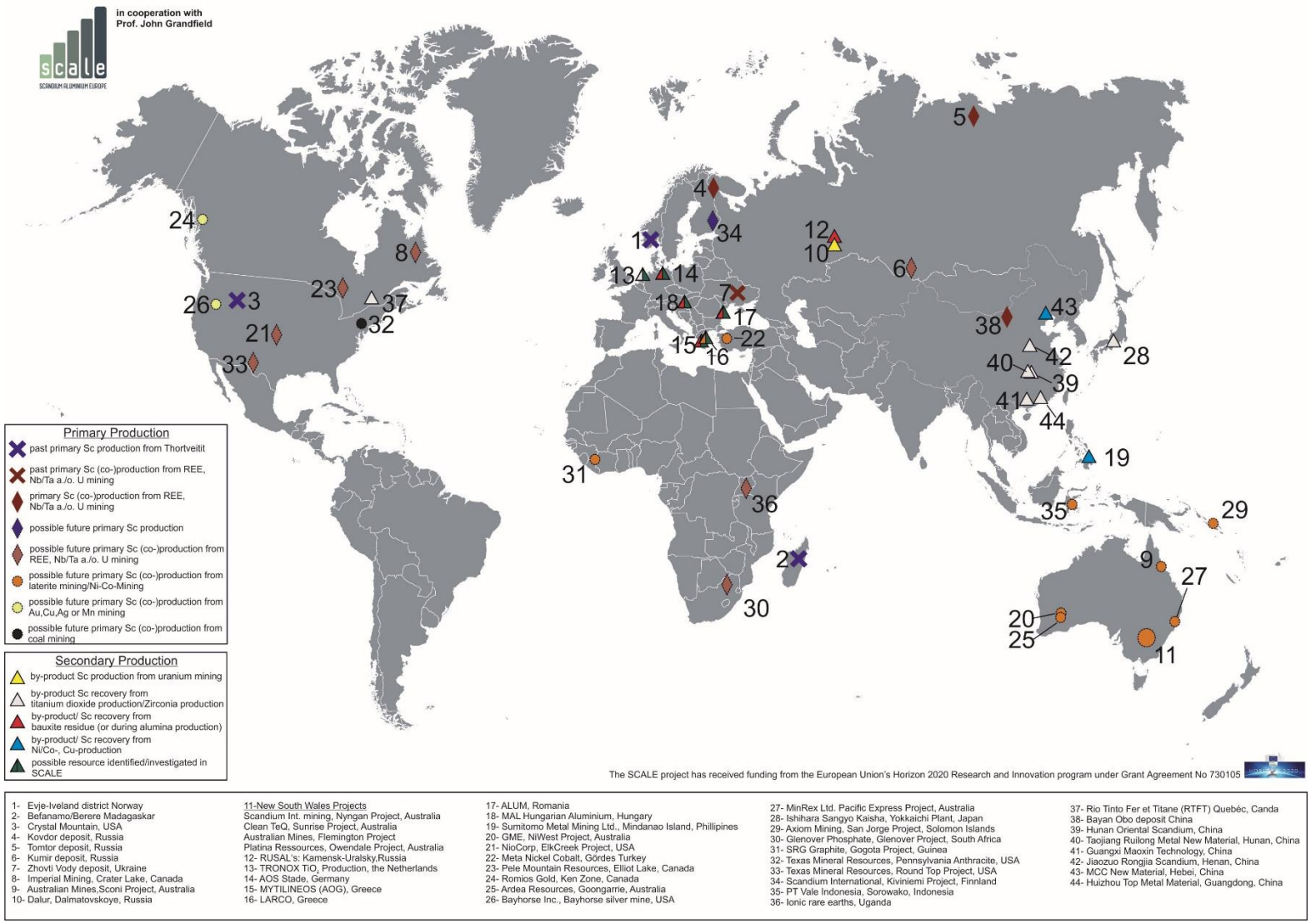

Figure 10 World map illustrating the important localities involved in Sc mining, exploration, recovery and production activities.

2.4 Discussion, conclusion and outlook

BRs, TiO_2 production wastes, Sn/Ni slags, EAF dusts and Al-Sc alloy dross are materials of very different origin as they accumulate during diverse paths of ore processing, refining or compound production. Even though these materials have significantly different chemical compositions, mineral assemblages and material characteristics (comp. chapter 2.3.1) they all have shown to be enriched in Sc. Apart from the dross, which is naturally high in Sc as it forms during Al-Sc alloy making, the FCs from TiO_2-production have the highest Sc mass fractions (>250 mg/kg). The other wastes from TiO_2 production i.e., AS (~50 mg/kg) and acidic liquid (~120 mg/kg) are also enriched in Sc. The BRs investigated in this work range from ~50-100 mg/kg Sc. This is similar to the EAF slag from Ni-production (ca. 80 ± 20 mg/kg) and EAF dust from steel production (92 mg/kg) which however showed a very high uncertainty. The investigated tin slag exhibited slightly higher mass fractions (>100 mg/kg). It can be concluded that all these materials are significantly enriched in Sc compared to natural rocks and could hence be considered as a Sc resource. As the price of Sc is currently high, a high theoretical monetary value is represented by the Sc content within the different materials. However, the complexity and diverse nature of these materials makes it necessary to develop different Sc recovery processes, adapted to the specific residues and wastes and/or integrated into existing processing schemes.

For TiO_2 production wastes these schemes are already developed and applied in several white pigment production facilities in China which currently supply the majority of Sc traded worldwide (comp. chapter 1.3). Therefore, the TiO_2 production route, which proved to concentrate Sc within both liquid and solid waste streams, has a high potential to also become a future supplier of Sc within Europe. Since part of the Sc inherited in the material flow is present in solution, the recovery does not necessarily include the handling of solid waste, which can be highly advantageous. This however also implies that the solid wastes investigated in this work are unlikely to be become secondary resources. In fact, the EIT-KIC project ScaVanger is working on the establishment of a European Sc supply chain from liquid TiO_2 production wastes (from the chloride route) and anticipates producing high purity Sc_2O_3 and ScF_3 by 2026 (Yagmurlu et al. 2021).

BRs are strongly investigated, and many different reuse possibilities are currently researched. The recovery of Sc represents one possible reuse of BR and could add value to the reutilization process due to the high monetary value represented by the Sc. However, BR is a complex material also rich in other valuable metals such as Fe, Ti and Al. Hence recovery schemes will likely be developed to recover not only trace elemental amounts but also some of these major elements before or subsequently to Sc extraction. Several different Sc recovery schemes by leaching and solvent extraction are currently under development and pilot plant operations are run in Russia and Greece (Balomenos et al. 2021; Petrakova et al. 2015). The

production of Sc compounds from European i.e., Greek BR is therefore likely to be established in the upcoming years if the overall BR reutilization process proves to be feasible and economically viable. Apart from the Greek alumina plant (MYTILINEOS) there are currently no other localities in the EU where Sc recovery from BR is investigated in pilot plant scale.

The slags from Ni- and Sn production, even though enriched in Sc, are currently not investigated in Europe for their Sc-recovery potential. Both Ni and Sn are mostly produced outside Europe (Raw Materials Information System 2021a, 2021b) and hence accumulation of processing residues is rather small. Furthermore, the specific characteristics of slags often make them interesting for applications in cement industry and as replacements for natural fine aggregates (Olukotun et al. 2021). Additionally, tin slag is used for extraction of Nb and Ta (Odo et al. 2014).

The EAF dust accumulating during EAF steel production is a residue which is in parts already reutilized in the Waelz process (Antrekowitsch and Rösler 2015). However, a significant amount of the EAF dust accumulating in European steelworks is still not reused. To the best of our knowledge, there are no in-depth investigations currently undertaken with regard to Sc recovery from those materials but they are investigated in terms of Zn recovery (Hamann et al. 2019). It would be interesting to look at the path of Sc during Zn recovery and evaluate the possibility of Sc co-recovery processes in the future.

It can be concluded that liquid acidic TiO_2 production waste as well as Greek BR have a high potential to become important secondary resources for a European Sc supply chain. Pilot plant operations and further in-depth research is ongoing for both of these cases and the demand for sustainably sourced Sc exists due to an increasing interest in SOFC production within Europe (Yagmurlu et al. 2021). Worldwide there are several localities, mainly in China, Russia and Canada, where Sc is produced or soon to be produced as a byproduct of TiO_2 and Al_2O_3 industry. TiO_2 production waste and BR will hence also be in the focus of European Sc production.

For future operations, it is therefore of high importance to not only identify Sc enriched materials, but also understand enrichment processes that result in the formation of potential Sc resources. For BR, the mineralogy of the residue is strongly connected to the mineralogy of the primary bauxite and its geochemical evolution. Finding geochemical links between the primary ore and the BR that enhance our understanding of the Sc occurrences in these materials was therefore the second major focus of this thesis. Thus, the following chapters will provide detailed insights on the geochemistry and mineralogy of Sc in BR.

3. Comparative study of Scandium in different bauxite residues

3.1 Investigation of scandium in bauxite residues of different origin

The content of this chapter was published in the paper:

Gentzmann, M. C., K. Schraut, C. Vogel, H.-E. Gäbler, T. Huthwelker, and C. Adam, 2021: Investigation of scandium in bauxite residues of different origin. Applied Geochemistry, 126, 104898.doi: https://doi.org/10.1016/j.apgeochem.2021.104898

The content of chapter 3.1 is based on the publication: *Gentzmann, M. C., K. Schraut, C. Vogel, H.-E. Gäbler, T. Huthwelker, and C. Adam, 2021: Investigation of scandium in bauxite residues of different origin. Applied Geochemistry, 126, 104898.doi: https://doi.org/10.1016/j.apgeochem.2021.104898,* the introduction was shortened

3.2 Understanding scandium leaching from bauxite residues of different geological backgrounds using statistical design of experiments

The content of this chapter was published in the paper:
Gentzmann, M. C, Paul, A., Serrano, J., Adam, C, 2022: Understanding scandium leaching from bauxite residues of different geological backgrounds using statistical design of experiments, Journal of Geochemical Exploration, Volume 240, 2022, 107041, ISSN 0375-6742. https://doi.org/10.1016/j.gexplo.2022.107041
.

The content of chapter 3.2 is based on the publication: Gentzmann, M. C, Paul, A., Serrano, J., Adam, C., 2022: Understanding scandium leaching from bauxite residues of different geological backgrounds using statistical design of experiments Journal of Geochemical Exploration, Volume 240, 2022, 107041, https://doi.org/10.1016/j.gexplo.2022.107041

4. Discussion and conclusion

Recent technological developments have shown that Sc is not only interesting for small scale, specialized utilizations, but it has the potential to enable widespread applications that facilitate green energy production and reduce CO_2 emissions. Currently Sc is solely produced as a by-product of other metals and minerals or recovered from metallurgical residues i.e., secondary resources. However, in Europe there is no supply chain for Sc and comprehensive knowledge about potential secondary resources is lacking. This work includes the first overview of potential resources for Sc recovery in Europe and provides a substantial contribution to fill in those knowledge gaps. Since Sc is known to be rarely concentrated in natural rocks and circular economy approaches become increasingly important, the work focuses on industrial wastes and residues. It particularly presents new findings regarding the occurrence of Sc in bauxite residues as the overall assessment of the residues investigated in this work showed that BRs have a high potential to become one of the important sources for Sc in Europe. Since studies that deal with mineralogical and geochemical aspects of Sc occurrences in these materials are extremely rare, this thesis shows under which conditions Sc is enriched in BRs, in which mineral phases it concentrates, and how these phases behave during Sc recovery by leaching. An in-depth knowledge about the influence of the primary bauxite ore on the resulting Sc association in the bauxite residue is furthermore presented as it is crucial to provide a basis for the development of efficient, material adapted recovery techniques.

4.1 The potential of secondary raw materials as Sc resources in Europe and beyond

Six different residues from TiO_2, alumina, steel, tin, nickel, and Al-Sc alloy production are enriched in Sc and represent potential secondary raw materials for the recovery of Sc and the subsequent production of Sc compounds (see chapter 2). The current high price of Sc_2O_3 and the correspondingly high value that would be created by its recovery represent an opportunity to enable the economically viable processing of a residue that might not otherwise be reused. Amongst the residues that were investigated, liquid acid waste from TiO_2 production and BR were identified as the most promising future sources for Sc in Europe.

The TiO_2 liquid acid waste has some major advantages. Firstly, the Sc is already present in solution, which eliminates the need for a complicated solvent extraction from solid residue and the handling of said residue. Secondly, the Sc extraction and production can be integrated into an already existing processing scheme and the production route can be built upon available infrastructure. The integration of Sc compound production from these wastes is already established in other countries such as China (Zhang et al. 2021) and Canada (RioTinto 2021), which demonstrates that it can be integrated successfully.

The Sc recovery from BR, which accumulates in large volumes wherever bauxites are processed, is to date only realized in pilot scale in Russia and Greece (Balomenos et al. 2021; Petrakova et al. 2015). However there is an increasing pressure on the aluminum industry to find reutilization possibilities (World Aluminium 2020). Efficient and economically viable recovery processes can only be developed when the Sc association and distribution within the treated materials is sufficiently understood which is why this thesis provides the fundamental knowledge for a better implementation of the Sc recovery process (chapter 3 and 4.2). This recovery and the production of a high value critical element like Sc can furthermore enable larger scale reutilizations such as the recovery of Fe, Ti, or Al and potential applications for concrete or geopolymers (Klauber et al. 2011).

The worldwide comparison provided in this work (chapter 2.3 4, Fig.10) shows that Sc sources could be manifold. The review of existing literature proves that various kinds of industrial waste streams have been investigated for their theoretical Sc recovery potential in the past (comp. chapter 1.3). The established recovery and production schemes are predominantly those from white pigment production. Additionally, there are other small scale or pilot plant operations with annual productions rates < 1 t/a where Sc is obtained as a byproduct (Grandfield 2021). Potential primary resources span from lateritic Ni-Co deposits to igneous REE and Nb enriched intrusions. In addition to those already mentioned above other secondary resources include uranium leach liquors, residues from zirconia and Zr production and residues from Ni, Co and Cu production.

Concludingly the global Sc market is currently characterized by a high diversity of potential resources and the developments in the upcoming years will show which of the numerous different approaches will prevail. The comprehensive overview given in this thesis provides a basic understanding of current trends and developments in the global Sc supply chain and enables an assessment of the European overall standing. It was determined that the most promising residues for Sc production in Europe are thus TiO_2 acid waste and BR. Finally, the overview and the assessment deliver a first foundation to reevaluate future trends for Sc production in Europe.

4.2 The association of Sc in BR from ore to waste

The combined investigations presented in chapter 3.1 and 3.2 revealed both significant similarities and differences between the Sc occurrences in BRs of different origin and they provide the first comprehensive comparison between those BRs.

Similarities were found to occur regarding the general Sc distribution amongst different particle size fractions. More specifically, the comparison between the Sc mass fraction in larger mineral particles and the fine-grained matrix showed that Sc in all BRs is rather homogeneously distributed amongst the different size fractions. Regarding the Sc occurrences

in the different mineral species present in BRs some common characteristics could be identified. In fact, the Al hydroxides gibbsite, boehmite and diaspore as well as the Ca rich phases lime and calcite exhibit low Sc mass fractions. In contrast, the Sc mass fractions of the Fe phases goethite, hematite and chamosite (chamosite only observed in Russian BR) are at the same level as those determined for the fine-grained matrix. In the BR samples from Greece, it was observed that goethite can contain higher mass fractions of Sc than hematite. The XANES investigations presented in chapter 3.1.3.3.2 revealed that Sc can be both incorporated into and adsorbed to hematite and goethite. In addition to these findings, several accessory phases exhibited higher Sc mass fractions. These included Ti phases like rutile and ilmenite in German and Greek BR, zircon in German BR and Mg-Ca rich phase accumulations in Russian BR (comp chapter 3.1.3.2.4, Fig. 16). The results substantiate previous findings in the literature and provide a more comprehensive understanding of the different aspects that define the Sc distribution in BRs. In fact, different authors described the affinity of Sc towards Fe oxides and hydroxides such as goethite and towards clay minerals such as chamosite (Horovitz 1975; Teitler et al. 2019). The importance of surface adsorption onto those minerals was highlighted in several publications including for example the works of Vind et al. (2018) and Qin et al. (2021). The homogenous distribution observed here agrees with previous observations on BR where Sc bulk mass fractions did not differ between different particle size fractions obtained by sieving (Vind et al. 2018). The enrichment of Sc in accessory phases like zircon, rutile and ilmenite can be explained by its affinity towards high field strength elements (Wang et al. 2021). High mass fractions of Sc in these minerals have been observed in BRs as well as in other residues and natural rocks (Vind et al. 2018; Zhong and Wu 2012).

The abovementioned general characteristics of Sc occurrences in BRs hold true for all the investigated samples yet some significant differences were identified as well. These can be linked to the respective geological background of the BR and were found to have a strong influence on the Sc recovery. One of the major differences in geological background is correlated to the type of primary bauxite used for alumina production. As described in chapter 1.2.3, two major types can be distinguished namely lateritic and karstic bauxite. While lateritic bauxites often exhibit rather low Sc mass fractions, karstic bauxites are prone to contain higher mass fractions (comp. Tab. 2). This phenomenon can be explained by the Sc and REE stabilization caused by the underlying karstic relief and corresponding increased pH values (chapter 3.1.3.4.2). Some major observations that were made for the Sc occurrence in the investigated BRs can be correlated to this aspect. To begin with, the German BR resulting from processing of lateritic bauxite exhibits the lowest Sc mass fractions amongst all the samples compared. Secondly, both Greek and Hungarian BR were found to contain a certain proportion of Fe-phases (goethite and hematite), which regardless of species and mineral chemistry exhibit a lower average Sc mass fraction. This can be attributed to the admixture of minor

amounts of lateritic bauxite ore to the Bayer process, which is often used in alumina plants that predominantly use karstic bauxites. The admixture is a measure to enable a higher alumina recovery. Therefore, a certain fraction of Fe-species in the resulting BR stems from lateritic bauxite and is likely to exhibit a lower average mass fraction of Sc.

Ultimately, not only the primary bauxite ore but also the additional input materials of the Bayer process can differ with bauxite type. In fact, Bayer processing plants that use karstic bauxites often add lime to decrease their caustic soda consumption. This influences the assemblage of new minerals that form during Bayer processing (Gräfe and Klauber 2011). Accordingly, the addition of lime often causes BRs derived from karstic bauxites to contain high mass fractions of katoite (also called hydrogarnet). In contrast, the lateritic bauxites that were treated without lime addition do not contain as high mass fractions of this mineral. The XRD measurements presented in chapter 3.1.3.1 and 3.2.4.2 reveal that Greek, Hungarian and Russian BR mainly derived from karstic bauxites contain a significantly higher percentage of katoite than German BR derived from lateritic bauxites. As presented in chapter 3.2, the katoite proved to be one of the secondary minerals that release a major part of the easily leachable fraction of Sc upon dissolution (comp. chapter. 3.2.5). Contrastingly, other secondary minerals such as cancrinite were found to release much smaller mass fractions of Sc when dissolved. Therefore, different primary bauxites require different processing schemes which evidently cause variations in the mineral assemblage of the BR and the distribution of Sc amongst those mineral phases.

In addition to the bauxite type, the atmospheric conditions during bauxitization, i.e., oxidizing or reducing, were found to influence the distribution of Sc within the bauxites and BRs. The effect of these conditions could for example be inferred from the observations made on Hungarian and Russian BR which were presented in chapter 3.1.3.4.4. Accordingly, predominantly reducing conditions during bauxitization favor the formation of clay minerals such as chamosite and the sequestering and/or adsorption of Sc by this mineral. Predominantly oxidizing conditions however favor the formation of goethite and hematite and the association of Sc with them. The atmospheric conditions during formation of the bauxite ore can influence how much Sc is associated with the Bayer process resistant minerals and vice versa. For example, as chamosite is partly soluble during Bayer processing, the proportion of Sc associated with it is prone to redistribution. In contrast, the Sc associated with hematite and goethite will to a large extent be transferred to the BR virtually unchanged. Therefore, the proportion of Sc that is redistributed in the Bayer process and hence associated with newly formed phases in the BR will be higher when reducing conditions were evident during the bauxitization of the primary ore. The variation in Sc species associated with the changes in physicochemical environment during weathering processes has been well documented on lateritic profiles in Australia, China and New Caledonia (Chassé et al. 2019; Qin et al. 2020;

Teitler et al. 2019). The in-depth investigations of the Sc distribution in those profiles showed that formation of Fe oxides and hydroxides, particularly goethite but also clay minerals, immobilize Sc by incorporation and surface adsorption (comp. chapter 1.2.3). The formation of those minerals is in turn known to be dependent on the atmospheric conditions during bauxitization (Bárdossy 1982) which will therefore directly affect the Sc distribution.

Finally, it is important to mention that the source rocks of a bauxite deposit will inevitably determine the Sc budget that can be mobilized, redistributed, and potentially concentrated in the bauxite ore. Therefore, laterites derived from mafic rocks are more likely to contain higher mass fractions of Sc than those derived from felsic rocks as can be deduced from the overview in Table 1. Nevertheless, if high mass fractions of Sc exist in a protolith, but are mobilized and leached due to weathering processes, the bauxite ore and the resulting BR might still exhibit low Sc mass fractions. It is important to note here, that all the above-mentioned redistribution processes during bauxitization will only affect the proportion of Sc in the minerals that are susceptible to bauxitic weathering. The proportion of Sc that is incorporated into weathering resistant minerals such as zircon will still be found in zircon after bauxitization and Bayer processing and its association from ore to waste remains largely unchanged.

To conclude, it is demonstrated that the combination of source rocks, underlying relief and physicochemical conditions during bauxitization influence the mass fraction and distribution of Sc within a bauxite ore which is in turn decisive for the association in the resulting BR. It is shown that it is important how this bauxite ore is processed, i.e., which bauxite mixtures and additives are used in the alumina plant. These aspects will determine the level of Sc accumulated in BR and how Sc is redistributed from the bauxite ore to the BR.

4.3 The release of Sc under variable leaching conditions

The comparison of the leaching behavior of three different BRs presented in this work revealed some fundamental differences between those materials but also showed systematic similarities. By evaluating these differences and similarities, the thesis provides a general understanding of the processes affecting the proportion of Sc that can be leached from a certain BR. This knowledge now makes it possible to link the geochemical and mineralogical background of a material to hydrometallurgical treatment possibilities.

Generally, the BRs contain an easily and a hardly leachable fraction of Sc. A large part of the easily leachable fraction of Sc is associated with the secondary mineral phases katoite and to a lesser extent cancrinite, which form during Bayer processing. The proportion of Sc that is released predominantly from those minerals differs significantly between the BRs investigated and ranges between ~20-50%. The hardly leachable fraction is associated with the Fe phases hematite goethite and chamosite (the latter only in Russian BR) as well as with leaching resistant minerals such as zircon and ilmenite. It comprises ~50-80% of the total Sc mass fraction. This wide range of recoverable Sc content, which is consistent with the various

results presented in the literature (comp. chapter 1.4.2 and Fig. 1), shows the strong influence of material properties and leaching conditions on Sc recovery. The statistical evaluation by means of “Design of Experiments” (DoE) underlined that the BR type had the strongest influence on the Sc recovery. Other very important factors were found to be temperature and acid type. Interactions between these factors furthermore revealed the differences in effects on both Sc and Fe leaching and hence the selectivity of Sc over Fe. While Sc leaching increases linearly with temperature, Fe leaching increases exponentially. The temperature is therefore a crucial factor for maximizing both Sc recovery and selectivity over iron.

In German BR up to 25% of Sc can be leached when mild leaching conditions are used and a high selectivity of Sc over iron can be maintained. In this context mild leaching conditions comprise citric acid leaching and sulfuric acid leaching at room temperature. Sc is readily released from cancrinite and then from katoite when high temperature citric acid leaching or room temperature sulfuric acid leaching is applied. The same pattern can be observed for Hungarian BR, but the proportion of easily leachable Sc in Hungarian BR is ~10% higher than in German BR. As Hungarian BR originates from processing of predominantly karstic bauxite the proportion of Sc that could be redistributed in the Bayer process and is available for incorporation into secondary phases such as katoite is higher (comp. previous chapter). The use of stronger leaching conditions, i.e., high temperature sulfuric acid leaching, will promote the dissolution of Fe-phases. Due to the association of Sc with Fe-phases (comp. chapter 3.1.3.4) this leads to an increased Sc recovery and Fe concentration in the leachate and a lower selectivity of Sc over Fe in the process. In contrast to Hungarian and German BR, the BR from Russia already shows the partial dissolution of the Fe-phase chamosite under mild leaching conditions (i.e., citric acid leaching at 85°C). The easily leachable fraction of Sc in Russian BR is therefore ~15-20% higher than in the other two examples.

Based on these results for Sc recovery the release of Sc from the BRs into the leachate can be approximated as a 4-step process which is illustrated in Figure 27.

1) cancrinite dissolution
2) katoite dissolution
3) Fe-phase dissolution
4) total dissolution of BR

However, the transitions in this four-stage process are to be regarded as smooth rather than sharp.

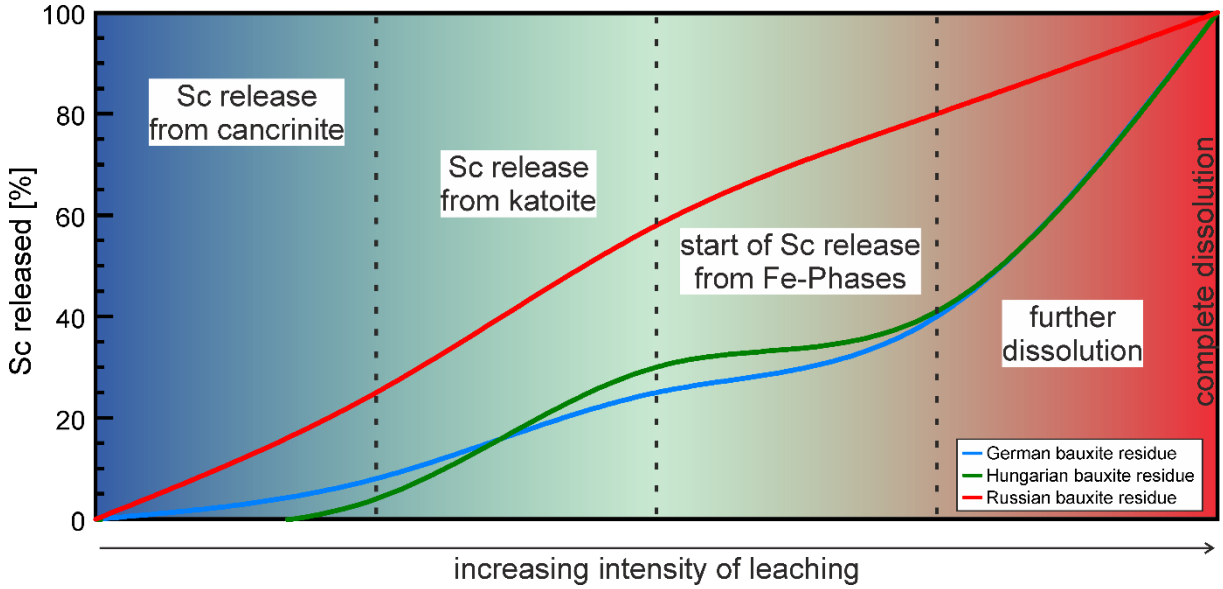

Figure 27 Schematic simplified representation of Sc release from different mineral phases during leaching of bauxite residues from Germany, Hungary and Russia. The leaching intensity increases from left to right. It should be noted that the minerals mentioned in this figure were identified as the major contributing phases. However, the dissolution of other crystalline and amorphous phases will also contribute to the Sc release.

It should also be noted that the total dissolution was not directly investigated in this study but could be compared to a total digestion process e.g., using strong acids and/or acid mixtures with hydrofluoric acid.

The physicochemical parameters that influence the dissolution pattern will be mainly the pH of the slurry during leaching and the temperature (Borra et al. 2015; Ochsenkuehn-Petropoulou et al. 2018). The pH of the slurry is in turn dependent on the acid type and concentration and the l/s ratio. It can be subject to changes during the leaching process as dissolution of alkaline phases can lead to buffering (Kong et al. 2017). The temperature has a high influence because it serves to overcome the activation energy needed to dissolve hematite and goethite (Taxiarchou et al. 1997; Zhang et al. 1985).

The investigations on BRs presented here make it possible determine he overall link between bauxite ore, BR and its characteristics regarding the leachability of Sc (Fig. 28). BRs stemming from a lateritic bauxite will exhibit a rather low proportion of easily leachable Sc. They will release this proportion under mild leaching conditions with low temperature sulfuric acid leaching or high temperature citric acid leaching and will show a comparatively high selectivity of Sc over iron during leaching. Under those same mild conditions, BR originating form karstic bauxite will release a higher proportion of Sc into the leachate. This is due to a higher proportion of Sc that is subject to redistribution in the Bayer process. In addition, BR originating from karstic bauxites bauxitized under partly reducing conditions will exhibit an even higher easily leachable fraction of Sc because the release from clay minerals such as

chamosite is already facilitated under mild leaching conditions. However, the selectivity of Sc over Fe will be lower in these BRs.

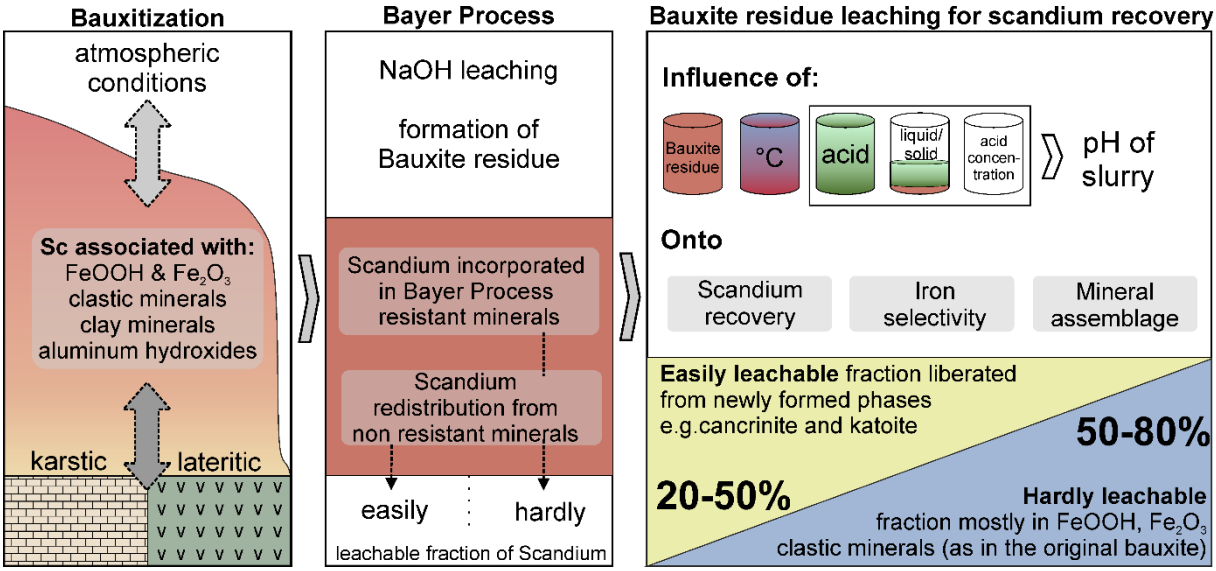

Figure 28 Schematic overview of factors influencing the Sc association and distribution from bauxite ore to bauxite residue and finally during bauxite residue leaching.

The investigations on the different BRs in this thesis revealed many links between primary ore and secondary waste material. Nevertheless, it is important to also mention the limitations of the interpretation which may point the way for future research of Sc in BRs. It should be noted that the bauxites and BRs considered in this study are by no means able to represent the whole variety of materials that exist all over the world. The examples served to compare some fundamentally different characteristics, but more bauxites and BRs need to be compared to expand the knowledge and provide an even larger comprehensive overview. Since the major focus of this work, was the association of Sc in the BR, studies on the actual primary bauxite were only performed on a small scale. However, a more in-depth understanding of the Sc behavior during bauxitization would require intensive research on bauxites and their respective source rocks. In addition, the actual process parameters of the Bayer process such as temperature, pressure or additives, to only name a few, may influence the chemistry and mineralogy of secondary precipitates and hence the association of Sc with those precipitates. Finally, it should be noted that this thesis primarily analyzed the behavior of crystalline phases in the bauxite residues during leaching and only provided limited knowledge about the potential influence of the amorphous phases within the material. Further special investigations would be necessary to understand how and to what extent these amorphous phases affect the Sc release during Bayer processing and BR leaching.

4.4 From the geochemistry of bauxite to the Sc recovery potential of bauxite residues and beyond

The outcome of this thesis is the comprehensive link between the bauxite and BR material properties with regards to their behavior during the Sc recovery process. Knowledge about the geological development of a bauxite determined by its mineralogy and geochemistry can ultimately help to assess whether a large part of Sc could be easily leachable or whether the material requires a more intense leaching procedure. This knowledge can facilitate the setup of suitable experiments and analytical methods to gain in depth knowledge about a specific material. In addition to the systematic conclusions that can be drawn about leaching procedures, the presented correlations can also be used to evaluate how the Sc will distribute when other processing schemes are applied. Those processing schemes could include other wet chemical procedures, thermochemical treatment, or beneficiation methods such as magnetic separation. BRs with low fractions of easily leachable Sc may be more suitable for other treatment flow sheets apart from direct leaching, e.g., smelting, or reductive roasting. These methods may enable a reutilization of the BR for building materials and the potential recovery of other valuable elements (e.g., Fe, Ti, Al etc.). Concludingly, the fundamental knowledge about the Sc association and distribution presented in this work defines the basis for the general assessment of the Sc recovery potential from BR.

References

Aiglsperger, T., J. A. Proenza, J. F. Lewis, M. Labrador, M. Svojtka, A. Rojas-Purón, F. Longo, and J. Ďurišová, 2016: Critical metals (REE, Sc, PGE) in Ni laterites from Cuba and the Dominican Republic. *Ore Geology Reviews*, **73,** 127-147.https://doi.org/10.1016/j.oregeorev.2015.10.010

Alipanah, M., D. M. Park, A. Middleton, Z. Dong, H. Hsu-Kim, Y. Jiao, and H. Jin, 2020: Techno-Economic and Life Cycle Assessments for Sustainable Rare Earth Recovery from Coal Byproducts using Biosorption. *ACS Sustainable Chemistry & Engineering*, **8,** 17914-17922.10.1021/acssuschemeng.0c04415

Alkan, G., B. Xakalashe, B. Yagmurlu, F. Kaussen, and B. Friedrich, 2017: Conditioning of red mud for subsequent titanium and scandium recovery–a conceptual design study. *World of metallurgy–ERZMETALL*, **70,** 5-12

Anderson, M. J., and P. J. Whitcomb, 2017: *DOE simplified: practical tools for effective experimentation.* 3rd ed. CRC press, 258 pp

Antrekowitsch, J., and G. Rösler, 2015: Steel mill dust recycling in the 21st century. *The publications of the MultiScience-XXIX. MicroCAD International Scientific Conference. University of Miskolc*

Balomenos, E., G. Nazari, P. Davris, G. Abrenica, A. Pilihou, E. Mikeli, D. Panias, S. Patkar, and W.-Q. Xu, 2021: Scandium Extraction from Bauxite Residue Using Sulfuric Acid and a Composite Extractant-Enhanced Ion-Exchange Polymer Resin. Cham, Springer International Publishing, 217-228.10.1007/978-3-030-65489-4_22

Bardossy, G., and G. Aleva, 1990: Lateritic Bauxites. Developments in economic geology, 27. *Elsevier Sci. Publ.***,** 624

Bárdossy, G., 1982: *Karst bauxites.* Vol. 14, Elsevier

Bau, M., 1999: Scavenging of dissolved yttrium and rare earths by precipitating iron oxyhydroxide: experimental evidence for Ce oxidation, Y-Ho fractionation, and lanthanide tetrad effect. *Geochimica et Cosmochimica Acta*, **63,** 67-77.https://doi.org/10.1016/S0016-7037(99)00014-9

Betancur, J. D., C. A. Barrero, J. M. Greneche, and G. F. Goya, 2004: The effect of water content on the magnetic and structural properties of goethite. *Journal of Alloys and Compounds*, **369,** 247-251.https://doi.org/10.1016/j.jallcom.2003.09.046

Blanchard, P. E. R., A. P. Grosvenor, J. Rowson, K. Hughes, and C. Brown, 2016: Identifying calcium-containing mineral species in the JEB Tailings Management Facility at McClean Lake, Saskatchewan. *Applied Geochemistry*, **73,** 98-108.https://doi.org/10.1016/j.apgeochem.2016.08.001

Bogatyrev, B. A., V. V. Zhukov, and Y. G. Tsekhovsky, 2009: Phanerozic bauxite epochs. *Geology of Ore Deposits*, **51,** 456-466.10.1134/S1075701509060038

Bogomazov, A. V., and A. S. Senyuta, 2017: Method for the acid treatment of red mud, Patent Nr. AU 2012385520 B2.

Bonomi, C., A. Alexandri, J. Vind, A. Panagiotopoulou, P. Tsakiridis, and D. Panias, 2018: Scandium and titanium recovery from bauxite residue by direct leaching with a Brønsted acidic ionic liquid. *Metals*, **8,** 834.10.3390/met8100834

Borra, C. R., Y. Pontikes, K. Binnemans, and T. Van Gerven, 2015: Leaching of rare earths from bauxite residue (red mud). *Minerals Engineering*, **76,** 20-27.https://doi.org/10.1016/j.mineng.2015.01.005

Borra, C. R., B. Blanpain, Y. Pontikes, K. Binnemans, and T. Van Gerven, 2016: Recovery of Rare Earths and Other Valuable Metals From Bauxite Residue (Red Mud): A Review. *Journal of Sustainable Metallurgy*, **2,** 365-386.10.1007/s40831-016-0068-2

Botelho Junior, A., D. Espinosa, J. Vaughan, and J. Tenório, 2021: Recovery of scandium from various sources: A critical review of the state of the art and future prospects. *Minerals Engineering*, **172,** 107148.https://doi.org/10.1016/j.mineng.2021.107148

Boulangé, B., and F. Colin, 1994: Rare earth element mobility during conversion of nepheline syenite into lateritic bauxite at Passa Quatro, Minais Gerais, Brazil. *Applied Geochemistry*, **9,** 701-711.https://doi.org/10.1016/0883-2927(94)90029-9

Büchele, D., M. Chao, M. Ostermann, M. Leenen, and I. Bald, 2019: Multivariate chemometrics as a key tool for prediction of K and Fe in a diverse German agricultural soil-set using EDXRF. *Scientific Reports*, **9,** 17588.10.1038/s41598-019-53426-5

Calvin, S., 2013: *XAFS for Everyone.* Taylor & Francis

Carlson, M., and S. Treves, 2005: The Elk Creek carbonatite, southeast Nebraska–an overview. *Natural Resources Research*, **14,** 39-45.10.1007/s11053-005-4677-x

Cashin, P., 2018: Towards the Developement of North Americas First Primary Scandium Resource: The Crater lake Project, Québec. Presentation during: European Scandium Inventory Workshop, Berlin 2018; http://scale-project.eu/scandium-workshop/

Chashchin, V., 2018: Production of Scandium at JSC Dalur. European Scandium Inventory Workshop, Berlin 2018; http://scale-project.eu/scandium-workshop/

Chassé, M., W. L. Griffin, S. Y. O. Reilly, and G. Calas, 2016: Scandium speciation in a world-class lateritic deposit. *Geochemical Perspectives Letters*, **3,** 105-114.http://dx.doi.org/10.7185/geochemlet.1711

Chassé, M., W. L. Griffin, S. Y. O'Reilly, and G. Calas, 2019: Australian laterites reveal mechanisms governing scandium dynamics in the critical zone. *Geochimica et Cosmochimica Acta*, **260,** 292-310.https://doi.org/10.1016/j.gca.2019.06.036

Chassé, M., W. L. Griffin, O. Alard, S. Y. O'reilly, and G. Calas, 2018a: Insights into the mantle geochemistry of scandium from a meta-analysis of garnet data. *Lithos*, **310,** 409-421.doi:10.1016/j.lithos.2018.03.026

Chassé, M., A. Juhin, D. Cabaret, S. Delhommaye, D. Vantelon, and G. Calasa, 2018b: Influence of Crystallographic Environment on Scan-dium K-Edge X-Ray Absorption Near-Edge Structure Spectra. *Physical Chemistry Chemical Physics*.https://doi.org/10.1039/C8CP04413A

Chassé, M., M. Blanchard, D. Cabaret, A. Juhin, D. Vantelon, and G. Calas, 2020: First-principles modeling of X-ray absorption spectra enlightens the processes of scandium sequestration by iron oxides. *American Mineralogist*, **105,** 1099-1103.doi:10.2138/am-2020-7308

Čížková, M., D. Mezricky, M. Rucki, T. M. Tóth, V. Náhlík, V. Lanta, K. Bišová, V. Zachleder, and M. Vítová, 2019: Bio-mining of lanthanides from red mud by green microalgae. *Molecules*, **24,** 1356.https://doi.org/10.3390/molecules24071356

Cusack, P. B., R. Courtney, M. G. Healy, L. M. T. O' Donoghue, and É. Ujaczki, 2019: An evaluation of the general composition and critical raw material content of bauxite residue in a storage area over a twelve-year period. *Journal of Cleaner Production*, **208,** 393-401.https://doi.org/10.1016/j.jclepro.2018.10.083

Das, B., B. Dash, B. Tripathy, I. Bhattacharya, and S. Das, 2007: Production of η-alumina from waste aluminium dross. *Minerals engineering*, **20,** 252-258.https://doi.org/10.1016/j.mineng.2006.09.002

Das, H., J. Zonderhuis, and H. van der Marel, 1971: Scandium in rocks, minerals and sediments and its relations to iron and aluminium. *Contributions to Mineralogy and Petrology*, **32,** 231-244.https://doi.org/10.1007/BF00643336

Davris, P., E. Balomenos, D. Panias, and I. Paspaliaris, 2018: Developing New Process for Selective Extraction of Rare Earth Elements from Bauxite Residue Based on Functionalized Ionic Liquids. Cham, Springer International Publishing, 149-156.https://doi.org/10.1007/978-3-319-72284-9_20

de Groot, F., G. Vankó, and P. Glatzel, 2009: The 1s x-ray absorption pre-edge structures in transition metal oxides. *Journal of Physics: Condensed Matter*, **21,** 104207.10.1088/0953-8984/21/10/104207

Deady, E., E. Mouchos, K. Goodenough, B. Williamson, and F. Wall, 2014: Rare Earth elements in Karst-bauxites: A novel untapped European resource? In: ERES 2014 : 1st conference on European Rare Earth Resources, Milos, Greece, 4-7 Sept 2014.**,** 364-375

Deady, É. A., E. Mouchos, K. Goodenough, B. J. Williamson, and F. Wall, 2016: A review of the potential for rare-earth element resources from European red muds: examples from Seydişehir, Turkey and Parnassus-Giona, Greece. *Mineralogical Magazine*, **80,** 43-61

Ditze, A., and K. Kongolo, 1997: Recovery of scandium from magnesium, aluminium and iron scrap. *Hydrometallurgy*, **44,** 179-184.https://doi.org/10.1016/S0304-386X(96)00041-2

Dobra, G., A. Kiselev, L. Filipescu, V. Alistarh, N. Anghelovici, and S. Iliev, 2016: Full analysis of Sierra Leone bauxite and possibilities of bauxite residue filtration.10.17516/1999-494X-20169-5-643-656

Doebelin, N., and R. Kleeberg, 2015: Profex: a graphical user interface for the Rietveld refinement program BGMN. *Journal of Applied Crystallography*, **48,** 1573-1580.10.1107/S1600576715014685

Dorin, T., M. Ramajayam, A. Vahid, and T. Langan, 2018: Chapter 12 - Aluminium Scandium Alloys. *Fundamentals of Aluminium Metallurgy*, R. N. Lumley, Ed., Woodhead Publishing, 439-494.https://doi.org/10.1016/B978-0-08-102063-0.00012-6

Dunkl, I., 1992: Origin of Eocene-covered karst bauxites of the Transdanubian Central Range (Hungary): evidence for early Eocene volcanism. *European Journal of Mineralogy***,** 581-596

Elsner, H., 2014: *DERA Rohstoffinformationen: Zinn-Angebot und Nachfrage bis 2020 (Tin - Supply and demand until 2020, in German).* DERA, Deutsche Rohstoffagentur in der BGR

European Commission, 2017: *Study on the review of the list of critical raw materials : final report (European Commission,Directorate-General for Internal Market, Industry, Entrepreneurship) SMEs;*Publications Office.doi/10.2873/876644

Fan, H.-R., K.-F. Yang, F.-F. Hu, S. Liu, and K.-Y. Wang, 2016: The giant Bayan Obo REE-Nb-Fe deposit, China: Controversy and ore genesis. *Geoscience Frontiers*, **7,** 335-344.https://doi.org/10.1016/j.gsf.2015.11.005

Feuling, R. J., 1991b: Recovery of scandium, yttrium and lanthanides from zircon sand. Google Patents

Filippou, D., and G. Hudon, 2020: Minerals, slags, and other feedstock for the production of titanium metal. *Extractive Metallurgy of Titanium*, Elsevier, 19-45.https://doi.org/10.1016/B978-0-12-817200-1.00003-X

Foord, E., S. D. Birmingham, F. Demartin, T. Pilati, C. M. Gramaccioli, and F. J. T. C. M. Lichte, 1993: Thortveitite and associated Sc-bearing minerals from Ravalli County, Montana. *Canadian Mineralogist*, **31,** 337-346.https://doi.org/10.3749/1499-1276-31.2.337

Fortier, S. M., N. T. Nassar, G. W. Lederer, J. Brainard, J. Gambogi, and E. A. McCullough, 2018: Draft critical mineral list—Summary of methodology and background information—U.S. Geological Survey technical input document in response to Secretarial Order No. 3359. 2018-1021,Reston, VA, 26 pp. [Available online at http://pubs.er.usgs.gov/publication/ofr20181021.]

Gamaletsos, P. N., A. Godelitsas, A. Filippidis, and Y. Pontikes, 2019: The Rare Earth Elements Potential of Greek Bauxite Active Mines in the Light of a Sustainable REE Demand. *Journal of Sustainable Metallurgy*, **5,** 20-47.10.1007/s40831-018-0192-2

Gentzmann, M. C., K. Schraut, C. Vogel, H.-E. Gäbler, T. Huthwelker, and C. Adam, 2021: Investigation of scandium in bauxite residues of different origin. *Applied Geochemistry*, **126,** 104898.https://doi.org/10.1016/j.apgeochem.2021.104898

Giovannini, A., A. Bastos Neto, C. Porto, V. Pereira, L. Takehara, L. Barbanson, and P. Bastos, 2017: Mineralogy and Geochemistry of Laterites from the Morro dos Seis Lagos Nb (Ti, REE) Deposit (Amazonas, Brazil). *Ore Geology Reviews*, **88,** 461-480.10.1016/j.oregeorev.2017.05.008

Graedel, T. E., R. Barr, C. Chandler, T. Chase, J. Choi, L. Christoffersen, E. Friedlander, C. Henly, C. Jun, N. T. Nassar, D. Schechner, S. Warren, M.-y. Yang, and C. Zhu, 2012: Methodology of Metal Criticality Determination. *Environmental Science & Technology*, **46,** 1063-1070.10.1021/es203534z

Gräfe, M., and C. Klauber, 2011: Bauxite residue issues: IV. Old obstacles and new pathways for in situ residue bioremediation. *Hydrometallurgy*, **108,** 46-59.https://doi.org/10.1016/j.hydromet.2011.02.005

Gräfe, M., G. Power, and C. Klauber, 2011: Bauxite residue issues: III. Alkalinity and associated chemistry. *Hydrometallurgy*, **108,** 60-79.https://doi.org/10.1016/j.hydromet.2011.02.004

Grandfield, J., 2018: 10-Year Outlook for the Global Scandium Market to 2028. Presentation during: European Scandium Inventory Workshop, Berlin 2018; http://scale-project.eu/scandium-workshop/

——, 2021: 10-Year Outlook for the Global Scandium Market to 2031. Presentation during: TMS Webinars: Scandium: Properties, Alloys, and Current Activities Webinar Series; https://www.tms.org/portal/PROFESSIONAL_DEVELOPMENT/Professional_Development_Resources/Webinar_Library/ScandiumWebinar/portal/Professional_Development/Professional_Development_Resources/Webinars/webinarScandium.aspx?hkey=9c4d0f22-d21c-4c41-9d49-a63a3fa315d9

Grant, C., G. Lalor, and M. Vutchkov, 2005: Comparison of bauxites from Jamaica, the Dominican Republic and Suriname. *Journal of Radioanalytical and Nuclear Chemistry*, **266,** 385-388.https://doi.org/10.1007/s10967-005-0921-4

Grondin, F., 2019: *Mineralogy and Fluid Inclusion Study of the Crystal Mountain Fluorite Mine, Ravalli County, Montana, MSc Thesis.* Montana Tech of The University of Montana

Guézennec, A.-G., J.-C. Huber, F. Patisson, P. Sessiecq, J.-P. Birat, and D. Ablitzer, 2005: Dust formation in Electric Arc Furnace: Birth of the particles. *Powder Technology*, **157,** 2-11.https://doi.org/10.1016/j.powtec.2005.05.006

Gunn, G., 2014: *Critical metals handbook.* John Wiley & Sons

Gusev, A. I., 2012: Types of endogenic rare earth mineralization in Gorny and Rudny

Altai.(in russian). *Uspekhi Sovremennogo Estestvoznaniya*, **12,** 92-97

Gusev, A. I., N. I. Gusev, and I. V. Efimova, 2009: Magnetism and mineralisation of Kumir, Altai. *Rudy i metally*, **v.6,** 21-28 (in Russian)

Habashi, F., 2016: A Hundred Years of the Bayer Process for Alumina Production. *Essential Readings in Light Metals*, Springer, 85-93.https://doi.org/10.1007/978-3-319-48176-0_12

Hagni, A. M., R. D. Hagni, and C. Demars, 1991: Mineralogical characteristics of electric arc furnace dusts. *JOM The Journal of The Minerals, Metals & Materials Society*, **43,** 28-30.https://doi.org/10.1007/BF03220543

Halkoaho, T., M. Ahven, O. T. Rämö, J. Hokka, and H. Huhma, 2020: Petrography, geochemistry, and geochronology of the Sc-enriched Kiviniemi ferrodiorite intrusion, eastern Finland. *Mineralium Deposita*, **55,** 1561-1580.10.1007/s00126-020-00952-2

Hamann, C., M. Spanka, D. Stolle, C. Adam, and G. Auer, 2019: Rückgewinnung von Zink aus Stahlwerksstäuben durch gemeinsame Behandlung mit chloridhaltigen Reststoffen. *Recycling und Rohstoffe*, S. Thiel, O. Holm, E. Thomé-Kozmiensky, D. Goldmann, and B. Friedrich, Eds., Thomé-Kozmiensky Verlag GmbH, 593-605

Hattendorf, B., U. Hartfelder, and D. Günther, 2019: Skip the beat: minimizing aliasing error in LA-ICP-MS measurements. *Analytical and Bioanalytical Chemistry*, **411,** 591-602.10.1007/s00216-018-1314-1

Hoffmann, M., V. Emese, U. Éva, I. Fekete-Kertész, M. Molnár, V. Feigl, and C. Adam, 2019: European inventory of Scandium containing by-products. SCALE Deliverable 6.1,Community Research and Development Information Service, 69 pp. [Available online at https://cordis.europa.eu/project/id/730105/results.]

Horovitz, C. T., 1975: *Scandium its occurrence, chemistry physics, metallurgy, biology and technology.* Elsevier

Imperial Mining Group Ltd.: Imperial Mining Receives Highly Encouraging NI 43-101 Resource Estimate for the TG Scandium-Rare-Earth Zone: Remains Open to Further Expansion. [Available online at https://imperialmgp.com/site/assets/files/5188/imperial_inaugural_43-101_resource_report_for_the_tg_z.pdf.]

Ivanyuk, G., A. Kalashnikov, Y. A. Pakhomovsky, J. A. Mikhailova, V. N. Yakovenchuk, N. Konopleva, V. A. Sokharev, A. Bazai, and P. M. Goryainov, 2016: *Economic minerals of the Kovdor baddeleyite-apatite-magnetite deposit, Russia: Mineralogy, spatial distribution and ore processing optimization.* Vol. 77.10.1016/j.oregeorev.2016.02.008

Ivers-Tiffée, E., A. Weber, and D. Herbstritt, 2001: Materials and technologies for SOFC-components. *Journal of the European Ceramic Society*, **21,** 1805-1811.https://doi.org/10.1016/S0955-2219(01)00120-0

Jeske, A., and B. Gworek, 2013: Distribution and mobility of scandium and yttrium in selected types of soils in Poland. *Chemical Speciation & Bioavailability*, **25,** 216-222.10.3184/095422913X13785465993582

Jiang, T., X.-l. Pan, Y. Wu, H.-y. Yu, and G.-f. Tu, 2018: Mineral transition of desilication products precipitated in synthetic sodium aluminate solution under atmospheric pressure. *Transactions of Nonferrous Metals Society of China*, **28,** 367-375.https://doi.org/10.1016/S1003-6326(18)64670-9

Kalashnikov, A. O., V. N. Yakovenchuk, Y. A. Pakhomovsky, A. V. Bazai, V. A. Sokharev, N. G. Konopleva, J. A. Mikhailova, P. M. Goryainov, and G. Y. Ivanyuk, 2016: Scandium of the Kovdor baddeleyite–apatite–magnetite deposit (Murmansk Region, Russia): Mineralogy, spatial distribution, and potential resource. *Ore Geology Reviews*, **72,** 532-537.https://doi.org/10.1016/j.oregeorev.2015.08.017

Kaya, S., 2018: Current State of the Sc Recovery Possibilities during Hydrometallurgical Treatment of Lateritic Ni Co Ores. Presentation during: European Scandium Inventory Workshop, Berlin 2018; http://scale-project.eu/scandium-workshop/

Kempe, U., and D. Wolf, 2006: Anomalously high Sc contents in ore minerals from Sn–W deposits: possible economic significance and genetic implications. *ore geology reviews*, **28,** 103-122.https://doi.org/10.1016/j.oregeorev.2005.04.004

Khan, R., S. Ghosal, D. Sengupta, U. Tamim, S. M. Hossain, and S. Agrahari, 2019: Studies on heavy mineral placers from eastern coast of Odisha, India by instrumental neutron activation analysis. *Journal of Radioanalytical and Nuclear Chemistry*, **319,** 471-484.10.1007/s10967-018-6250-1

Kiskira, K., T. Lymperopoulou, L.-A. Tsakanika, C. Pavlopoulos, K. Papadopoulou, K.-M. Ochsenkühn, G. Lyberatos, and M. Ochsenkühn-Petropoulou, 2021: Study of Microbial Cultures for the Bioleaching of Scandium from Alumina Industry By-Products. *Metals*, **11,** 951.https://doi.org/10.3390/met11060951

Klauber, C., M. Gräfe, and G. Power, 2011: Bauxite residue issues: II. options for residue utilization. *Hydrometallurgy*, **108,** 11-32.https://doi.org/10.1016/j.hydromet.2011.02.007

Kong, X., M. Li, S. Xue, W. Hartley, C. Chen, C. Wu, X. Li, and Y. Li, 2017: Acid transformation of bauxite residue: Conversion of its alkaline characteristics. *Journal of Hazardous Materials*, **324,** 382-390.https://doi.org/10.1016/j.jhazmat.2016.10.073

Kravchenko, S. M., and B. G. Pokrovsky, 1995: The Tomtor alkaline ultrabasic massif and related REE-Nb deposits, northern Siberia. *Economic Geology*, **90,** 676-689.10.2113/gsecongeo.90.3.676 %J Economic Geology

Lacroix, A., 1920: Sur l'existence à Madagascar d'un silicate de scandium et d'yttrium, la thortveitite. *Acad: Sci. (Paris) Comptes Rendus* **171,** 421-423

Lafuente, B., R. T. Downs, H. Yang, and N. Stone, 2015: 1. The power of databases: The RRUFF project. *Highlights in Mineralogical Crystallography*, A. Thomas, and D. Rosa Micaela, Eds., De Gruyter (O), 1-30.doi:10.1515/9783110417104-003

Lapin, A. V., A. V. Tolstov, and I. M. J. G. I. Kulikova, 2016: Distribution of REE, Y, Sc, and Th in the unique complex rare-metal ores of the Tomtor deposit, **54,** 1061-1078.10.1134/s0016702916120065

LARCO, cited 2022: Our Products ─ Slag. [Available online at http://www.larco.gr/slag.php.]

Laskou, M., and M. Economou-Eliopoulos, 2007: The role of microorganisms on the mineralogical and geochemical characteristics of the Parnassos-Ghiona bauxite deposits, Greece. *Journal of Geochemical Exploration*, **93,** 67-77.doi:10.1016/j.gexplo.2006.08.014

Lebedev, V., 2007: Extraction and refining of scandium upon the processing of baddeleyite concentrates. *Theoretical Foundations of Chemical Engineering*, **41,** 718-722.10.1134/S0040579507050466

Levard, C., D. Borschneck, O. Grauby, J. Rose, and J. P. Ambrosi, 2018: Goethite, a tailor-made host for the critical metal scandium: The FexSc(1-x)OOH solid solution. *Geochemical Perspectives Letters*, **9,** 16-20.https://doi.org/10.7185/geochemlet.1832

Li, D., and C. Wang, 1998: Solvent extraction of Scandium (III) by Cyanex 923 and Cyanex 925. *Hydrometallurgy*, **48,** 301-312.https://doi.org/10.1016/S0304-386X(97)00080-7

Liu, X., N. Zhang, H. Sun, J. Zhang, and L. Li, 2011: Structural investigation relating to the cementitious activity of bauxite residue — Red mud. *Cement and Concrete Research*, **41,** 847-853.https://doi.org/10.1016/j.cemconres.2011.04.004

Lockwood, C. L., R. J. G. Mortimer, D. I. Stewart, W. M. Mayes, C. L. Peacock, D. A. Polya, P. R. Lythgoe, A. P. Lehoux, K. Gruiz, and I. T. Burke, 2014: Mobilisation of arsenic from bauxite residue (red mud) affected soils: Effect of pH and redox conditions. *Applied Geochemistry*, **51,** 268-277.https://doi.org/10.1016/j.apgeochem.2014.10.009

Lozano, A., C. Ayora, and A. Fernández-Martínez, 2020a: Sorption of rare earth elements on schwertmannite and their mobility in acid mine drainage treatments. *Applied Geochemistry*, **113,** 104499.https://doi.org/10.1016/j.apgeochem.2019.104499

Lozano, A., C. Ayora, F. Macías, R. León, M. J. Gimeno, and L. Auqué, 2020b: Geochemical behavior of rare earth elements in acid drainages: Modeling achievements and limitations. *Journal of Geochemical Exploration*, **216,** 106577.https://doi.org/10.1016/j.gexplo.2020.106577

Lymperopoulou, T., P. Georgiou, L.-A. Tsakanika, K. Hatzilyberis, and M. Ochsenkuehn-Petropoulou, 2019: Optimizing conditions for scandium extraction from bauxite residue using taguchi methodology. *Minerals*, **9,** 236.https://doi.org/10.3390/min9040236

Machado, J. G., F. A. Brehm, C. A. M. Moraes, C. A. Dos Santos, A. C. F. Vilela, and J. B. M. Da Cunha, 2006: Chemical, physical, structural and morphological characterization of the electric arc furnace dust. *Journal of hazardous materials*, **136,** 953-960.https://doi.org/10.1016/j.jhazmat.2006.01.044

Manoj, B., and A. Kunjomana, 2012: Study of stacking structure of amorphous carbon by X-ray diffraction technique. *Int. J. Electrochem. Sci*, **7,** 3127-3134

Mansfeldt, T., and R. Dohrmann, 2004: Chemical and mineralogical characterization of blast-furnace sludge from an abandoned landfill. *Environmental science & technology*, **38,** 5977-5984.https://doi.org/10.1021/es040002+

Maulana, A., K. Sanematsu, and M. Sakakibara, 2016: An Overview on the Possibility of Scandium and REE Occurrence in Sulawesi, Indonesia. *Indonesian Journal on Geoscience*, **3,** 139-147.DOI:10.17014/ijog.3.2.139-147

McCormick, P., T. Picaro, and P. Smith, 2002: Mechanochemical treatment of high silica bauxite with lime. *Minerals Engineering*, **15,** 211-214.https://doi.org/10.1016/S0892-6875(01)00207-2

McNulty, G., 2007: Production of titanium dioxide. *Proceedings of NORM V international conference, Seville, Spain*, Citeseer, 169-189

Mikeli, E., E. Balomenos, and D. Panias, 2021: Utilizing Recyclable Task-Specific Ionic Liquid for Selective Leaching and Refining of Scandium from Bauxite Residue. *Molecules*, **26,** 818.https://doi.org/10.3390/molecules26040818

Molchanova, T., I. Akimova, K. Smirnov, O. Krylova, and E. Zharova, 2017: Hydrometallurgical methods of recovery of scandium from the wastes of various technologies. *Russian Metallurgy (Metally)*, **2017,** 170-174.DOI: 10.1134/S0036029517030065

Mongelli, G., M. Boni, G. Oggiano, P. Mameli, R. Sinisi, R. Buccione, and N. Mondillo, 2017: Critical metals distribution in Tethyan karst bauxite: The cretaceous Italian ores. *Ore Geology Reviews*, **86,** 526-536.http://dx.doi.org/10.1016/j.oregeorev.2017.03.017

Montgomery, D. C., 2017: *Design and analysis of experiments.* 9th ed. John wiley & sons, 734 pp

Mordberg, L., C. Stanley, and K. Germann, 2001: Mineralogy and geochemistry of trace elements in bauxites: the Devonian Schugorsk deposit, Russia. *Mineralogical Magazine*, **65,** 81-101.https://doi.org/10.1180/002646101550145

Myers, J. E., P. F. Ervin, N. D. Eckhoff, and D. G. Brookins, 1970: The Scandium Content of the Utopia Limestone, Greenwood County, Kansas. *Transactions of the Kansas Academy of Science (1903)***,** 481-485.https://doi.org/10.2307/3627076

O'Neill, L. C., B. A. Elliott, and J. R. Kyle, 2017: Mineralogy and crystallization history of a highly differentiated REE-enriched hypabyssal rhyolite: Round Top laccolith, Trans-Pecos, Texas. *Mineralogy and Petrology*, **111,** 569-592.10.1007/s00710-017-0511-5

Ochsenkuehn-Petropoulou, M., L.-A. Tsakanika, T. Lymperopoulou, K.-M. Ochsenkuehn, K. Hatzilyberis, P. Georgiou, C. Stergiopoulos, O. Serifi, and F. Tsopelas, 2018: Efficiency of sulfuric acid on selective scandium leachability from bauxite residue. *Metals*, **8,** 915.10.3390/met8110915

Ochsenkühn-Petropoulou, M. T., K. S. Hatzilyberis, L. N. Mendrinos, and C. E. Salmas, 2002: Pilot-Plant Investigation of the Leaching Process for the Recovery of Scandium from Red Mud. *Industrial & Engineering Chemistry Research*, **41,** 5794-5801.10.1021/ie011047b

Ochsenkühn-Petropulu, M., T. Lyberopulu, and G. Parissakis, 1994: Direct determination of landthanides, yttrium and scandium in bauxites and red mud from alumina production. *Analytica Chimica Acta*, **296,** 305-313.http://dx.doi.org/10.1016/0003-2670(94)80250-5

Ochsenkühn-Petropulu, M., T. Lyberopulu, K. M. Ochsenkühn, and G. Parissakis, 1996: Recovery of lanthanides and yttrium from red mud by selective leaching. *Analytica Chimica Acta*, **319,** 249-254.https://doi.org/10.1016/0003-2670(95)00486-6

Odo, J. U., W. C. Okafor, S. O. Ekpe, and C. C. Nwogbu, 2014: Extraction of Niobium from Tin Slag. *International Journal of Scientific and Research Publications*, **4**

Olukotun, N., A. R. M. Sam, N. H. A. S. Lim, M. Abdulkareem, I. Mallum, and O. Adebisi, 2021: Mechanical Properties of Tin Slag Mortar. *Recycling*, **6,** 42.https://doi.org/10.3390/recycling6020042

Oqilov, B., M. Botalov, V. Rychkov, E. Kirillov, D. Smyshlyaev, A. Malyshev, A. Taukin, and A. Yuldashbaeva, 2020: Study of scandium leaching from the red mud by succinic acid. *AIP Conference Proceedings*, AIP Publishing LLC, 050022

Pedram, H., M. R. Hosseini, and A. Bahrami, 2020: Utilization of A. niger strains isolated from pistachio husk and grape skin in the bioleaching of valuable elements from red mud. *Hydrometallurgy*, **198,** 105495.10.1016/j.hydromet.2020.105495

Peters, E. M., Ş. Kaya, C. Dittrich, and K. Forsberg, 2019: Recovery of Scandium by Crystallization Techniques. *Journal of Sustainable Metallurgy*, **5,** 48-56.10.1007/s40831-019-00210-4

Petrakova, O. V., A. V. Panov, S. N. Gorbachev, G. N. Klimentenok, A. V. Perestoronin, S. E. Vishnyakov, and V. S. Anashkin, 2015: Improved efficiency of red mud processing through scandium oxide recovery. *Light Metals 2015*, Springer, 93-96.https://doi.org/10.1007/978-3-319-48248-4_17

Petrella, L., A. E. Williams-Jones, J. Goutier, and J. Walsh, 2014: The nature and origin of the rare earth element mineralization in the Misery syenitic intrusion, northern Quebec, Canada. *Economic Geology*, **109,** 1643-1666.https://doi.org/10.2113/econgeo.109.6.1643

Philander, C., and A. Rozendaal, 2009: Mineral intricacies of the Namakwa Sands mineral resource. *The 7th International Heavy Minerals Conference 'What next*

Pingitore, N., J. Clague, and D. Gorski, 2014: Round Top Mountain rhyolite (Texas, USA), a massive, unique Y-bearing-fluorite-hosted heavy rare earth element (HREE) deposit. *Journal of Rare Earths*, **32,** 90-96.10.1016/S1002-0721(14)60037-5

Plotnikov, I., and Y. D. Milovidov, 1963: Origin of bauxites of the northern urals. *International Geology Review*, **5,** 71-78.DOI:10.1080/00206816309474680

Power, G., M. Gräfe, and C. Klauber, 2011: Bauxite residue issues: I. Current management, disposal and storage practices. *Hydrometallurgy*, **108,** 33-45.https://doi.org/10.1016/j.hydromet.2011.02.006

Qin, H.-B., S. Yang, M. Tanaka, K. Sanematsu, C. Arcilla, and Y. Takahashi, 2020: Chemical speciation of scandium and yttrium in laterites: new insights into the control of their partitioning behaviors. *Chemical Geology*, **552,** 119771.https://doi.org/10.1016/j.chemgeo.2020.119771

——, 2021: Scandium immobilization by goethite: Surface adsorption versus structural incorporation. *Geochimica et Cosmochimica Acta*, **294,** 255-272.https://doi.org/10.1016/j.gca.2020.11.020

Qu, Y., and B. Lian, 2013: Bioleaching of rare earth and radioactive elements from red mud using Penicillium tricolor RM-10. *Bioresource Technology*, **136,** 16-23.https://doi.org/10.1016/j.biortech.2013.03.070

Qu, Y., H. Li, X. Wang, W. Tian, B. Shi, M. Yao, and Y. Zhang, 2019: Bioleaching of Major, Rare Earth, and Radioactive Elements from Red Mud by using Indigenous Chemoheterotrophic Bacterium Acetobacter sp. *Minerals*, **9,** 67.10.3390/min9020067

Radusinović, S., and A. Papadopoulos, 2021: The Potential for REE and Associated Critical Metals in Karstic Bauxites and Bauxite Residue of Montenegro. *Minerals*, **11,** 975.https://doi.org/10.3390/min11090975

Raw Materials Information System, cited 2021: RMIS – Raw Materials Profiles - Tin. [Available online at https://rmis.jrc.ec.europa.eu/apps/rmp2/#/Tin.]

——, cited 2021: RMIS – Raw Materials Profiles - Nickel. [Available online at https://rmis.jrc.ec.europa.eu/apps/rmp2/#/Nickel.]

Reinhardt, N., J. A. Proenza, C. Villanova-de-Benavent, T. Aiglsperger, T. Bover-Arnal, L. Torró, R. Salas, and A. Dziggel, 2018: Geochemistry and mineralogy of rare earth elements (REE) in Bauxitic ores of the Catalan Coastal Range, NE Spain. *Minerals*, **8,** 562.doi:10.3390/min8120562

Remmen, K., R. Schäfer, S. Hedwig, T. Wintgens, M. Wessling, and M. Lenz, 2019: Layer-by-layer membrane modification allows scandium recovery by nanofiltration. *Environmental Science: Water Research & Technology*, **5,** 1683-1688.10.1039/C9EW00509A

Retallack, G. J., 2010: Lateritization and bauxitization events. *Economic Geology*, **105,** 655-667.DOI: 10.2113/gsecongeo.105.3.655

RioTinto: Rio Tinto enters scandium market with construction of new plant in Canada. [Available online at https://www.riotinto.com/news/releases/2021/Rio-Tinto-enters-scandium-market-with-construction-of-new-plant-in-Canada.]

Rudnick, R. L., and S. Gao, 2014: *Composition of the continental crust.* Oxford, Elsevier.https://doi.org/10.1016/B978-0-08-095975-7.00301-6

RUSAL, cited 2022: Scandium-oxide. [Available online at https://rusal.ru/en/innovation/technology/scandium-oxide/.]

Rüttinger, L., R. Treimer, G. Tiess, and L. Griestop, 2016: Umwelt- und Sozialauswirkungen der Bauxitgewinnung und –weiterverarbeitung in der Boké und Kindia-Region, Guinea. *adelphi*

Rychkov, V., M. Botalov, E. Kirillov, S. Kirillov, V. Semenishchev, G. Bunkov, and D. Smyshlyaev, 2021: Intensification of carbonate scandium leaching from red mud (bauxite residue). *Hydrometallurgy*, **199,** 105524.https://doi.org/10.1016/j.hydromet.2020.105524

Rychkov, V. N., E. Kirillov, S. Kirillov, G. Bunkov, M. Mashkovtsev, M. Botalov, V. Semenishchev, and V. Volkovich, 2016: *Selective ion exchange recovery of rare earth elements from uranium mining solutions.* Vol. 1767, 020017 pp.10.1063/1.4962601

Samson, I. M., and M. Chassé, 2016: Scandium. *Encyclopedia of Geochemistry: A Comprehensive Reference Source on the Chemistry of the Earth*, W. M. White, Ed., Springer International Publishing, 1-5.10.1007/978-3-319-39193-9_281-1

Schetelig, J., 1911: Über thortveitit, ein neues Mineral. *Centralblatt für Mineralogie, Geologie, und Paläontologie*, **721,** 726

Schmid, T., R. Jungnickel, and P. Dariz, 2020: Insights into the CaSO4–H2O System: A Raman-Spectroscopic Study. *Minerals*, **10,** 115.https://doi.org/10.3390/min10020115

Schrijvers, D., A. Hool, G. Blengini, W. Chen, J. Dewulf, R. Eggert, L. van Ellen, R. Gauss, J. Goddin, K. Habib, C. Hagelüken, A. Hirohata, M. Hofmann-Amtenbrink, J. Kosmol, M. Gleuher, M. Grohol, A. Ku, M.-H. Lee, G. Liu, and P. Wäger, 2020: A review of methods and data to determin raw material criticality. *Resources, Conservation and Recycling*, **155**.10.1016/j.resconrec.2019.104617

Semenishchev, V., 2018: Recovery of rare earths and scandium from uranium leachates. Presentation during: European Scandium Inventory Workshop, Berlin 2018; http://scale-project.eu/scandium-workshop/

Siegfried, P., and F. Wall, 2018: *In search of the forgotten rare earth.* Vol. 28, 10-15 pp.10.1144/geosci2018-021

Singhal, S. C., 2007: Solid Oxide Fuel Cells. *The Electrochemical Society Interface*, **16,** 41-44.10.1149/2.f06074if

Smirnov, A. L., S. M. Titova, V. N. Rychkov, G. Bunkov, V. Semenishchev, E. Kirillov, N. N. N. Poponin, and I. A. Svirsky, 2017: *Study of scandium and thorium sorption from uranium leach liquors.* Vol. 312, 277-283 pp.10.1007/s10967-017-5234-x

Snars, K., and R. J. Gilkes, 2009: Evaluation of bauxite residues (red muds) of different origins for environmental applications. *Applied Clay Science*, **46,** 13-20.http://dx.doi.org/10.1016/j.clay.2009.06.014

Sofilic, T., V. Novosel-Radovic, S. Cerjan-Stefanovic, and A. Rastovcan-Mioc, 2005: The mineralogical composition of dust from an electric arc furnace. *Materiali in tehnologije*, **39,** 149

Stambouli, A. B., and E. Traversa, 2002: Solid oxide fuel cells (SOFCs): a review of an environmentally clean and efficient source of energy. *Renewable and Sustainable Energy Reviews*, **6,** 433-455.https://doi.org/10.1016/S1364-0321(02)00014-X

Stoy, L., V. Diaz, and C.-H. Huang, 2021: Preferential Recovery of Rare-Earth Elements from Coal Fly Ash Using a Recyclable Ionic Liquid. *Environmental Science & Technology*, **55,** 9209-9220.10.1021/acs.est.1c00630

Sugita, K., Y. Kobayashi, Y. Taguchi, S. Takeda, Y. Ota, M. Ojiri, K. Oda, and H. Sano, 2015: Method of recovering rare-earth elements, Patent Nr. US 2015/0086449 A1. C22B59/00 ed.

Suss, A., 2018: Bauxite residue as raw material for scandium oxide recovery- UC RUSAL experience. Presentation during: European Scandium Inventory Workshop, Berlin 2018; http://scale-project.eu/scandium-workshop/

Suss, A., N. Kuznetsova, A. Kozyrev, A. Panov, and S. Gorbachev, 2018: Specific features of scandium behavior during sodium bicarbonate digestion of red mud. *TMS Annual Meeting & Exhibition*, Springer, 165-173.https://doi.org/10.1007/978-3-319-72284-9_22

Sutar, H., S. C. Mishra, S. K. Sahoo, and H. Maharana, 2014: Progress of red mud utilization: an overview. *American Chemical Science Journal*, **4**

Taggart, R. K., J. C. Hower, G. S. Dwyer, and H. Hsu-Kim, 2016: Trends in the Rare Earth Element Content of U.S.-Based Coal Combustion Fly Ashes. *Environmental Science & Technology*, **50,** 5919-5926.10.1021/acs.est.6b00085

Taxiarchou, M., D. Panias, I. Douni, I. Paspaliaris, and A. Kontopoulos, 1997: Dissolution of hematite in acidic oxalate solutions. *Hydrometallurgy*, **44,** 287-299.https://doi.org/10.1016/S0304-386X(96)00075-8

Tayibi, H., M. Choura, F. A. Lopez, F. J. Alguacil, and A. López-Delgado, 2009: Environmental impact and management of phosphogypsum. *Journal of environmental management*, **90,** 2377-2386

Teitler, Y., M. Cathelineau, M. Ulrich, J. P. Ambrosi, M. Munoz, and B. Sevin, 2019: Petrology and geochemistry of scandium in New Caledonian Ni-Co laterites. *Journal of Geochemical Exploration*, **196,** 131-155.https://doi.org/10.1016/j.gexplo.2018.10.009

Texas Mineral Resources: TEXAS MINERAL RESOURCES CONSORTIUM AWARDED SECOND PHASE OF U.S. DEPARTMENT OF ENERGY (DOE) CONTRACT TARGETING PRODUCTION OF MIXED RARE EARTH OXIDES FROM PENNSYLVANIA COAL-BASED RESOURCES. [Available online at http://tmrcorp.com/news/press_releases/index.php?content_id=237.]

The International Aluminium Institute, cited 2020: Opportunities for use of bauxite residue in Supplementary Cementitious Materials. [Available online at http://www.world-aluminium.org/media/filer_public/2020/03/16/opportunities_for_use_of_bauxite_residue_in_supplementary_cementitious_materials_2020.pdf.]

Tolstov, A., and A. Gunin, 2001: Comprehensive assessment of the Tomtor deposit. *Vestnik VGU*, **11,** 144-160

U.S. Geological Survey, 1996: Mineral Commodity Summaries 1996. 1996. [Available online at http://pubs.er.usgs.gov/publication/mineral1996.]

——, 2019: Mineral Commodity Summaries 2019,Reston, VA. [Available online at http://pubs.er.usgs.gov/publication/70202434.]

——, 2021: Mineral commodity summaries 2021,Reston, VA, 200 pp. [Available online at http://pubs.er.usgs.gov/publication/mcs2021.]

Ujaczki, É., Y. S. Zimmermann, C. A. Gasser, M. Molnár, V. Feigl, M. Lenz, and Biotechnology, 2017: Red mud as secondary source for critical raw materials–extraction study. *Journal of Chemical Technology & Biotechnology*, **92,** 2835-2844.https://doi.org/10.1002/jctb.5300

Ujaczki, É., V. Feigl, M. Molnár, P. Cusack, T. Curtin, R. Courtney, L. O'Donoghue, P. Davris, C. Hugi, M. W. Evangelou, E. Balomenos, and M. Lenz, 2018: Re-using bauxite residues: benefits beyond (critical raw) material recovery, **93,** 2498-2510.10.1002/jctb.5687

Ulrich, M., M. Cathelineau, M. Muñoz, M.-C. Boiron, Y. Teitler, and A. M. Karpoff, 2019: The relative distribution of critical (Sc, REE) and transition metals (Ni, Co, Cr, Mn, V) in some Ni-laterite deposits of New Caledonia. *Journal of Geochemical Exploration*, **197,** 93-113.https://doi.org/10.1016/j.gexplo.2018.11.017

Ulrich, T., B. Kamber, P. Jugo, and D. Tinkham, 2009: Imaging element-distribution patterns in minerals by laser ablation - Inductively coupled plasma - Mass spectrometry (LA-ICP-MS). *Canadian Mineralogist - CAN MINERALOG*, **47,** 1001-1012.10.3749/canmin.47.5.1001

Valeton, I., 1962: Petrographie und Genese von Bauxitlagerstätten, Petrography and genesis of bauxite deposits (in German). *Geologische Rundschau*, **52,** 448-474

Valeton, I., 1972: *Bauxites.* Vol. 1, Elsevier, 226 pp

Valeton, I., M. Biermann, R. Reche, and F. Rosenberg, 1987: Genesis of nickel laterites and bauxites in greece during the jurassic and cretaceous, and their relation to ultrabasic parent rocks. *Ore Geology Reviews*, **2,** 359-404.http://dx.doi.org/10.1016/0169-1368(87)90011-4

Vanderpool, C. D., M. B. MacInnis, and J. A. Ladd, 1986: Recovery of tungsten, scandium, iron, and manganese values from tungsten bearing material, Patent Nr. 46,247,03.

Verbaan, N., M. Johnson, T. Grammatikopoulos, E. Larochelle, S. Honan, K. Smith, and R. Sixberry, 2018: A Process Flowsheet for the Extraction of Niobium, Titanium, and Scandium from Niocorp's Elk Creek Deposit. Cham, Springer International Publishing, 2523-2539.10.1007/978-3-319-95022-8_213

Vind, J., A. Malfliet, C. Bonomi, P. Paiste, I. E. Sajó, B. Blanpain, A. H. Tkaczyk, V. Vassiliadou, and D. Panias, 2018: Modes of occurrences of scandium in Greek bauxite and bauxite residue. *Minerals Engineering*, **123,** 35-48.https://doi.org/10.1016/j.mineng.2018.04.025

Vogel, C., M. C. Hoffmann, O. Krüger, V. Murzin, W. Caliebe, and C. Adam, 2020: Chromium (VI) in phosphorus fertilizers determined with the diffusive gradients in thin-films (DGT) technique. *Environmental Science and Pollution Research***,** 1-9.https://doi.org/10.1007/s11356-020-08761-w

von Billerbeck, E., A. Ruh, and D.-S. Kim, 2014: Verarbeitung von Filterstäuben aus der Elektrostahlerzeugung im Wälzprozess. *Mineralische Nebenprodukte und Abfälle–Flaschen, Schlacken, Stäube und Baurestmassen. Neuruppin: TK Verlag***,** 387-398

Von Knorring, O., and E. Condliffe, 1987: Mineralized pegmatites in Africa. *Geological Journal*, **22,** 253-270.https://doi.org/10.1002/gj.3350220619

Von Knorring, O., T. Clifford, and I. Gass, 1970: Mineralogical and geochemical aspects of pegmatites from orogenic belts of equatorial and southern Africa. *African Magmatism and Tectonics***,** 157-184

Wagh, A. S., and W. R. Pinnock, 1987: Occurrence of scandium and rare earth elements in Jamaican bauxite waste. *Economic Geology*, **82,** 757-761.https://doi.org/10.2113/gsecongeo.82.3.757

Wakui, Y., H. Matsunaga, and T. M. Suzuki, 1989: Selective Recovery of Trace Scandium from Acid Aqueous Solution with (2-Ethylhexyl hydrogen 2-ethylhexylphosphonate)-Impregnated Resin. *Analytical Sciences*, **5,** 189-193.10.2116/analsci.5.189

Wang, L., P. Wang, W.-Q. Chen, Q.-Q. Wang, and H.-S. Lu, 2020: Environmental impacts of scandium oxide production from rare earths tailings of Bayan Obo Mine. *Journal of Cleaner Production*, **270,** 122464.https://doi.org/10.1016/j.jclepro.2020.122464

Wang, W., Y. Pranolo, and C. Y. Cheng, 2011: Metallurgical processes for scandium recovery from various resources: A review. *Hydrometallurgy*, **108,** 100-108.https://doi.org/10.1016/j.hydromet.2011.03.001

——, 2013: Recovery of scandium from synthetic red mud leach solutions by solvent extraction with D2EHPA. *Separation and Purification Technology*, **108,** 96-102

Wang, Z., M. Y. H. Li, Z.-R. R. Liu, and M.-F. Zhou, 2021: Scandium: Ore deposits, the pivotal role of magmatic enrichment and future exploration. *Ore Geology Reviews*, **128,** 103906.https://doi.org/10.1016/j.oregeorev.2020.103906

Webminerals, cited 2022: The Evje and Iveland Pegmatite District. [Available online at http://www.smartminerals.com/norvegia/trip/Evje_Iveland.htm.]

Willey, L. A., 1971: Aluminum Scandium Alloy, Patent Nr. US US3619181A.

Williams-Jones, A. E., and O. V. Vasyukova, 2018: The Economic Geology of Scandium, the Runt of the Rare Earth Element Litter. *Economic Geology*, **113,** 973-988.10.5382/econgeo.2018.4579

World Aluminium, cited 2020: Opportunities for use of bauxite residue in Supplementary Cementitious Materials. [Available online at https://bauxite.world-aluminium.org/fileadmin/user_upload/Opportunities_for_use_of_bauxite_residue_in_Supplementary_Cementious_Materials.pdf.]

World Steel Association, 2020: Steel Statistical Yearbook 2020 concise version. [Available online at https://www.worldsteel.org/steel-by-topic/statistics/steel-statistical-yearbook.html.]

Wu, F., 2012: Aluminous goethite in the Bayer process and its impact on alumina recovery and settling, PhD Thesis, Curtin University.

Xue, A., X.-h. Chen, and X.-n. Tang, 2010: The technological study and leaching kinetics of scandium from red mud. *Nonferrous Metals Extr. Metall*, **2,** 51-53

Yagmurlu, B., W. Zhang, M. J. Heikkilä, R. T. Koivula, and B. Friedrich, 2019: Solid-State Conversion of Scandium Phosphate into Scandium Oxide with Sodium Compounds. *Industrial & Engineering Chemistry Research*, **58,** 14609-14620.10.1021/acs.iecr.9b02411

Yagmurlu, B., W. Zhang, D. Avdibegovic, M. Regadío, R. Koivula, C. Dittrich, K. Binnemans, and B. Friedrich, 2018: Advances in scandium recovery beyond state of the art. *Proceedings of the ALTA 2018 Uranium-REE-Lithium Conference, Perth (Australia), 19-26 May 2018.*, ALTA Metallurgical Services (ALTA); Perth. Australia, 85-93

Yagmurlu, B., B. Orberger, C. Dittrich, G. Croisé, R. Scharfenberg, E. Balomenos, D. Panias, E. Mikeli, C. Maier, R. Schneider, B. Friedrich, P. Dräger, F. Baumgärtner, M. Schmitz, P. Letmathe, K. Sakkas, C. Georgopoulos, and H. van den Laan, 2021: Sustainable Supply of Scandium for the EU Industries from Liquid Iron Chloride Based TiO2 Plants. *Materials Proceedings*, **5,** 86

Yamamoto, T., 2008: Assignment of pre-edge peaks in K-edge x-ray absorption spectra of 3d transition metal compounds: electric dipole or quadrupole? *X-Ray Spectrometry*, **37,** 572-584.10.1002/xrs.1103

Zhang, B., X. Xue, X. Huang, H. Yang, and J. Han, 2017: Study on Leaching Valuable Elements from Bayan Obo Tailings. *Proceedings of the 3rd Pan American Materials Congress*, Cham, Springer International Publishing, 633-641

Zhang, J.-j., Z.-g. Deng, and T.-h. Xu, 2005: Experimental investigation on leaching metals from red mud. *Light Metals*, **2,** 13-15

Zhang, L., T.-A. Zhang, G. Lv, W. Zhang, T. Li, and X. Cao, 2021: Separation and Extraction of Scandium from Titanium Dioxide Waste Acid. *JOM*, **73,** 1301-1309.10.1007/s11837-021-04629-7

Zhang, N., H.-X. Li, and X.-M. Liu, 2016: Recovery of scandium from bauxite residue—red mud: a review. *Rare Metals*, **35,** 887-900.https://doi.org/10.1007/s12598-016-0805-5

Zhang, Y., N. Kallay, and E. Matijevic, 1985: Interaction of metal hydrous oxides with chelating agents. 7. Hematite-oxalic acid and-citric acid systems. *Langmuir*, **1,** 201-206.https://doi.org/10.1021/la00062a004

Zhong, X., and Y. Wu, 2012: Recovery of uranium and thorium from zirconium oxychloride by solvent extraction. *Journal of Radioanalytical and Nuclear Chemistry*, **292,** 355-360

Zinoveev, D., P. Grudinsky, E. Zhiltsova, D. Grigoreva, A. Volkov, V. Dyubanov, and A. Petelin, 2021: Research on High-Pressure Hydrochloric Acid Leaching of Scandium, Aluminum and Other Valuable Components from the Non-Magnetic Tailings Obtained from Red Mud after Iron Removal. *Metals*, **11,** 469.https://doi.org/10.3390/met11030469

Appendix

Appendix A – Additional information to introduction

Table A 1 Compilation of reported Sc recoveries in % achieved by leaching of BR with different approaches and the respective reference. This table comprises the data underlying Figure 1 in the introduction.

Nr	Inorganic acid	Organic acid	Bio leaching	Alkaline leaching	Ionic liquid	Reference	leaching agent
1	50					Ochsenkuehn-Petropoulou et al. (2018)	H_2SO_4
2	48					Ochsenkühn-Petropulu et al. (1996)	HNO_3
3	75					Ochsenkühn-Petropulu et al. (1996)	HNO_3
4	80					Ochsenkühn-Petropulu et al. (1996)	HNO_3
5	74					Ochsenkühn-Petropulu et al. (1996)	HNO_3
6	78					Ochsenkühn-Petropulu et al. (1996)	HNO_3
7	79					Ochsenkühn-Petropulu et al. (1996)	HNO_3
8	80					Ochsenkühn-Petropulu et al. (1996)	HNO_3
9	68					Ochsenkühn-Petropulu et al. (1996)	HCl
11		24				Borra et al. (2015)	Acetic acid
12		49				Borra et al. (2015)	Methanosulfonic
13		43				Borra et al. (2015)	Citric acid
14	48					Borra et al. (2015)	HCl
15	48					Borra et al. (2015)	H_2SO_4
16	46					Borra et al. (2015)	HNO_3
17	47					Borra et al. (2015)	HCl, 0.5N
18	49					Borra et al. (2015)	HCl, 1.5N
19	55					Borra et al. (2015)	HCl, 3N
20	77					Borra et al. (2015)	HCl, 6N
21	45					Borra et al. (2015)	HCl, 0.5N
22	49					Borra et al. (2015)	HCl, 3N
23	80					Xue et al. (2010)	H_2SO_4
24	80					Zhang et al. (2005)	HCl
25	54					Ochsenkühn-Petropoulou et al. (2002)	HNO_3

Nr	Inorganic acid	Organic acid	Bio leaching	Alkaline leaching	Ionic liquid	Reference	leaching agent
26	51					Ochsenkühn-Petropoulou et al. (2002)	HNO_3
27	44					Ochsenkühn-Petropoulou et al. (2002)	HNO_3
28	51					Ochsenkühn-Petropoulou et al. (2002)	HNO_3
29	68					Ochsenkühn-Petropoulou et al. (2002)	HNO_3
30	73					Ochsenkühn-Petropoulou et al. (2002)	HNO_3
31	10					Sugita et al. (2015)	H_2SO_4
32	57					Sugita et al. (2015)	H_2SO_4
33	26					Sugita et al. (2015)	H_2SO_4
34	32					Sugita et al. (2015)	H_2SO_4
35	36					Sugita et al. (2015)	H_2SO_4
36	1					Sugita et al. (2015)	H_2SO_4
37	11					Sugita et al. (2015)	H_2SO_4
38	14					Sugita et al. (2015)	H_2SO_4
39	16					Sugita et al. (2015)	H_2SO_4
40	23					Sugita et al. (2015)	H_2SO_4
41	29					Sugita et al. (2015)	H_2SO_4
42	36					Sugita et al. (2015)	H_2SO_4
43	17					Sugita et al. (2015)	H_2SO_4
44	11					Sugita et al. (2015)	H_2SO_4
45	43					Sugita et al. (2015)	H_2SO_4
46	16					Sugita et al. (2015)	H_2SO_4
47	5					Sugita et al. (2015)	HCl
48	2					Sugita et al. (2015)	HNO_3
49	6					Sugita et al. (2015)	H_2SO_4
50	13					Sugita et al. (2015)	H_2SO_4
51	6					Sugita et al. (2015)	HNO_3
52	2					Sugita et al. (2015)	H_3PO_4
53	0.2					Sugita et al. (2015)	H_2SO_4

Nr	Inorganic acid	Organic acid	Bio leaching	Alkaline leaching	Ionic liquid	Reference	leaching agent
54	32					Wang et al. (2013)	H_2SO_4
55	48					Wang et al. (2013)	H_2SO_4
56	18					Wang et al. (2013)	HCl
57	22					Wang et al. (2013)	HNO_3
58				26		Petrakova et al. (2015)	$NaHCO_3$
59				22.9		Rychkov et al. (2021)	CO_2
60				39.3		Rychkov et al. (2021)	CO_2
61					66	Bonomi et al. (2018)	1-ethyl-3-methyllimidazolium hydrogensulfate [Emim][HSO_4]
62					66	Bonomi et al. (2018)	[Emim][HSO_4]
63					65	Bonomi et al. (2018)	[Emim][HSO_4]
64					69	Bonomi et al. (2018)	[Emim][HSO_4]
65					35	Davris et al. (2018)	hydrophobic ionic liquid betainium bis(trifluoromethylsulfonyl)imide [Hbet][Tf2N]
66					37	Davris et al. (2018)	[Hbet][Tf2N]
67					37	Davris et al. (2018)	[Hbet][Tf2N]
68					44	Davris et al. (2018)	[Hbet][Tf2N]
69			70			Qu and Lian (2013)	Penicillium tricolor
70			40			Qu and Lian (2013)	Aspergillus niger
71	32					Ujaczki et al. (2017)	HCl
72	30					Ujaczki et al. (2017)	H_2SO_4
73	31					Ujaczki et al. (2017)	HNO_3
74		36				Ujaczki et al. (2017)	Citric acid
75		2				Ujaczki et al. (2017)	Oxalic acid
76			42			Kiskira et al. (2021)	Acerobacter tropicalis
77			38			Pedram et al. (2020)	Aspergillus niger

Nr	Inorganic acid	Organic acid	Bio leaching	Alkaline leaching	Ionic liquid	Reference	leaching agent
78		72				Bogomazov and Senyuta (2017)	Formic acid
79		65				Bogomazov and Senyuta (2017)	Acetic acid
80		68				Bogomazov and Senyuta (2017)	Mixture formic acetic acid
81			52			Qu et al. (2019)	Acetobacter sp.
Number	**56**	**8**	**5**	**3**	**8**		

Appendix B – Additional Information to chapter 2

Table B 1 Major element mass fractions (%) expressed as oxides determined by X-ray fluorescence for secondary materials analyzed for Scandium inventory.

Element oxide in wt%	Greek Bauxite Residue		German Bauxite residue			Hungarian Bauxite Residue		Russian Bauxite residue		Acid Slurry*	Filtercake	
	1	2	1	2	3	1	2	1	2		1	2
Al_2O_3	15.96	18.91	17.91	15.94	14.67	16.00	16.83	14.38	17.75	0.21	5.62	5.23
B_2O_3	*b.d.*	*b.d.*	*b.d.*	*b.d.*	*b.d.*	*b.d.*	*b.d.*	*b.d.*	*b.d.*	*b.d.*	0.00	0.00
BaO	*b.d.*	*b.d.*	*b.d.*	*b.d.*	*b.d.*	*b.d.*	*b.d.*	*b.d.*	*b.d.*	0.02	0.05	0.03
CO_2	*b.d.*	*b.d.*	*b.d.*	*b.d.*	*b.d.*	2.30	0.00	*b.d.*	*b.d.*	57.91	0.00	0.00
CaO	10.28	9.03	4.30	3.21	3.67	13.37	13.68	13.31	7.11	0.11	7.68	7.76
CeO_2	0.06	0.07	0.07	0.06	0.07	0.05	0.08	0.09	0.10	*b.d.*	0.10	0.26
Cl	0.13	0.07	0.17	0.05	0.05	0.02	0.01	0.02	0.04	0.30	13.53	12.97
Cr_2O_3	0.30	0.33	0.44	0.23	0.35	0.10	0.14	0.05	0.05	0.07	1.00	0.96
F	*b.d.*	*b.d.*	*b.d.*	*b.d.*	*b.d.*	0.04	*b.d.*	*b.d.*	*b.d.*	*b.d.*	*b.d.*	*b.d.*
Fe_2O_3	49.02	49.66	46.19	56.72	58.23	40.80	38.21	52.49	51.72	0.05	27.47	25.01
I	*b.d.*	*b.d.*	*b.d.*	*b.d.*	*b.d.*	*b.d.*	*b.d.*	*b.d.*	*b.d.*	*b.d.*	*b.d.*	*b.d.*
K_2O	0.10	0.09	0.11	0.11	0.08	0.11	0.10	0.08	0.48	*b.d.*	0.03	0.05
MgO	0.24	0.27	0.14	*b.d.*	0.14	0.51	0.87	1.01	1.12	0.02	3.11	2.84
MnO	0.01	0.02	0.57	0.05	0.06	0.32	0.18	0.32	0.75	0.01	6.45	5.58
Na_2O	5.55	3.15	7.21	6.72	6.04	7.31	6.14	2.37	8.04	*b.d.*	0.12	0.08
NiO	0.11	0.14	b.d.	*b.d.*	*b.d.*	0.05	0.05	0.03	0.06	0.01	0.08	0.06
P_2O_5	0.13	0.17	0.60	0.43	0.54	0.31	0.30	1.28	0.49	0.07	0.12	0.13
SO_3	0.49	0.47	0.66	0.74	0.32	0.63	1.02	2.18	1.54	5.45	3.27	3.02
Sc_2O_3	0.01	b.d.	0.01	0.01	*b.d.*	0.01	b.d.	0.01	*b.d.*	0.01	0.05	0.05
SiO_2	9.14	6.53	9.81	7.75	7.09	11.85	10.69	7.07	*b.d.*	13.45	2.44	3.22
SnO_2	*b.d.*	*b.d.*	*b.d.*	*b.d.*	*b.d.*	*b.d.*	*b.d.*	*b.d.*	*b.d.*	*b.d.*	0.03	0.03
SrO	0.01	0.01	0.01	0.02	0.01	0.06	0.07	0.47	0.08	*b.d.*	0.01	0.01
Ta_2O_5	*b.d.*	*b.d.*	*b.d.*	*b.d.*	*b.d.*	*b.d.*	*b.d.*	*b.d.*	0.01	0.04	0.07	0.06
TiO_2	6.21	5.95	11.86	7.32	8.98	3.62	4.24	4.74	4.75	36.36	20.56	25.43
WO_3	*b.d.*	0.02	*b.d.*	*b.d.*	*b.d.*	*b.d.*	*b.d.*	*b.d.*	0.02	0.05	0.03	0.03
ZrO_2	0.16	0.14	0.35	0.24	0.30	0.09	0.09	0.14	0.13	0.23	1.30	1.49

*Prepared with wax, b.d.= below detection limit

Table B 1 (continued) Major element mass fractions (%) expressed as oxides determined by X-ray fluorescence for secondary materials analyzed for Scandium inventory.

Element oxide in wt%	EAF Slag Ni-prod.	Sn slag	Phosphogypsum				Dross
			African	Greek	Lithuania 1	Lithuania 2	
Al_2O_3	4.67	10.04	0.16	0.15	0.08	0.20	balance
B_2O_3	*b.d.*	*b.d.*	*b.d.*	*b.d.*	*b.d.*	*b.d.*	*b.d.*
BaO	*b.d.*	0.21	*b.d.*	0.03	0.06	0.04	*b.d.*
CO_2	*b.d.*	2.85	2.07	6.24	5.84	*b.d.*	*b.d.*
CaO	4.10	17.68	35.61	37.53	36.62	36.34	0.18
CeO_2	*b.d.*	0.68	0.12	*b.d.*	0.24	0.15	*b.d.*
Cl	0.21	0.01	*b.d.*	0.01	*b.d.*	*b.d.*	0.65
Cr_2O_3	n.d.	0.26	*b.d.*	*b.d.*	*b.d.*	*b.d.*	0.02
F	*b.d.*	0.25	0.45	1.46	0.32	0.68	0.64
Fe_2O_3	37.75	18.97	0.10	0.04	0.15	0.06	0.51
I	*b.d.*	0.29	*b.d.*	*b.d.*	*b.d.*	*b.d.*	*b.d.*
K_2O	0.46	0.78	0.04	*b.d.*	0.03	0.06	0.43
MgO	6.38	2.70	b.d.	*b.d.*	*b.d.*	*b.d.*	2.43
MnO	0.31	0.58	*b.d.*	*b.d.*	*b.d.*	*b.d.*	0.02
Na_2O	0.32	1.11	0.10	0.04	0.02	0.15	1.02
NiO	0.08	*b.d.*	*b.d.*	*b.d.*	*b.d.*	*b.d.*	0.01
P_2O_5	0.02	0.88	1.83	0.63	0.56	1.60	0.02
SO_3	0.34	0.91	66.83	50.55	52.20	46.41	0.02
Sc_2O_3	*b.d.*	0.01	*b.d.*	*b.d.*	*b.d.*	*b.d.*	5.47
SiO_2	28.60	20.80	0.09	1.30	0.35	1.11	0.08
SnO_2	*b.d.*	2.36	*b.d.*	*b.d.*	*b.d.*	*b.d.*	*b.d.*
SrO	0.01	0.02	0.37	0.11	1.85	0.70	0.02
Ta_2O_5	*b.d.*	0.52	*b.d.*	*b.d.*	*b.d.*	*b.d.*	*b.d.*
TiO_2	0.24	5.14	*b.d.*	0.02	0.15	0.03	0.07
WO_3	0.12	1.94	0.01	*b.d.*	*b.d.*	*b.d.*	0.13
ZrO_2	*b.d.*	2.15	*b.d.*	*b.d.*	*b.d.*	*b.d.*	0.23

n.d.= not determined, b.d.= below detection limit, balance= Al_2O_3 was set to make up the residual mass fraction

Table B 2 Sc and total rare earth element (REE) mass fractions for the investigated wastes and residues determined by ICP-MS. The average (avg.) share of Sc of the total REE and the avg. and minimum Sc_2O_3 share of monetary value of all rare earth oxides (REO) is also given.

Sector	Sample	Sc	Sum of all REE	Avg. share of Sc of all REE	Avg. share of monetary value of Sc_2O_3 of total REO	Minimum share of monetary value of Sc_2O_3 of total REO
		mg/kg	mg/kg	%	%	%
Al_2O_3	**Bauxite residue Greece 1**	104 ± 1.6	800 ± 17.7	13	89	85
	Bauxite residue Greece 2	99 ± 8.4	876 ± 51.5	11	88	73
	Bauxite residue Germany 1	55 ± 3.8	527 ± 18.3	11	85	74
	Bauxite residue Germany 2	52 ± 6.5	458 ± 11.2	11	86	68
	Bauxite residue Germany 3	57 ± 5.9	522 ± 22.8	11	87	69
	Bauxite residue Hungary 1	94 ± 1.6	1143 ± 20.7	8	83	79
	Bauxite residue Hungary 2	84 ± 1.2	1033 ± 8.6	8	82	79
	Bauxite residue Russia 1	102 ± 5.3	1605 ± 27.9	6	75	67
	Bauxite residue Russia 2	70 ± 4.2	1269 ± 37.5	6	74	63
TiO_2	**TiO_2 liquid**	119 ± 10.5	707 ± 67.4	17	91	73
	TiO_2 solid	51 ± 0.6	321 ± 4.7	16	87	85
	TiO_2 Filtercake 1	333 ± 1	2138 ± 17.9	16	90	89
	TiO_2 Filtercake 2	259 ± 3.1	1750 ± 28.9	15	89	86
Ni	**Electric arc furnace slag**	79 ± 21.5	133 ± 23.2	60	98	56
Zn	**Tin slag**	123 ± 6.8	9367 ± 750.5	1	38	28
H_3PO_4 (fertilizer)	**PG Africa**	1 ± 0.1	2523 ± 50.1	< 1	2	1
	PG Greece	12 ± 10.9	252 ± 15.9	5	66	4
	PG Lithuania 1	1 ± 0.1	3672 ± 150.5	< 1	1	1
	PG Lithuania 2	1 ± 0.2	3457 ± 81.7	< 1	2	1
Steel	**Blast furnace sludge**	6 ± 0.7	91 ± 15	6	73	59
	Electric arc furnace dust	92 ± 65.7	116 ± 70	80	99	17
Al	**Al-Sc Alloy dross**	6981 ± 463.5	6988 ± 465.7	> 99	> 99	88

Table B 3 Supporting information to Scandium world map (as of July 2021). (Mt =Million tonnes, kt= kilo tonnes)

Nr.	Name	Company	Country	Grouped as	Avg. Sc grade	comment	Reference or Source
1	**Evje-Iveland-District**	-	Norway	past primary Sc prod. from thortveitite	-	first description of thortveitite	http://www.smartminerals.com/norvegia/trip/Evje_Iveland.htm ; Neumann 1961; Segalstadt & Raade 2003; https://www.mindat.org; (Landverk 3 is the source region of Thortveitit)
2	**Befanamo/Berere**	-	Mada-gaskar	past primary Sc prod. from thortveitite	-		Lacroix 1920 (in French), (Von Knorring and Condliffe 1987; Von Knorring et al. 1970); https://zh.mindat.org/loc-2263.html
3	**Crystal Mountain**	-	USA	past primary Sc prod. from thortveitite	-		Foord et al. (1993)
4	**Kovdor deposit**	-	Russia	primary Sc (co-) production from REE, Nb/Ta a./o. U mining	ca. 0.05 in baddeleyite concentrate	inferred resource 420t Sc_2O_3	Kalashnikov et al. (2016)
5	**Tomtor deposit**	-	Russia	primary Sc (co-) production from REE, Nb/Ta a./o. U mining	ca. 0.03	approx. 100 Mt	Kalashnikov et al. 2016; Lapin et al. (2016);Tolstov and Gunin (2001); Kravchenko and Pokrovsky (1995) https://www.mindat.org/loc-67560.html
6	**Kumir deposit**	-	Russia	possible future primary Sc (co-) production from REE, Nb/Ta a./o. U mining	up to 0.065	inferred hypothetical resource > 100t	Kalashnikov et al. 2016; Gusev (2012); Gusev et al. (2009) https://www.mindat.org/loc-192609.html
7	**Zhovti Vody deposit**	-	Ukraine	past primary Sc (co-) production from REE, Nb/Ta a./o. U mining	0.0105, 105ppm	resource comprised 7.4 Mt, closed in 2003	Williams-Jones & Vasyukova 2018
8	**Crater lake**	Imperial mining	Canada	possible future primary Sc (co-) production from REE, Nb/Ta a./o.U mining	0.02-0.05		https://imperialmgp.com/projects/crater-lake/
9	**Sconi Project**	Australian Mines Ltd.	Australia	possible future primary Sc (co-) production from laterite mining/Ni-Co Mining		75 mt resource	https://australianmines.com.au/sconi
10	**Dalmatovs-koye/ Khokhlovskoye**	Dalur	Russia	by-product Sc-production from uranium mining	~ca. 1 mg/l in uranium leach liquors	resource and stockpiles ca. 400 t	**Chashchin (2018); Semenishchev (2018)** https://www.mindat.org/loc-194650.html

Nr.	Name	Company	Country	Grouped as	Avg. Sc grade	comment	Reference or Source
11	**Nyngan Project**	Scandium Int. Mining	Australia	possible future primary Sc (co-) production from laterite mining/Ni-Co Mining	0.0235 %; 235 ppm	16.9 Mt resource	http://www.scandiummining.com/projects/nyngan-scandium-project/
11	**Sunrise Project**	Clean TeQ	Australia	possible future primary Sc (co-) production from laterite mining/Ni-Co Mining	ca. 0.04-0.06 %	measured resource 2635 t (cut off grades > 300 ppm)	https://www.cleanteq.com/wp-content/uploads/2016/12/9772_Clean-Teq-SYERSTON-PROJECT-GEOLOGY-AND-RESOURCE_31-1-17.pdf; https://www.cleanteq.com/sunrise-project/; Chassé et al. 2016, Chassé et al. 2019
11	**Owendale Project**	Platina Resources	Australia	possible future primary Sc (co-) production from laterite mining/Ni-Co Mining	0.0395 %, 395ppm	33.7 Mt	https://www.platinaresources.com.au/projects/owendale/; https://hyleametals.com.au/hylea-cobalt-project/
11	**Flemington Project**	Australian Mines Ltd.	Australia	possible future primary Sc (co-) production from laterite mining/Ni-Co Mining	0.0403%, 403ppm	measured resource 2.5 Mt	https://mining.com.au/high-grade-cobalt-and-scandium-intersections-at-flemington-project/
12	**Kamensk-Uralsky, Russia**	RUSAL	Russia	by-product / Sc recovery from bauxite residue (or during alumina production)	0.009-0.023%, 90-230ppm	approx. 20 kt	Suss (2018); Suss et al. 2018
13	**TiO_2 Prod. Rotterdamm**	TRONOX	the Nether-lands	possible resource identified/investigated in SCALE /by-product Sc recovery from titanium dioxide production/zirconia production	dependent on residue 0.01-0.03 %	approx. 15t/a accumulating	SCALE research, Deliverable 6.1
14	**Red Mud deposit**	AOS Stade	Germany	possible resource identified/investigated in SCALE	ca. 0.005%, 50ppm	ca. 930 t resource in storage bauxite residues facilities	SCALE research, Deliverable 6.1

Nr.	Name	Company	Country	Grouped as	Avg. Sc grade	comment	Reference or Source
15	**Red Mud deposit**	MYTILINEOS (AOG)	Greece	possible resource identified/investigated in SCALE	ca. 0.01%, 100ppm	ca. 450 t resource in storage bauxite residues facilities	SCALE research, Deliverable 6.1
16	**Laterite deposit/ EAF slag**	LARCO	Greece	possible resource identified/investigated in SCALE	ca. 0.006%, 60ppm	ca. 90 t resource in storage bauxite residues facilities	SCALE research, Deliverable 6.1
17	**Red Mud deposit**	ALUM	Romania	possible resource identified/investigated in SCALE	ca. 0.008%, 80ppm	ca. 330 t resource in storage bauxite residues facilities	SCALE research, Deliverable 6.1
18	**Red Mud deposit**	MAL Hungarian Aluminium	Hungary	possible resource identified/investigated in SCALE	ca. 0.009%, 90ppm	ca. 1.7 kt resource in storage bauxite residues facilities	SCALE research, Deliverable 6.1
19	**Mindanao Island**	Sumitomo Metal Mining	Philippines	by-product Sc recovery from Ni/Co-, Cu-production	-	-	http://www.smm.co.jp/E/csr/activity_highlights/persistence/highlights2.html
20	**NiWEST Project**	GME	Australia	possible future primary Sc (co-) production from laterite mining/Ni-Co Mining	-	-	https://gmeresources.com.au/projects/niwestproject/
21	**Elk Creek Project**	NioCorp	USA	possible future primary Sc (co-) production from REE, Nb/Ta a./o. U mining	indicated 0.0057%, 57 ppm	indicated resource ca. 10.5 kt	https://www.niocorp.com/wp-content/uploads/180001_FINAL_43-101_FS_NioCorp_AS_FILED.pdf

Nr.	Name	Company	Country	Grouped as	Avg. Sc grade	comment	Reference or Source
22	**Gördes Laterite deposit**	Meta Nickel Cobalt	Turkey	possible future primary Sc (co-) production from laterite mining/Ni-Co Mining	0.004-0.012 %, 40-120 ppm	500t/a production capacity in "worst case scenario"	Kaya (2018)
23	**Elliot Lake**	Pele Mountain Resources	Canada	possible future primary Sc (co-) production from REE, Nb/Ta a./o. U mining	-	-	https://www.newsfilecorp.com/release/5298/Pele-Mountain-Resources-Advancing-Rare-Earths-Uranium-and-Scandium-Deposit-in-Elliot-Lake
24	**Ken Zone**	Romios Gold	Canada	possible future primary Sc (co-) production from Au, Cu, Ag or Mn mining	-	-	http://www.romios.com/
25	**Goongarrie**	Ardea Resources	Australia	possible future primary Sc (co-) production from laterite mining/Ni-Co Mining	ca. 0.005-0.01%, 50-100ppm	-	https://ardearesources.com.au/projects-goongarrie; https://www.australianmining.com.au/news/scandium-scouted-goongarrie-south/
26	**Bayhorse Silver Mine**	Bayhorse Inc.	USA	possible future primary Sc (co-) production from Au, Cu, Ag or Mn mining	ca. 0.002, 20ppm	-	https://www.newsfilecorp.com/release/33535/Bayhorse-Silver-Inc.-Significant-Scandium-Values-Up-to-26-GT-Sc-Accompany-High-Grade-Silver-Bayhorse-Mine-Oregon-USA; http://www.bayhorsesilver.com/
27	**Pacific Express Projects**	MinRex Ltd.	Australia	possible future primary Sc (co-) production from laterite mining/Ni-Co Mining	approx. 0.004 %, 40ppm	inferred resource ca. 27 t	https://smallcaps.com.au/minrex-resources-maiden-cobalt-pacific-express-project/
28	**Yokkaichi Plant**	Ishihara Sangyo kaisha	Japan	by-product Sc recovery from titanium dioxide production/zirconia production	-	-	personal communication Prof. Grandfield
29	**San Jorge Projects**	Axiom Mining	Solomon Islands	possible future primary Sc (co-) production from laterite mining/Ni-Co Mining	0.004-0.008 %, 40-80ppm	-	http://www.axiommining.com.au/irm/showdownloaddoc.aspx?AnnounceGuid=112705ed-9354-44e4-ab26-5f943a798166&TE=cmcleod@resourceinvestingnews.com

Nr.	Name	Company	Country	Grouped as	Avg. Sc grade	comment	Reference or Source
30	**Glenover Project**	Glenover Phosphate	South Africa	possible future primary Sc (co-) production from REE, Nb/Ta a./o. U mining	-	-	http://www.glenover.com/
31	**Gogota Project**	SRG Graphite	Guinea	possible future primary Sc (co-) production from laterite mining/Ni-Co Mining	ca. 0.003%, 30ppm	estimated base case mineral resource 1.17t Sc	http://srggraphite.com/gogota/
32	**Pennsylvania Anthracite**	Texas Mineral resources	USA	possible future primary Sc (co-)production from coal mining	-	-	https://www.globenewswire.com/news-release/2019/04/12/1803248/0/en/Texas-Mineral-Resources-Consortium-Successfully-Produces-Multiple-High-Purity-Rare-Earth-Elements-from-Pennsylvania-Coal-Mining-Waste-Material.html
33	**Round Top Projects**	Texas Mineral resources	USA	possible future primary Sc (co-) production from REE, Nb/Ta a./o. U mining	-	-	http://tmrcorp.com/projects/rare_earths/; https://www.globenewswire.com/news-release/2019/06/04/1863768/0/en/Texas-Mineral-Resources-and-JV-Partner-USA-Rare-Earth-Advance-Round-Top-Rare-Earth-Project.html
34	**Kiviniemi Project**	Scandium Int. Mining	Finland	possible future primary Sc production	ca. 0.017 %, 170ppm	12.6Mt total potential tonnage (cut off 60ppm, av grade 170ppm) resulting in potential og 0.2 Mt of Sc	http://www.scandiummining.com/site/assets/files/5743/kiviniemi-property-technical-characteristics.pdf
35	**Sorako, Sulavesi**	PT Vale Indonesia Tbk	Indonesia	possible future primary Sc (co-) production from laterite mining/Ni-Co Mining	< 100 ppm	no exact information about grades available yet	Maulana et al. (2016)
36	**Makuutu Project**	Ionic rare earth	Uganda	possible future primary Sc (co-) production from REE, Nb/Ta a./o. U mining	ca. 0.003%, 30ppm	inferred resource	https://wcsecure.weblink.com.au/pdf/IXR/02468915.pdf

Nr.	Name	Company	Country	Grouped as	Avg. Sc grade	comment	Reference or Source
37	**Rio Tinto Fer et Titane, Quebec, Sc_2O_3 demonstration plant**	Rio Tinto Fer et Titane	Canada	by-product Sc recovery from titanium dioxide production/zirconia production	-		https://www.riotinto.com/news/releases/2021/Rio-Tinto-enters-scandium-market-with-construction-of-new-plant-in-Canada
38	**Bayan Obo deposit**	-	China	primary Sc (co-)production from REE, Nb/Ta a./o. U mining	0.03% in tailings		Zhang et al. (2017)
39	**Hunan Oriental Scandium**	Hunan Oriental Scandium	China	by-product Sc recovery from titanium dioxide production/zirconia production	-		personal communication Prof. Grandfield
40	**Taojiang Ruilong Metal New Material**	Taojiang Ruilong Metal New Material	China	by-product Sc recovery from titanium dioxide production/zirconia production	-		personal communication Prof. Grandfield
41	**Guangxi Maoxin Technology**	Guangxi Maoxin Technology	China	by-product Sc recovery from titanium dioxide production/zirconia production	-		personal communication Prof. Grandfield
42	**Jiaozou Rongjia Scandium**	Jiaozou Rongjia Scandium	China	by-product Sc recovery from titanium dioxide production/zirconia production	-		personal communication Prof. Grandfield
43	**MCC New Material**	MCC New Material	China	by-product Sc recovery from Ni/Co-, Cu-production	-		personal communication Prof. Grandfield
44	**Huizhou Top Metal Material**	Huizhou Top Metal Material	China	by-product Sc recovery from titanium dioxide production/zirconia production	-		personal communication Prof. Grandfield

Appendix C – Additional Information to chapter 3.1

The content of this appendix was published in the paper:

Gentzmann, M. C., K. Schraut, C. Vogel, H.-E. Gäbler, T. Huthwelker, and C. Adam, 2021: Investigation of scandium in bauxite residues of different origin. Applied Geochemistry, 126, 104898.doi: https://doi.org/10.1016/j.apgeochem.2021.104898

Appendix D – Additional Information to chapter 3.2

The content of this appendix was published in the paper:

Gentzmann, M. C, Paul, A., Serrano, J., Adam, C, 2022: Understanding scandium leaching from bauxite residues of different geological backgrounds using statistical design of experiments, Journal of Geochemical Exploration, Volume 240, 2022, 107041, ISSN 0375-6742. https://doi.org/10.1016/j.gexplo.2022.107041

Eigenständigkeitserklärung

Hiermit erkläre ich, dass ich vorliegende Dissertation selbstständig verfasst habe und keine anderen als die angegebenen Hilfsmittel benutzt habe. Alle benutzten Hilfsmittel wurden durch entsprechende Angaben der Quellen kenntlich gemacht. Diese Arbeit hat in gleicher oder ähnlicher Form noch keiner anderen Prüfungsbehörde vorgelegen.

Marie Christin Gentzmann

Berlin, Mai 2022